Sustainable Futures 11 (2026) 101721

Contents lists available at ScienceDirect

Sustainable Futures

journal homepage: www.sciencedirect.com/journal/sustainable-futures

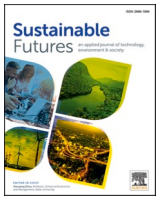

Green hydrogen production in a semi-arid region: A system dynamics analysis of water supply alternatives

Luís Matheus Tavares Silva [a,*], Cosme Polese Borges [b], Mônica Cavalcanti Sá De Abreu [c], Mauricio Uriona Maldonado [d], Flávia Mendes De Almeida Collaço [e]

[a] Federal University of Ceará – Av. da Universidade, 2431 – Benfica – CEP 60.020-180, Fortaleza, Ceará, Brazil
[b] Federal University of Santa Catarina, Rua Delfino Conti, 1000 - Trindade - CEP 88040-900, Florianópolis, Santa Catarina, Brazil
[c] Federal University of Ceará – Business Departament – Av. da Universidade, 2470 – Benfica – CEP 60.020-180, Fortaleza, Ceará, Brazil
[d] Federal University of Santa Catarina - Industrial Manufacturing Department - Rua Delfino Conti, 1000 - Trindade - CEP 88.040-900, Florianópolis, Santa Catarina, Brazil
[e] University of Sao Paulo - São Carlos School of Engineering - Av. Trabalhador Sãocarlense, 400 - São Carlos - CEP 13.566-590, São Paulo, Brazil

ARTICLE INFO

Keywords:
Green hydrogen
System dynamics
Recycled water
Seawater desalination
Circular economy
Semi-arid region

ABSTRACT

This study applies a system dynamics model to assess how alternative water-supply strategies, recycled water and seawater desalination, shape the viability of large-scale green hydrogen production in Ceará. Simulations from 2026 to 2050 show that water architecture is a strategic determinant of hydrogen output and operational burdens. Desalination-based scenarios produce moderate hydrogen volumes, reaching ≈397 kt/year and ≈509 kt/year, but impose the highest energy demand and brine loads, reinforcing pressures on coastal ecosystems and communities. A transitional configuration with gradually increasing recycled water yields the lowest output, ≈252 kt/year, due to the misaligned timing of desalination decline and recycled water expansion, a transition penalty relevant for incremental or poorly coordinated policy approaches. In contrast, a fully circular scenario based on recycled water delivers the highest production, ≈862 kt/year, eliminates brine discharge and lowers energy intensity while strengthening wastewater infrastructure and generating broader territorial co-benefits. Although ecological and social impacts are not modelled directly, the magnitude of brine and sludge flows identifies where regulatory oversight and multi-sectoral coordination are most urgently required. The findings send a clear message to policymakers: water choices are not operational details but structural decisions that can lock Ceará into an extractive, marine-burdening model or enable a regenerative pathway that expands productive capacity while distributing benefits across urban and industrial systems. Aligning hydrogen development with sanitation expansion, water governance and long-term environmental safeguards is therefore essential to prevent new inequalities and ensure that the emerging hydrogen economy contributes to a just and resilient future for semi-arid regions.

1. Introduction

Hydrogen (H2) is increasingly regarded as a strategic solution in global energy transition efforts, with the potential to decarbonize hard-to-abate sectors, modernize energy infrastructure, and accelerate the shift toward low-carbon economies [1,2]. Unlike conventional energy carriers, hydrogen acts as a chemical energy carrier in molecular form, enabling storage and transportation in ways that differ fundamentally from the movement of electrons in electrical systems. This property allows hydrogen to be integrated into existing supply chains for fuels such as oil, coal, biomass, and natural gas [3]. Nevertheless, the effectiveness of hydrogen in reducing emissions remains under debate, as current production methods are still largely dependent on fossil fuels, thereby limiting its potential climate benefits [4].

Technological advances have enabled hydrogen's integration into renewable energy systems, and the international community is mobilizing to unlock its full potential [5]. When derived from renewables, hydrogen offers applications without greenhouse gas emissions or air pollutants [6]. Yet, the expansion of hydrogen, particularly green hydrogen produced from renewable electricity, faces substantial

* Corresponding author at: Federal University of Ceará - Av. da Universidade, 2431 - Benfica - CEP 60.020-180, Fortaleza, Ceará, Brazil.
E-mail addresses: luismatheus@alu.ufc.br (L.M.T. Silva), cosme.polese@posgrad.ufsc.br (C.P. Borges), mabreu@ufc.br (M.C.S.D. Abreu), m.uriona@ufsc.br (M.U. Maldonado), flavia.collaco@usp.br (F.M.D.A. Collaço).

https://doi.org/10.1016/j.sftr.2026.101721
Received 23 December 2024; Received in revised form 11 December 2025; Accepted 1 February 2026
Available online 12 February 2026

challenges regarding water use and environmental sustainability [7].

The global race to deploy green hydrogen hubs is intensifying, and Brazil stands out due to its renewable-dominated electrical grid, with over 80 % of electricity generated from renewables in 2022 [8]. Brazil's competitive costs for renewable generation and its business environment have fostered interest in positioning the country as one of the major producers and exporters of green hydrogen [9,10].

As the green hydrogen agenda accelerates in Brazil, particular attention is being given to the country's semi-arid regions, where large-scale renewable energy and green hydrogen projects intersect with environmental, social, and regulatory challenges. Ceará, a state with roughly 95 % of its territory classified as semi-arid, has emerged as a focal point for major hydrogen investments [11]. Plans include the installation of an 11-gigawatt electrolyser hub in the Fortaleza Metropolitan Region, within the Industrial and Port Complex of Pecém. While the region offers significant potential for harnessing wind and solar energy, it faces persistent freshwater scarcity, historical droughts, and ongoing conflicts over water allocation among private companies, communities, and urban centres [12,13]. These constraints intensify the challenge of supplying both the local population and incoming green hydrogen projects with adequate water resources.

In this context, finding sustainable alternatives to conventional freshwater supplies is crucial for the future of green hydrogen production in Ceará. The main initiatives are evaluating the use of recycled water from wastewater treatment plants and seawater desalination [11, 12,14]. Each alternative entails different degrees of technological complexity, infrastructure requirements, environmental impacts, and social implications. Seawater desalination, for example, is energy-intensive and generates significant brine waste, which can adversely affect coastal ecosystems [15,16]. In contrast, recycled water aligns with circular economy principles and has the potential to reduce environmental pressures and promote resource efficiency, but its adoption depends on expanded sewage collection infrastructure, regulatory adjustments, and public acceptance [17,18].

Despite increasing attention to green hydrogen, there remains a notable gap in the literature regarding environmental and social implications of water supply strategies in semi-arid contexts [19]. Most existing studies emphasize technical and economic aspects, often using optimization or static models, and do not fully consider long-term environmental feedback, systemic interactions, or distributive effects [20–22]. For instance, Santana [23] analysed multiple water source alternatives for hydrogen production in Camaçari, Bahia, also a state located on Brazil's semiarid, highlighting cost impacts of transport distances but not assessing the use of recycled water or integrating cumulative environmental and social pressures.

Water supply emerges as a critical issue in the deployment of hydrogen hubs, especially as water demand extends beyond process feedstock and influences cooling and downstream uses [24,25]. Depending on electrolyser technology and system design, water-to-hydrogen ratios can vary significantly [21] and cumulative demands may put further stress on already fragile local resources. Given this scenario, there is a clear need to move beyond traditional technocratic and static perspectives that frame water supply as a purely technical or economic issue. It is essential to understand not only how hydrogen is produced, but also which socio-environmental logics, extractive and linear versus circular and regenerative, are being reinforced [26–28].

In this context, this study investigates the systemic impacts associated with alternative water supply strategies, specifically, recycled water versus seawater desalination, for green hydrogen production in semi-arid regions such as Ceará. To address this issue, a system dynamics approach is employed, drawing on literature, stakeholder interviews, and document analysis to simulate four scenarios with different shares of recycled water and seawater desalination between 2026 and 2050.

Therefore, the key methodological distinction of this study is the use of system dynamics modelling, which allows the analysis of complex, long-term feedback among infrastructure, water availability, energy demand, waste generation, and potential social and environmental impacts. Unlike optimization or static models, system dynamics provides a framework to capture cumulative, indirect, and feedback effects of policy and investment decisions, offering a more comprehensive basis for planning in highly interconnected socio-environmental systems [29–32]. By modelling these dynamics for Ceará, the study aims to contribute to more just and sustainable infrastructure planning. The results move beyond narrow techno-economic frameworks, providing actionable insights for public policy and stakeholder decision-making in the context of green hydrogen deployment in semi-arid regions.

2. Theoretical background

This section presents the theoretical foundations that frame the analysis of water supply strategies. It contrasts the principles of linear and circular economy, highlighting how seawater desalination and recycled water reflect different logics of resource use, waste generation, and environmental and social integration.

2.1. Linear economy and seawater desalination

Linear economy is the traditional system of producing and consuming which raw materials are converted into goods and services and then are disposed [33]. Its logic is known as "take, make, and disposal" [34]. This historical system is marked by resource inefficiency and negligence under the waste and emissions generation, jeopardizing the balance within the environmental system and putting the economic system under pressure, since more finite raw materials are needed to be taken in order to maintain manufacturer activities [35,36]. The most common disposal methods are land-filling and open burning [37]. This linear pattern can be observed in water supply strategies implemented under conditions of scarcity. A clear example is seawater desalination, which relies on the continuous extraction of saline water, energy-intensive processing, and discharge of residual waste, without incorporating regenerative or circular mechanisms.

Seawater desalination has been adopted to expand freshwater availability in arid and semi-arid regions [38,39], especially considering that about 66 % of the Earth's surface is covered by saline water [40]. Currently, 60 % of desalinated water is used for human supply and 30 % for industrial activities [41]. Among existing technologies, reverse osmosis is the most widespread. In this process, high-pressure pumps force seawater through a semipermeable membrane, separating freshwater from brine. The average recovery rate is 42 %, depending on salinity levels and system configuration [41,42].

A major concern in desalination is brine management. Table 1 summarizes the general characteristics of brine from the reverse osmosis process. These properties contribute to its persistence and potential

Table 1
General characteristics of brine from the reverse osmosis process.

Parameter	Characterization
Salinity	65 to 85 *g* of salt per 1 litter of brine.
Anti-scalant	2 ppm.
Flocculants/coagulants	Coagulant dosage between 1 and 30 mg/L (generally iron (III) salts); auxiliary coagulant dosage between 0.1 and 5 mg/L.
Heavy metals	Metallic equipment made of corrosion-resistant stainless steel; the concentrate may contain low levels of iron, chromium, nickel, and molybdenum if low-quality steel is used.
Total Dissolved Solids (TDS) mg/L	$\leq$ 70 mg/L.
Chemical cleaning products	Alkaline (pH 11–12) or acidic (pH 2–3) solutions containing additives such as detergents, complexing agents, oxidants, and biocides.

Source: Gomes et al. (2023).

toxicity when discharged into natural ecosystems without prior treatment [43,44].

The environmental impacts of brine discharge are evident in several regions. Approximately 142 million cubic meters of brine are generated daily, with 55 % of this volume concentrated in Saudi Arabia, Kuwait, Qatar, and the United Arab Emirates [41]. In the Persian Gulf, a region with climatic similarities to Ceará [13], field and laboratory studies report adverse effects on benthic organisms, macroalgae, and coral reefs [45]. Brine discharge contributes to reductions in plankton and epifauna abundance and favours salinity-tolerant species [45,46].

When combined with climate change, these impacts can intensify. For instance, the release of heated brine in the Persian Gulf may raise coastal sea temperatures by at least 3 °C, affecting fisheries and local livelihoods [47]. At a smaller scale, studies in rural communities in Rio Grande do Norte, bordering Ceará, show that brine from groundwater desalination units, when discharged directly onto the soil, increases pH, base saturation, and electrical conductivity [48]. Although such systems serve limited populations, they illustrate the potential for localized environmental degradation in the absence of proper brine handling.

Depending on the discharge method, the affected marine area can extend up to 23 square kilometres [44]. To assess these cumulative impacts, an integrated analytical framework is required. The structure of current desalination practices reflects a linear use of resources based on extraction, use, and disposal [49]. According to Moon et al. [43], the environmental consequences of high-salinity seawater desalination are often underestimated due to limited modelling approaches. Existing tools emphasize physical dispersion and overlook chemical toxicity, thermal effects, and long-term ecological interactions. Moreover, they rarely account for cumulative impacts from multiple plants operating in shared ecosystems.

A comprehensive assessment should combine different techniques to assess the environmental impacts from the operation of a reverse osmosis seawater desalination plant. Tools such as CORMIX and Delft3D support the modelling of brine dispersion and concentration, while exergo-environmental analysis helps identify energy inefficiencies across the system, and life cycle assessment captures resource use, emissions, and environmental impacts such as global warming potential, abiotic depletion potential, and marine aquatic ecotoxicity potential [43].

Seawater desalination exemplifies how infrastructure solutions can reproduce linear dynamics by prioritizing extraction and disposal over regeneration. Its widespread adoption in water-scarce regions highlights the need to critically assess not only technical performance, but also the broader implications for sustainability, and long-term resource governance.

2.2. Circular economy and recycled water

Circular economy is a regenerative system that reduces resource input, waste, emissions, and energy leakage by slowing, closing, or narrowing material and energy loops through maintenance, repair, reuse, remanufacturing, recycling, and long-lasting design [35]. It contrasts with the linear economy, which follows the “take, make, and dispose” logic, leading to inefficiencies and resource depletion [50].

Although both circular economy and sustainability involve collaboration among stakeholders, interdisciplinarity, and opportunities for value co-creation, circular economy focuses more explicitly on waste elimination and resource circularity, while sustainability addresses a broader range of environmental, social, and economic objectives [51,52]. In this context, the circular economy is considered a promising strategy to reduce carbon emissions and mitigate climate change by lowering energy and resource demand [53].

Water is particularly relevant to the circular economy since it is a non-substitutable resource under pressure from climate change, population growth, and economic development [17,18]. In the water sector, circular economy principles promote sustainable resource management and rational wastewater treatment. Table 2 summarizes circular economy principles and its corresponding actions, with water reuse and recycling combined under a single principle due to their functional overlap.

Recycled water reduces pressure on surface and groundwater sources by reintegrating treated effluents into productive cycles [54]. Wastewater treatment plants enable environmental restoration and support water reuse strategies when effluents are redirected to new uses [55]. As illustrated in Table 3, wastewater treatment follows a multi-stage structure that includes pre-treatment, primary, secondary, and tertiary treatments, disinfection, and sludge processing [55].

Recycled water can be directed to industrial processes, including hydrogen production, when its quality meets technical standards [56,57]. To produce high-purity water suitable for electrolysis, the effluent must undergo additional purification stages [56]. The treatment process must address a wide range of contaminants, including salts, pathogens, heavy metals, and persistent micropollutants such as pharmaceuticals and personal care products, which are not easily removed by conventional technologies [55,58]. Advanced purification methods, such as membrane filtration, oxidation processes, reverse osmosis, and ion-exchange resins, are therefore required to achieve the high-water quality standards needed for hydrogen production [56].

Nonetheless, even after these treatments, residual traces of contaminants may persist and pose operational challenges, particularly by affecting the stability of electrolyser membranes or triggering unwanted chemical reactions. These considerations highlight the importance of stringent monitoring and robust treatment protocols to ensure the safe and stable use of recycled water in green hydrogen applications. The complexity of the treatment depends on the origin of the effluent and the intended end use of the recycled water (e.g., agriculture, industrial use, hydrogen production) [59,60].

Wastewater treatment plants reduce pollution and mitigate health risks by preventing the direct discharge of contaminated water into the environment [61]. In addition to supplying recycled water, these systems can also recover energy and nutrients from sludge through processes like anaerobic digestion and nutrient extraction [62]. These recovery strategies enhance the alignment of water infrastructure with circular economy principles.

Despite these benefits, wastewater treatment has its own environmental impacts. Greenhouse gas emissions occur during biological and tertiary treatment stages, and endocrine-disrupting compounds may persist in treated effluents. Moreover, excess concentrations of heavy metals, such as mercury, are often detected in sludge, requiring careful disposal [63]. The sustainability of wastewater treatment systems also depends on their scale. A study conducted in Spain demonstrated that larger plants, serving populations over 50,000, achieved higher pollutant removal efficiency and lower operational costs per unit of treatment, especially in energy use [64]. Similar findings were observed in industrial reuse scenarios. In Taiwan, combined ultrafiltration and reverse osmosis systems were found to be economically and technologically viable, treating more water and at lower cost than conventional processes [65].

By integrating circular economy principles into wastewater treatment, recycled water becomes a strategy for minimizing freshwater

Table 2
Circular economy principles applied to the water sector.

Principle	Actions
Reduction	Reduce water use and pollution at the source.
Restoration	Apply technologies to remove pollutants from water and sludge.
Reuse/ Recycle	Recover treated effluent for non-potable or potable uses.
Recovery	Extract nutrients and energy from wastewater and sludge.
Rethink	Redesign systems to support a waste-free and emission-free circular water economy.

Source: Smol, Adam, and Preisner (2020).

Table 3
Stages and process of wastewater treatment.

Stage	Processes
Pre-treatment	Screening, grit removal
Primary treatment	Filtration, sedimentation, coagulation, flotation
Secondary treatment	Aerobic and anaerobic biological processes
Tertiary treatment	Membrane separation, distillation, ion exchange, oxidation, irradiation
Disinfection	Chlorination, ozonation, UV radiation
Sludge processing	Thickening, stabilization (e.g., digestion), dewatering, final disposition (e.g., landfill, reuse)

Source: Salgot and Folch (2018).

extraction and improving system resilience. Its use in green hydrogen hubs can reduce environmental burdens while promoting water reuse within the same territory [66]. Fig. 1 illustrates the systemic differences between seawater desalination and recycled water pathways. While the former follows a linear flow with limited reintegration, the latter supports a circular logic by enabling resource recovery and reuse of treated effluents.

As technological and institutional capacities evolve, the role of recycled water may expand beyond its current applications, fostering new synergies between infrastructure and environmental policy. This potential reinforces the importance of aligning water management with circular economy strategies, especially in regions facing increasing pressure on freshwater availability.

3. Materials and methods

Our study employs the system dynamics (SD) approach using the Stella Professional and Stella Architecture software. This approach was chosen due to its suitability for analysing intricate and interconnected systems [32]. The SD model's capacity to incorporate causal feedback loops makes it particularly well-suited for investigating the dynamic relationships between societal, environmental, and technological factors. Moreover, the model's flexibility in handling data scarcity and its ability to simulate long-term trends make it a valuable tool for exploring and evaluating complex system behaviour processes [67,68].

According to Sterman[32], SD approach comprises five phases: (i) problem articulation, which involves identifying and defining the system's critical issues hindering objective achievement; (ii) dynamic hypothesis formulation, which involves developing causal loop diagrams (CLD) to elucidate the system behaviour, including reinforcing and balancing feedback loops; (iii) stock and flow diagram (SFD) formulation, which entails transforming conceptual diagrams into a quantitative model with clear boundaries; (iv) testing and validation, comparing model outputs with empirical data and conducting sensitivity analysis; and (v) scenarios development, proposing scenarios and identifying leverage points to optimise system performance.

3.1. Problem articulation phase

The “problem articulation” phase identified critical factors influencing the Ceará state's water supply system and green hydrogen production. A mixed-methods strategy was developed encompassing both in-depth interviews and document analysis, as shown in Table 4. The interviews explored strategies for green hydrogen production hub implementation in the Industrial and Port Complex of Pecém in the Ceará state. The first goal was to identify who were the actors responsible for developing the green hydrogen production hub.

Then, identify what were the technological routes adopted for the Industrial and Port Complex’s green hydrogen production hub, as well as their respective operational challenges. Furthermore, as it became clear that water electrolysis would be the primary technology adopted, interviews examined water management in Ceará, highlighting the region’s specific soil and climate characteristics. Finally, interviewees were asked about the planned use of recycled water and seawater desalination, focusing on their potential environmental impacts and how each approach reflects a broader development model based on either circular or linear logic. In all, 11 interviews were conducted,

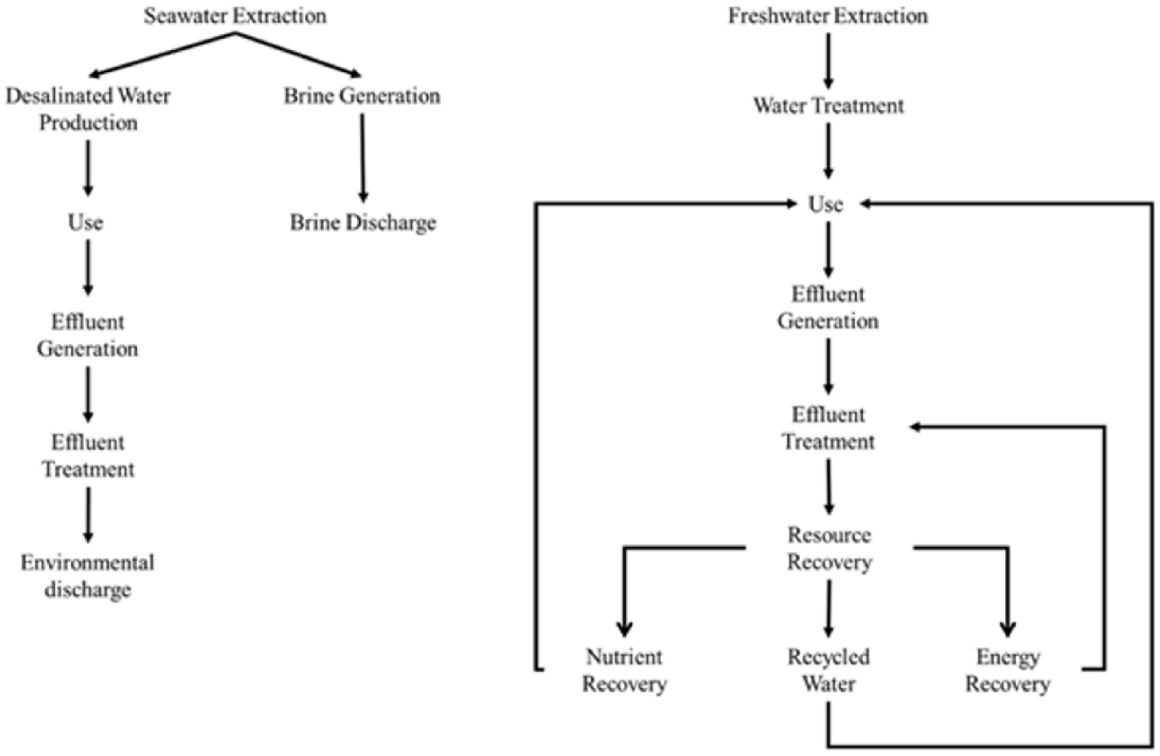

Fig. 1. Comparative water flow in general linear and circular systems.

Table 4
Data source overview.

Type of data	Subject	Sector	Acronym	Profile
Interview	Political and Technological Issues in GH Production	GH development group	E1	Energy Coordinator of State of Ceará
		Industrial and Port Complex	E4	Chief Executive Officer
		Electrolyzers company	E7	Engineering specialist
	Water Resources Management	Academia	E2	Professor and Researcher in Hydrology
			E3	Professor and Researcher in Wastewater treatment
		Water & Sewage Company	E5	Chemical engineer for innovation
	Technological Issues from Water Supply	Sanitary and Environmental Engineering Association	E6	Coordinator of the desalination and recycled water chamber
		Recycled water company	E9	Operations and engineering coordinator
		Water and industrial effluent treatment company	E11	Industrial wastewater treatment manager
	Environmental impacts	Academia	E8	Professor and Researcher in Marine Ecology
		Civil Society	E10	Indigenous leader
Document Analysis	Recycled water applications in Ceará	Ceará's State Law No 16.033/2016	Regulation	Establishes a policy for the reuse of non-potable water in the state of Ceará
	GH production projection	State of Ceará Official Gazettes	Communication reports	Official actions about green hydrogen development in Ceará
	GH production projection	Website companies	Communication reports	Information on memorandum of understanding signed by companies and Ceará Government
	Water resources planning in Ceará	Water infrastructure interventions, management and governance planning	Guidelines	Strategic action plan for water resources in Ceará (2018 – 2027)
		Water supply State company strategic planning	Guidelines	CAGECE's strategic management and business plan (2023 – 2027)
	Technical data of GH production and water supply	GH production projects and environmental impacts	Technical document	Environmental impact assessment for GH hub at CIPP
			Technical document	Environmental impact assessment for GH production by Fortescue industries

totalling 628 min of material.

The document analysis was centred on official gazettes, government agencies and companies' websites, as well as reports on green hydrogen production in Pecém Industrial And Port Complex. The Gazettes were available on the State Government's Civil House website, in which the term "green hydrogen" was searched from 01/01/2020 to 05/06/2023, yielding 20 relevant issues.

Key documents included the CAGECE's strategic management and business plan (2023 – 2027) [69], the Strategic Action Plan for Water Resources of Ceará [14] and Law No 16,033 on the Reuse of Non-Potable Water [70]. Additionally, the Environmental Impact Assessment (EIA) of Fortescue Future Industries [11], which aim to be the first green hydrogen production company to operate in the Industrial and Port Complex of Pecém, and the EIA of the green hydrogen production hub at Industrial and Port Complex of Pecém [71] were examined to gather operational data.

Taken together, the interviews and documentary evidence provide a coherent foundation for the subsequent modelling stages. They clarify the institutional configurations, technical constraints and environmental trade-offs that shape water supply routes for green hydrogen in Ceará, and they illuminate how recycled water and seawater desalination are embedded in distinct development logics. This combined evidence base substantiates the problem definition adopted in the model and ensures that the dynamic structure reflects the operational, regulatory, social and ecological realities of the Pecém context.

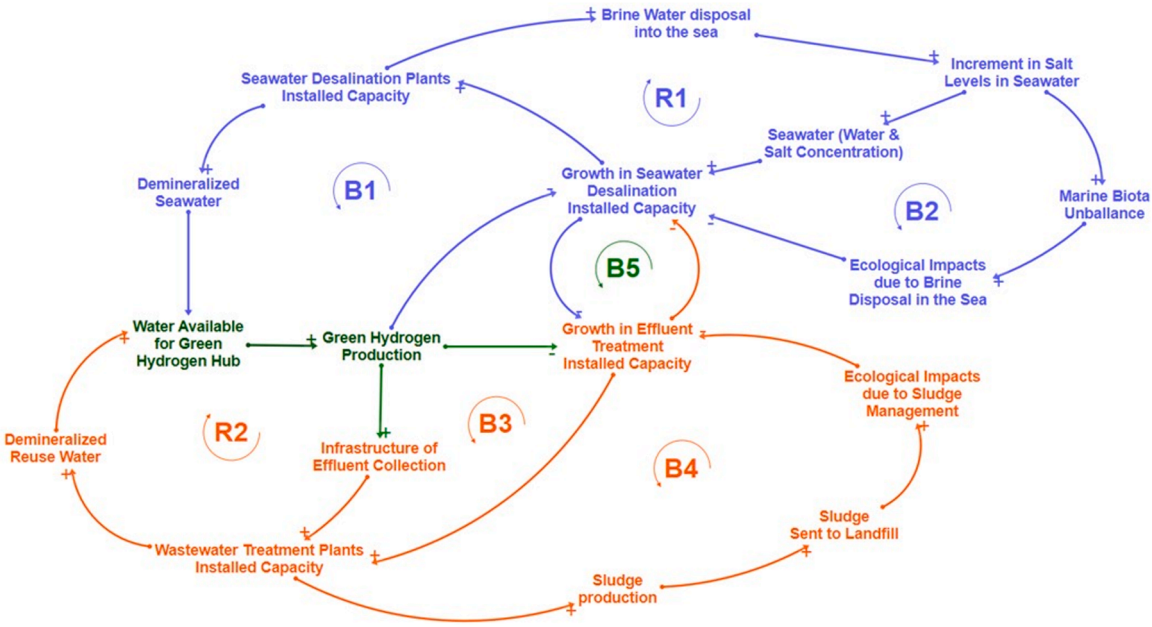

Fig. 2. Causal loop diagram of water supply.

3.2. Dynamic hypothesis formulation phase

During the "dynamic hypothesis formulation" phase, the CLD was developed with two complementary perspectives, one considering a multifaceted interaction among technological, environmental and social factors, and the other comparing circular and linear economy approaches. Fig. 2 elucidates the system's variables and the identified feedback loops, where B is for a balancing loop and R is for a reinforcing loop. From the first perspective, structurally, loops B1 and B3 are concerned with technological factors, encompassing variables related to installed capacity and its growth, as well as green hydrogen production. The loops B2 and B4 involve the environmental effects, encompassing variables related to the byproducts from both water supply technologies.

The loop R1 is pertinent to the environmental and technological factors, considering variables related to increment of salt concentrations in the seawater and the subsequent growth in desalination installed capacity. The loop R2 relates to socio-technological factors, encompassing the effluent collection increment and growth of recycled water installed capacity.

The second perspective in Fig. 2 compares the upper and lower parts of the CLD. It considers the linear economy approach, featuring loops B1 and B2, along with loop R1. Subsequently, it considers the circular economy approach, incorporating loops B3 and B4, and loop R2. At last, loop B5 highlights water supply sources' selection preferences.

Loop B1 outlines the positive feedback between seawater desalination installed capacity and green hydrogen production. However, loop B1 is counteracted by loop R1, wherein elevated brine discharge from desalination raises seawater salinity. This increase in salinity necessitates higher energy consumption and membrane replacement for the desalination process, hindering growth in desalination installed capacity. Moreover, loop B2 highlights the negative ecological consequences of increased salinity, including disruptions in marine ecosystems and reduced fishery yields, which may further discourage growth in seawater desalination installed capacity.

The circular economy approach initiates with loop B3, showing the installed capacity of the wastewater treatment plant. This loop influences the supply of demineralized recycled water, enhancing green hydrogen production while reducing recycled water installed capacity growth due to a limited supply of sewage. The loop R2 begins with the same logic as B3, however, the green hydrogen production leads to an increase in the effluent collection infrastructure, which raises the recycled water installed capacity.

Loop B4 begins with the positive impact of green hydrogen production on the infrastructure of effluent collection, which increases the capacity of wastewater treatment plant, thereby raising sludge production and its delivery to landfill. Increasing the number of landfill sites exacerbates sludge management challenges due to potential ecological effects, such as leachate leakage and greenhouse gas emission. The CLD behaviour is driven by the magnitude of circular versus linear economy approaches, which is settled via loop B5. This loop demonstrates the policy preferences about the growth in the seawater desalination capacity, which would lead to a reduction in the growth in sewage treatment capacity, and vice versa.

3.3. Stock and flow diagram formulation phase

The stock and flow diagram (SFD) formulation phase's objective is to build the model to represent the green hydrogen production in Ceará, Brazil, under different scenarios for water supply. The simulation period starts in 2026, when the first hydrogen plant is expected to begin the operation in Ceará [11], and ends in 2050, the target year for net-zero emissions in the energy sector [72]. The SFD developed is unpacked between figures three to nine, being composed of seven sectors.

Sector 1, entitled "Recycled Water Installed Capacity", represents the expansion and retirement of recycled water treatment infrastructure that can supply water to the hydrogen hub. The central stock in this sector is the recycled water installed capacity, denoted CR. Its evolution over time follows the standard stock–flow formulation in Eq. (S1.01), where NR, New Recycled Water Installed Capacity per Year, is the inflow and DR, Decommissioning of Recycled Water Installed Capacity per Year, is the outflow, both expressed in water cubic metres per second and converted internally to yearly values by the integration step, set at 0.25:

$$CR(t) = CR(t - dt) + [NR(t) - DR(t)]dt \tag{S1.01}$$

The model uses scenario-dependent initial conditions imported from Sector 7. The parameter Initial Recycled Water Installed Capacity, CR_0, defines the starting value of CR, ensuring that the recycled-water system begins the simulation aligned with the baseline water-supply configuration. Eq. (S1.01) states that the installed capacity in any period equals the previous capacity plus net additions over the time step. A positive difference between NR and DR yields expansion of water treatment capacity, whereas a negative difference leads to gradual decline. The inflow NR is governed by a conditional structure that reflects both (i) the availability of secondary effluent and (ii) the losses on the water distribution system. NR is activated only when CR is lower than ninety per cent of the effective secondary effluent available for recycled water treatment plant, which is the product of WT, Treated Water Available for Recycled Water Plant, and the conveyance factor $1 - WL$, where WL represents Water Losses during Distribution in Northeast Brazil. Variable WT is defined in Sector 2.

$$NR = \begin{cases} DELAYN\left(WT \times (1 - WL) \times FY,\ TR,\ 5,\ \dfrac{CR}{TR}\right), & if\ CR < 0.9 \times WT \times (1 - WL) \\ 0, & otherwise \end{cases} \tag{S1.02}$$

In this formulation, FY is Fix Year Unit ($\frac{1}{Year}$), and TR is the Time to Increase Recycled Water Installed Capacity. The delay order is set to five to reflect the gradual adjustment typical of infrastructure development. The final argument of the DELAYN function, $\frac{CR}{TR}$, defines the initial outflow of the delay chain. Using $\frac{CR}{TR}$ therefore produces realistic early-simulation behaviour by recognising that recycled water infrastructure already embeds a development pipeline that influences the pace of new capacity additions. The retirement of recycled water infrastructure is modelled through a parallel DELAYN structure that mirrors the ageing process of reverse osmosis treatment systems. The outflow DR is specified as:

$$DR = DELAYN\left(NR,\ YD,\ 5,\ \frac{CR}{YD}\right) \tag{S1.03}$$

Where YD represents Years for Reverse Osmosis Recycled Water Decommissioning. This reflects the fact that every batch of NR eventually becomes DR after its technical and regulatory lifetime elapses. The initial value $\frac{CR}{YD}$ ensures that the pre-existing infrastructure begins retiring at a rate consistent with its assumed remaining lifespan. The effective flow of recycled water supplied to the green hydrogen hub is

represented by RW, Recycled Water for Green Hydrogen Hub. It is constrained by both the installed capacity of the recycled water system and the effluent supply available upstream, depicted in sector 2. The variable OR, Operational Capacity of Recycled Water Plant, is derived from the scenario variable P, Percentage of Recycled Water. Equations below presents the calculation for RW and OR.

$$RW = \begin{cases} (1 - WL) \times WT \times OR \times RR, \ if \ CR > WT \\ (1 - WL) \times RR \times OR \times CR, \ otherwise \end{cases} \quad \text{(S1.04)}$$

$$OR = P \quad \text{(S1.05)}$$

The volumetric flow of recycled water supplied to the hub is limited by installed recycled water capacity, CR, or by upstream effluent availability, represented by WT and by the variable Treated Water Available for Recycled Water Plant in the model. Water Losses during Distribution in Northeast Brazil is represented by WL, while RR is Recycled Water Recovery Rate. In hydraulic terms, the model assumes that the effective feed to the recycled water plant corresponds to the minimum between WT and CR, reduced by distribution losses (1 − WL), and then adjusted by plant utilisation OR and recovery rate RR. When CR exceeds WT, the system is effluent-limited; when CR is lower than or equal to WT, the bottleneck is the recycled water plant capacity. This structure ensures that recycled-water deliveries cannot exceed either the upstream effluent supply or the treatment capacity at any point in time, and that all flows are consistently exposed to the same distribution losses.

The recycled water system also entails an energy requirement associated with advanced treatment processes. The annual energy consumption of recycled water, denoted EE (Recycled Water Energy Consumption per Year), is calculated in Eq. (S1.06). EE depends directly on the volumetric flow of recycled water sent to the hydrogen hub, RW, multiplied by the specific energy consumption per cubic metre of recycled water, EW (Recycled Water Energy per Water Cubic Metres), and scaled by the number of seconds per year, SY:

$$EE = RW \times EW \times SY \quad \text{(S1.06)}$$

The parameter EW represents the average electricity demand of treatment involving ultrafiltration, reverse osmosis and post-treatment conditioning. This value remains constant throughout the simulation, reflecting the assumption that no major technological shifts in energy intensity occur over the evaluated period. In addition to energy use, water treatment generates waste streams that must be managed. This effect is represented by SL, Sludge to Landfill, defined in Eq. (S1.07). SL depends on the volume of effluent effectively processed by the recycled water plant, which is limited either by upstream effluent availability or by the installed recycled water capacity, the same logic used in Eq. (S1.04). When the system is effluent-limited (CR > WT), sludge production is proportional to the treated effluent that reaches the plant after distribution losses. When the system is capacity-limited (CR ≤ WT), sludge is determined by the operated recycled water plant capacity, CR, also adjusted by the same distribution-loss factor (1−WL). In both cases, the resulting flow is multiplied by the complement of the recovery rate (1−RR), by SE and by SY (Seconds per Year):

$$SL = \begin{cases} OR \times (1 - WL) \times WT \times (1 - RR) \times SE \times SY, \ if \ CR > WT \\ (1 - WL) \times OR \times CR \times (1 - RR) \times SE \times SY, \ otherwise \end{cases} \quad \text{(S1.07)}$$

This formulation ensures that sludge generation is always tied to the actual volume of effluent processed by the recycled water system, while preserving the same bottleneck logic used to define recycled water deliveries to the hydrogen hub. Because SE is a pure unit-conversion factor equal to one, it does not affect magnitudes and serves only to maintain dimensional consistency in the model. The Fig. 3 presents the SFD for sector 1. The variables in orange (HTML = #fb8500) are the parameters from recycled water.

Sector 2, entitled "Effluent Collection System", represents the collection infrastructure that supplies effluent to recycled water treatment in Sector 1. This sector governs how the sewerage system expands in response to growing hydrogen production, how this infrastructure retires over its lifetime, and how much treated effluent becomes available for the recycled water treatment plant. The central stock in this sector is the effluent collection capacity, denoted EC, Infrastructure of Effluent Collection Capacity. Its evolution follows the standard stock–flow formulation shown in Eq. (S2.01), where NC, New Collection Capacity, is the inflow and RC, Retirement of Collection Capacity, is the outflow:

$$EC(t) = EC(t - dt) + [NC(t) - RC(t)]dt \quad \text{(S2.01)}$$

The initial value of the effluent collection infrastructure is set to 1 m^3/s, representing a normalised baseline that allows expansion and retirement dynamics to be captured relative to an established collection network. Following the interviews, the maximum value for EC is 3 m^3/s. This value is better explained in the section 3.4, Validation Phase. The inflow NC represents the rate at which new collection capacity is added. It depends on the existing level of effluent collection capacity, EC, and on the effective drivers of expansion. A key variable in this determination is RI, the Real Increment in Effluent Collection Capacity, defined as the product of the incremental driver derived from hydrogen production and the operational capacity of the recycled water treatment system, shown in Eq. (S2.04). Eq. (S2.02) specifies NC using a nested conditional formulation that distinguishes between an active expansion regime and a saturation regime:

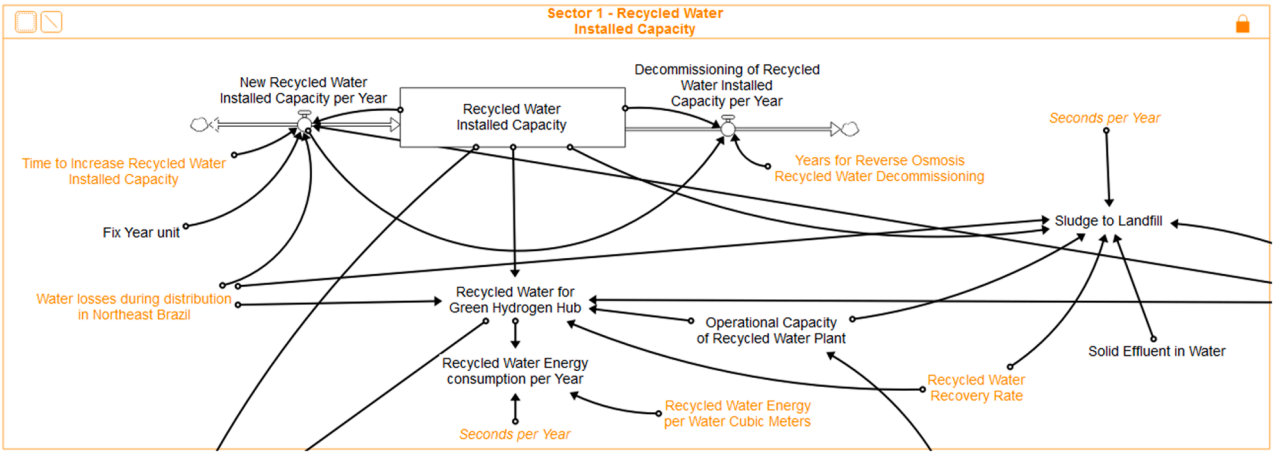

Fig. 3. Recycled water installed capacity.

$$NC = \begin{cases} 0.01, \ if \ EC \ \geq 3, \ else \\ \begin{cases} 0.01, \ if \ RI = 0.9, \\ DELAYN(RI, \ TI, \ 5, \ I_0), \ otherwise \end{cases} \end{cases} \quad \text{(S2.02)}$$

Where the initial value of the delay, I_0, is defined as:

$$I_0 = \begin{cases} 0, \ if \ RI = 0 \\ \frac{EC}{TI}, \ if \ RI > 0 \end{cases} \quad \text{(S2.02.01)}$$

The formulation for variable NC incorporates two levels of decision-making: a structural limit and an operational response. When the existing collection capacity reaches or exceeds 3 m^3/s, the system enters a saturation regime in which only marginal annual increases are admitted. When EC < 3, expansion is governed by a second condition based on the real increment signal RI. If RI = 0.9, the upper bound of the incremental function, NC is likewise constrained to 0.01, reflecting that no further acceleration is justified once the system reaches its maximum incremental threshold. In all other cases, NC is determined by an nth-order delay that represents the multi-year pipeline associated with planning, permitting and constructing sewerage infrastructure.

The initial value of the delay, I_0, incorporates a safeguard: when RI = 0, the pipeline is initialised at zero to prevent artificial propagation of capacity additions; when RI > 0, the initial value becomes $\frac{EC}{TI}$, representing the effective throughput implied by the existing infrastructure and its implementation time. This structure ensures that expansion of the effluent collection network responds coherently to system conditions while preserving the temporal inertia characteristic of large wastewater systems. The incremental driver of effluent collection expansion is the Increment in Effluent Collection Capacity, denoted IN It is defined as a graphical function of HP, Green Hydrogen Production per Year:

$$IN = GRAPH(HP) \quad \text{(S2.03)}$$

The GRAPH function is implemented as a piecewise-linear relationship, starting from IN = 0.10 at lower hydrogen production levels and reaching IN = 1.00 at 2000,000 tonnes of green hydrogen per year. The intermediate breakpoints are modeller assumptions that specify how quickly expansion incentives grow as hydrogen production increases. In contrast to the analogous function used in the seawater desalination sector, which will be presented later, the slope of this curve is more gradual. This reflects interview evidence indicating that desalination plants are easier for companies to expand autonomously, whereas effluent collection infrastructure depends on public coordination, integration with existing networks and more complex regulatory procedures. The Real Increment in Effluent Collection Capacity, denoted RI, translates this incremental driver into an effective expansion signal by adjusting for the operational status of the recycled water treatment system. It is calculated as the product of IN and the Operational Capacity of the Recycled Water Plant, OR, which is defined in Sector 1:

$$RI = IN \ \times OR \quad \text{(S2.04)}$$

This formulation implies that even if hydrogen production creates strong incentives for expansion, high IN, effluent collection will only be expanded when the recycled water plant is expected to operate. When OR is low, RI decreases, signalling that there is limited value in increasing collection capacity if recycled water treatment is not being fully utilised. Conversely, when OR approaches one, RI converges towards IN, meaning that the collection system responds more directly to the hydrogen-driven demand for effluent.

Retirement of sewerage infrastructure is represented by the outflow RC. Effluent collection networks are known by its long-lived assets that retire gradually. This process is modelled using a DELAYN structure:

$$RC = DELAYN\left(NC, \ LS, \ 5, \ \frac{EC}{LS}\right) \quad \text{(S2.05)}$$

Where LS denotes the Life Span of Effluent Collection Infrastructure and the initial value $\frac{EC}{LS}$ ensures that, at the start of the simulation, the existing collection system begins to retire at a rate consistent with its remaining lifetime. Eq. (S2.05) therefore captures the gradual, cohort-based turnover of infrastructure, in which each tranche of NC eventually becomes RC once it reaches the end of its service life. Finally, Sector 2 determines the volume of effluent that becomes available for recycled water treatment in Sector 1, being represented by WT, Treated Water Available for Recycled Water Plant:

$$WT = EC \ \times FT \quad \text{(S2.06)}$$

The parameter FT represents the proportion of collected effluent that is treated to the quality required for subsequent recycled water processing. By linking WT directly to EC, Eq. (S2.06) couples the performance of the effluent collection system to the recycled water system in Sector 1. Increases in EC raise WT proportionally, enabling higher recycled water production, whereas limited EC constrains WT and, in turn, the amount of recycled water that can be supplied to the hydrogen hub. Fig. 4 presents the sector 2. The variables in brown (HTML = #bd7e00) are the parameters, which will be defined in section 3.4, Validation Phase.

Sector 3, entitled "Seawater Desalination Installed Capacity", represents the infrastructure responsible for supplying desalinated seawater to the hydrogen hub. The central stock in this sector is denoted as CS, Seawater Desalination Installed Capacity, whose evolution over time follows the standard stock–flow relationship:

$$CS(t) = CS(t - dt) + [NS(t) - RS(t)]dt \quad \text{(S3.01)}$$

Where NS is New Desalination Installed Capacity per Year and RS is Retirement of Desalination Capacity per Year. When NS exceeds RS, installed desalination capacity expands; when RS exceeds NS, capacity declines gradually. The initial value of CS is imported directly from the parameter Initial Seawater Desalination Installed Capacity, defined in Sector 7 and based on project-level engineering data for the Industrial and Port Complex of Pecém. Expansion of desalination capacity responds to increment driven by hydrogen production and is defined using an nth-order delay to represent the multi-year cycle of planning, permitting, procurement and construction associated with large-scale seawater desalination facilities:

$$NS(t) = DELAYN\left(RS, \ TS, \ 5, \ \frac{CS}{TS}\right) \quad \text{(S3.02)}$$

Where RSI is the Real Increment in Seawater Desalination Installed Capacity and TS is the Time to Implement Seawater Desalination Expansion. The delay order is set to five to represent the multi-year cycle of planning, permitting, procurement and construction of large-scale seawater desalination facilities. The initial value $\frac{CS}{TS}$ ensures that, at the start of the simulation, the delay pipeline contains an increment flow consistent with the existing installed capacity, avoiding artificial suppression of NS in the early years. The Real Increment in Seawater Desalination Installed Capacity converts the incremental driver ID into an effective increment signal by accounting for the operational status of the desalination system, being RSI defined as:

$$RSI = ID \ \times OS \quad \text{(S3.03)}$$

The Increment in Seawater Desalination Installed Capacity, denoted ID, represents the increment incentive generated by hydrogen production while OS, Operational Capacity of the Seawater Desalination System, depends on the scenario variable P, Percentage of Recycled Water. The equations are defined as follows:

$$ID = GRAPH(HP) \quad \text{(S3.04)}$$

$$OS = 1 - P \quad \text{(S3.05)}$$

At Eq. (S3.04), the GRAPH function maps hydrogen production between 10,000 and 2000,000 tonnes per year onto a monotonic increase

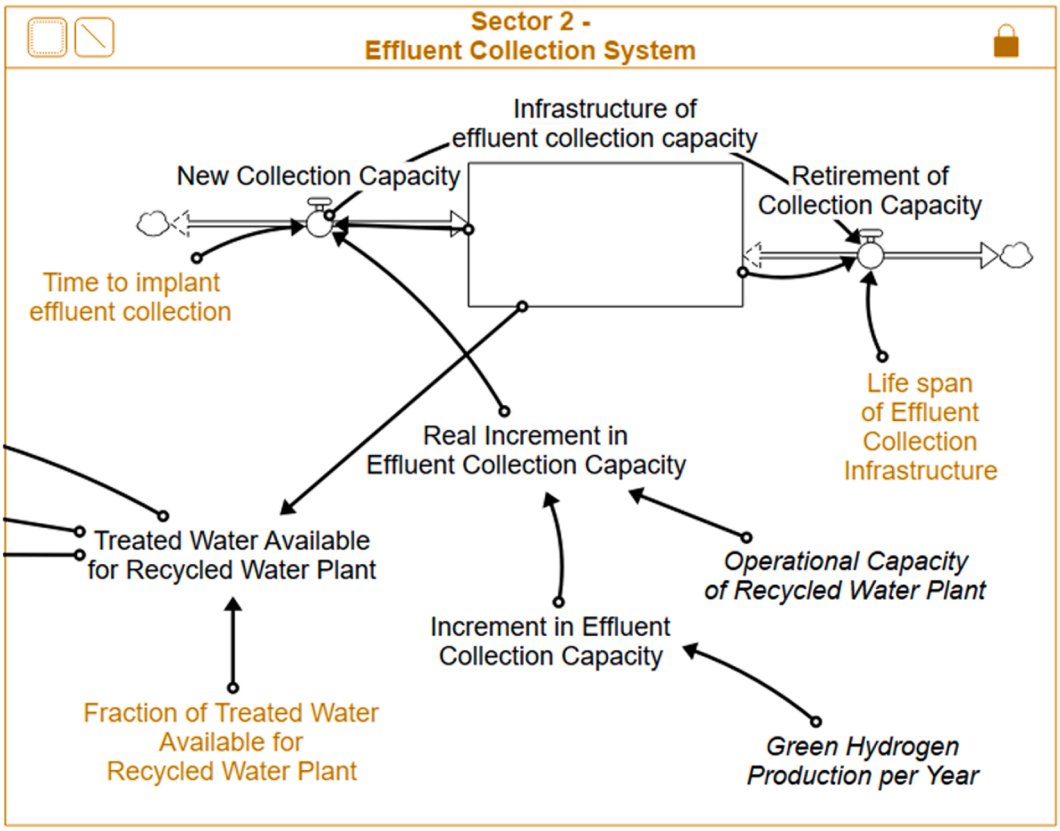

Fig. 4. Effluent collection system.

in ID from 0.50 to 1.0. Interviewees consistently explained that desalination is institutionally easier to expand than recycled water because the infrastructure is privately owned, modular, and less dependent on integration with urban sanitation networks. As a result, the slope of the desalination GRAPH is steeper than the analogous function used in Sector 2. Retirement of desalination capacity is governed by a parallel DELAYN function representing the ageing of reverse osmosis membranes and associated high-pressure equipment:

$$RS(t) = DELAYN\left(NS,\ YS,\ 5,\ \frac{CS}{YS}\right) \tag{S3.06}$$

Where YS denotes Years for Reverse Osmosis Seawater Decommissioning. Each tranche of NS is thus transferred to RS once it reaches the end of its assumed lifetime YS. The initial value CS/YS ensures that the pre-existing desalination capacity begins to retire at a rate consistent with its remaining lifetime at the start of the simulation. The volumetric flow of desalinated water delivered to the hydrogen hub is denoted SW, Seawater for Green Hydrogen Hub. It depends on the installed desalination capacity, its operational utilisation and the effective recovery rate:

$$SW = CS \times OS \times SR \tag{S3.07}$$

Where SR is Seawater Recovery Rate. For a given CS, increases in OS or SR raise SW proportionally, while reductions in either variable lower the product water available for hydrogen production. The total volumetric flow processed by the desalination system, WD (Water Processed in Desalination), is the sum of the product water SW and the BF:

$$WD = SW + BF \tag{S3.08}$$

BF represents the Brine Water Discharge Flow. Brine discharge arises as the complement of the recovery process, denoted by SR. The BF, Brine Water Discharge Flow, is given by:

$$BF = CS \times OS \times (1 - SR) \tag{S3.09}$$

This expression uses the same CS and OS terms as Eq. (S3.07), but scales them by the fraction of feedwater that is not recovered as permeate. Any increase in desalination capacity or utilisation therefore generates a proportional increase in brine discharge, given the recovery rate SR. The annual brine volume discharged to the sea is represented BY (Brine Water in the Sea per Year):

$$BY = BF \times SY \tag{S3.10}$$

Where SY denotes Seconds per Year. BY provides an annualised measure of brine discharge that can be used to support longer-term assessments of brine volumes, but it does not directly participate in the near-field salinity feedback described below, which is based on instantaneous mixing, following equations from Khangaonkar et al. [73].. Near-field salinity dynamics are represented through a steady-state mixing relationship between the brine plume and the surrounding seawater in the immediate vicinity of the outfall. The mixed salinity in the near field, SM (Salinity Mix Near-Field), is given by:

$$SM = \frac{(BF \times SB) + ((ND - 1) \times BF \times SN)}{BF + ((ND - 1) \times BF)} \tag{S3.11}$$

Where SB is Salinity of Brine Water, SN is Salinity Near Field (ambient), BF is Brine Water Discharge Flow, and ND is Near-Field Dilution. The term $(ND-1) \times BF$ represents the volume of ambient seawater entrained by the brine jet, so Eq. (S4.03) expresses SM as the flow-weighted average of brine and entrained seawater salinities

Regarding to energy consumption, the Eq. (S3.12) ensures that all seawater drawn into the plant is accounted for as either useful freshwater or concentrate brine. For a given SW, lower SR implies a larger BF and hence a larger WD, consistent with the need to process more feedwater to obtain the same volume of permeate when recovery is reduced. The total energy consumption required to operate the seawater

desalination system is represented by EY (Seawater Desalination Energy Consumption per Year), calculated as:

$$EY = DW \times WD \times SY \tag{S3.12}$$

Where DW is Seawater Desalination Energy per Water Cubic Metre, WD is Water Processed in Desalination, defined at Eq. (S3.08), and SY is Seconds per Year. This formulation ensures that any change in throughput WD, whether driven by expansion of CS, variations in OS or changes in recovery SR, is translated consistently into annual electricity demand. The model incorporates a feedback between near-field salinity around the outfall and desalination performance. The term ER, Expected Decrements in Recovery Rate Efficiency, is defined as a graphical function of SN, Salinity Near Field, which belongs to sector 4 and will be explained later in this subsection:

$$ER = GRAPH(SN) \tag{S3.13}$$

The GRAPH function maps SN, defined in Eq. (S4.02), values between 35 and 45 kg/m^3 onto a gradual decrease in ER from 1.00 to 0.75, with intermediate points defined by the modeller to match hydrodynamic and desalination studies. The effective seawater recovery rate SR is obtained by scaling the initial design recovery rate SI (Seawater Initial Recovery Rate) by ER:

$$SR = ER \times SI \tag{S3.14}$$

When SN remains at baseline levels, ER equals one and SR coincides with SI. As SN increases above baseline, ER falls below one and SR declines proportionally, reducing both SW at Eq. (S3.07) and increasing BF at Eq. (S3.09) for a given CS and OS. Fig. 5 presents the sector 3. The variables in blue (HTML = #0091 da) represent the parameters.

Sector 4, entitled "Salinity Near Field", represents how local seawater salinity in the vicinity of the desalination outfall evolves over time in response to brine discharge and subsequent dispersion. The salinity increment in the near field, DS (ΔSalinity Near Field), is then defined as the difference between the mixed salinity SM and the ambient salinity SN:

$$DS = SM - SN \tag{S4.01}$$

DS quantifies the localised salinity elevation resulting from brine discharge in the immediate mixing zone, driving input for the near-field salinity accumulation mechanism and subsequent dispersion. This allows the model to capture how changes in desalination operations propagate into coastal salinity conditions. The central stock in this sector is SN (Salinity Near Field), which tracks the average salt concentration in the near-field mixing zone. Its dynamics follow a standard stock–flow relationship:

$$SN(t) = SN(t - dt) + [SA(t) - WS(t)] \times dt \tag{S4.02}$$

Where SA is Salinity in Surrounding Areas, the net annualised inflow of salt to the near field, and WS is Water Spreading, the outflow associated with dispersive processes. The model links the salinity increment to the evolution of SN through a dimensionless measure of relative change. The Expected Salinity Level Increment, denoted EI, is defined as the ratio between the near-field salinity increment DS and the current near-field salinity SN:

$$EI = \frac{DS}{SN} \tag{S4.03}$$

EI therefore quantifies how large the brine-induced salinity increment is in proportion to the ambient near-field salinity. When DS is small relative to SN, EI remains close to zero; when DS becomes large relative to SN, EI approaches or exceeds unity, signalling a strong localised increase.

$$SA = \begin{cases} 0, \ if \ EI \times SN \times FY = NAN \\ EI \times SN \times FY, \ otherwish \end{cases} \tag{S4.04}$$

Where FY is Fix Year Unit (equal to 1 year^{-1}) used to express SA in kg/m^3/year. The explicit formulation in Eq. (S4.04) incorporates a safeguard that prevents numerical failure when no seawater desalination is operating. In scenarios where desalination is not used, brine discharge BF equals zero, which implies that the salinity increment DS also becomes zero. Because EI is defined as DS divided by SN, this produces an indeterminate $\frac{0}{0}$ expression that Stella evaluates as "not-a-number". When this occurs, the model may crash due to propagation of undefined values. To avoid this, the conditional-structure forces SA to zero, maintaining numerical stability throughout the simulation. Salinity reduction due to dispersion and mixing with surrounding waters is represented by the outflow WS, Water Spreading, being activated only when near-field salinity exceeds the baseline ambient value of 36.03 kg/m^3:

$$WS = \begin{cases} SS, \ if \ SN > 36.03 \\ 0 \ , \ otherwish \end{cases} \tag{S4.05}$$

Where SS is Salt Spreading, a parameter with units of kg/m^3/year. SS is set to 0.94 kg/m^3/year, based on the limited but convergent evidence that basin-scale salinity changes from current desalination discharges are small. Paparella et al. [74]. and Ibrahim et al. [75]. report salinity increases below about 0.5–1.0 kg/m^3 in comparable coastal systems, while interview E8 stresses that strong coastal currents along Ceará favour rapid dispersion. The chosen value of SS provides a conservative representation of annual salinity relaxation that keeps SN within ranges

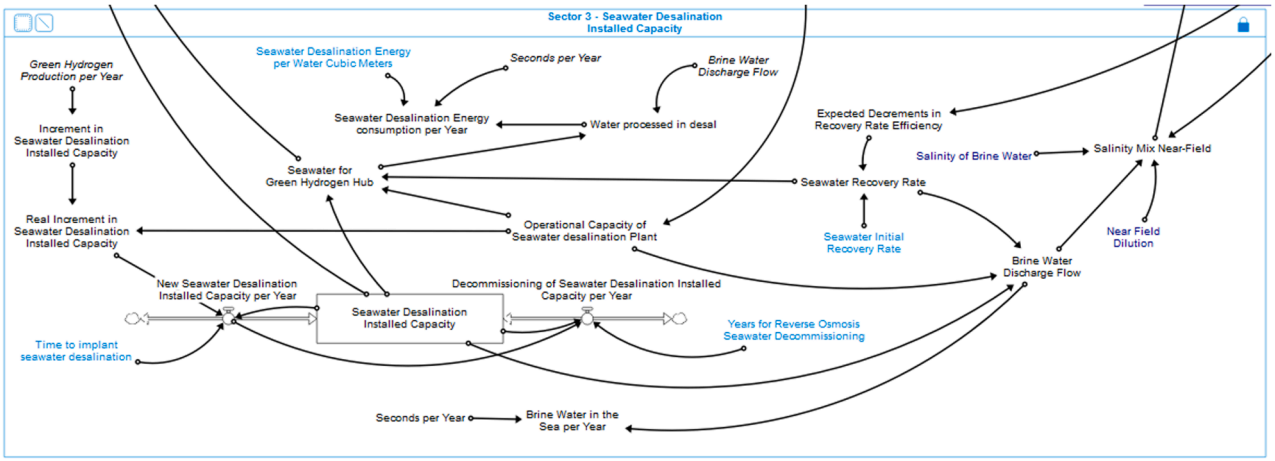

Fig. 5. Seawater desalination installed capacity.

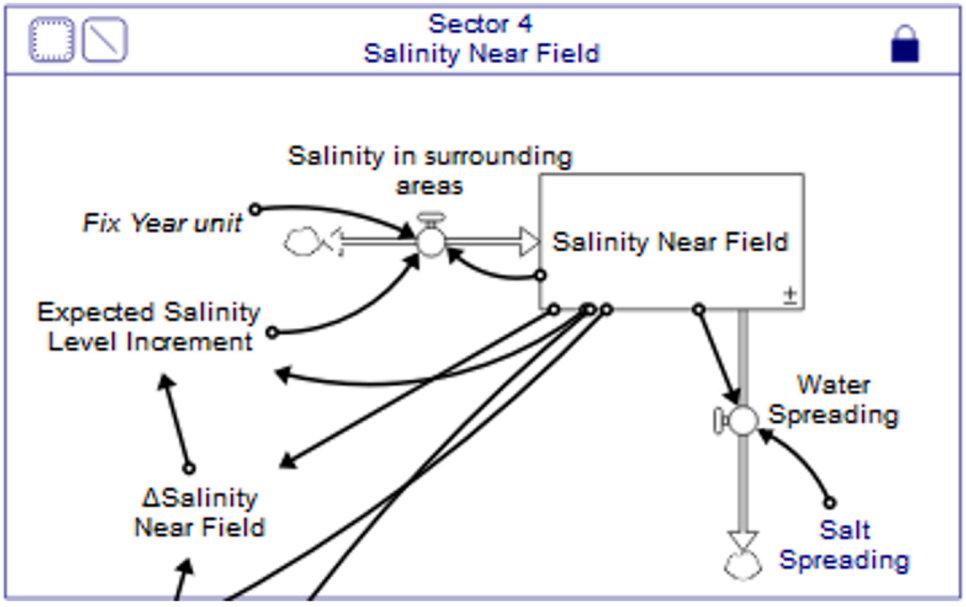

Fig. 6. Salinity near field.

consistent with the hydrodynamic results of Pereira et al. [76]., while still allowing localised elevation when brine discharge grows. Fig. 6 presents the sector 4. The variables in dark blue (HTML = #00007f) represent the parameters.

Sector 5, entitled "Green Hydrogen Hub – Water Supply", aggregates all water delivered from the recycled water system (Sector 1) and the seawater desalination system (Sector 3) to determine the volumes available for cooling and electrolysis. The sector does not include a stock; instead, it defines a set of algebraic relationships that partition the total incoming water into its cooling and production components. The total amount of water delivered to the hydrogen hub, denoted WH (Water for Green Hydrogen Hub), RW and SW:

$$WH = RW + SW \tag{S5.01}$$

The variable Fraction of Water for Cooling, FC, partitions WH into its evaporative cooling component WC, Water for Green Hydrogen Cooling, while FP, Fraction of Water for Green Hydrogen Production, partitions WH for effective green hydrogen production, WP, Water for Green Hydrogen Production, as depicted in the following equations:

$$WC = WH \times FC \tag{S5.02}$$

$$FP = (1 - FC) \tag{S5.03}$$

$$WP = WH \times FP \tag{S5.04}$$

The variable Total Installed Capacity of Water, TC, is the sum of desalination capacity CS and recycled water capacity CR:

$$TC = CS + CR \tag{S5.05}$$

The Fig. 7 presents the sector 5. The variable in royal blue (HTML = #2519d9) represents a parameter.

Sector 6, Green Hydrogen Production, translates the water actually available for electrolysis, from Sector 5, into green hydrogen output. The core of this sector is the relationship between water mass flow, electrolyser efficiency and hydrogen production. The variable Electrolyser Efficiency for GH_2 Production, denoted EF, is defined as the ratio between the theoretical and real specific energy consumption of electrolysis:

$$EF = \frac{TE}{RE} \tag{S6.01}$$

Where TE is the Theoretical Energy Consumption for GH_2 Production (HHV basis) and RE is the Real Energy Consumption for GH_2 Production (HHV basis). Both TE and RE are treated as constant parameters. The mass flow of water available for electrolysis, TW (Tonnes of Water), depends on the volumetric flow WP (Water for Green Hydrogen

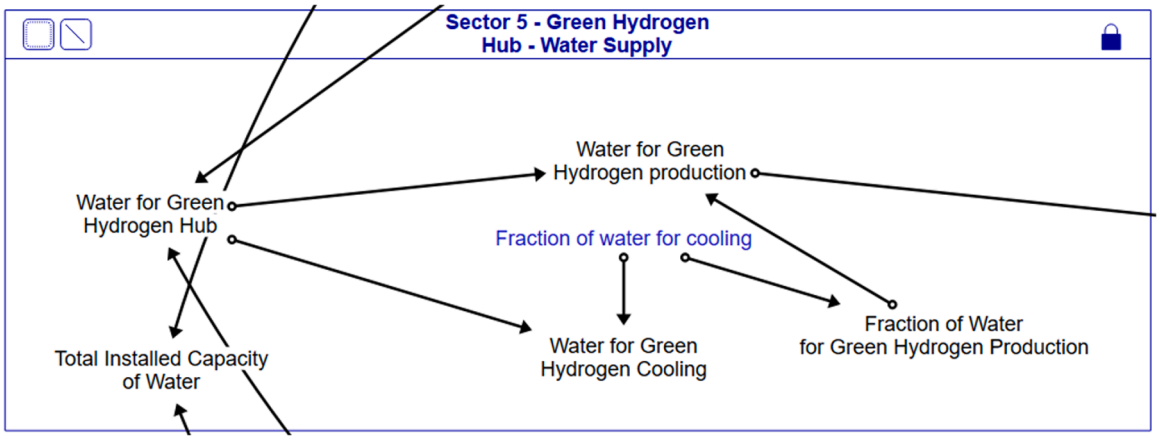

Fig. 7. Green hydrogen hub (water supply).

Production, defined in Sector 5) and the density of water, ρ_W(Water Density):

$$TW = \rho_W \times WP \tag{S6.02}$$

Hydrogen production per unit of time is then derived from the mass ratio between water and hydrogen. Green hydrogen production per second, denoted HS, is given by:

$$HS = \left(\frac{TW}{WM}\right) \times EF \tag{S6.03}$$

Where WM is Water per Hydrogen (Mass), expressed as tonnes of water per tonne of hydrogen. Eq. (S6.03) states that hydrogen output per second equals the water mass flow divided by the water requirement per tonne of hydrogen, adjusted by the electrolyser efficiency EF. To obtain the annual hydrogen output, HS is scaled by the number of seconds per year, SY (Seconds per Year). Green hydrogen production per year, denoted HP, is therefore:

$$HP = HS \times SY \tag{S6.04}$$

Finally, the share of recycled water in the hub's water portfolio, P (Percentage of Recycled Water), is treated in the model as an exogenous scenario parameter that directly influences the operational shares of recycled water and desalinated water in Sectors 1 and 3:

$$P = Percentage\ of\ Recycled\ Water \tag{S6.05}$$

This parameter links the water-supply configuration to both the hydrogen production sector and the infrastructure expansion sectors and is better described on section 3.5 Scenario Development Phase. Fig. 8 presents the sector 6. The variables in green (HTML = #005,500) represents the parameters, while the variable in red (HTML = #aa0000), represents the scenarios decision rule.

Sector 7 defines the initial values of the two main water-supply infrastructures: recycled water treatment and seawater desalination. These initial conditions are scenario-dependent and provide the starting point for the capacity dynamics described in Sectors 1 and 3. The initial installed capacity of recycled water, denoted CR_0 (Initial Recycled Water Installed Capacity), is specified as a conditional function of the recycled-water share P (Percentage of Recycled Water):

$$CR_0 = \begin{cases} 0, & if\ P = 0 \\ 0.206, & if\ P = 1 \\ 0.0206, & otherwise \end{cases} \tag{S7.01}$$

This formulation captures three configurations: no recycled water use ($P = 0$), full reliance on circular economy ($P = 1$), and an intermediate configuration in which recycled water accounts for other percentages of total supply, represented by 0.0206 m^3/s. The initial installed desalination capacity, denoted CS_0 (Initial Seawater Desalination Installed Capacity), is defined analogously:

$$CS_0 = \begin{cases} 0, & if\ P = 1 \\ 0.206, & otherwise \end{cases} \tag{S7.02}$$

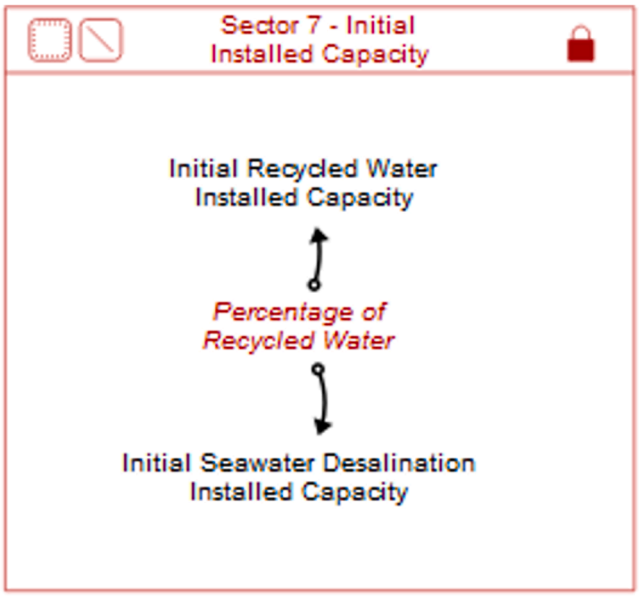

Fig. 9. Initial installed capacity.

The Fig. 9 presents the sector 7. The variable in red (HTML = #aa0000), represents the scenarios decision rule.

To facilitate transparency and reproducibility, each of the seven sectors is presented separately in Figs. 3–9, allowing readers to trace how specific physical, operational and institutional processes were represented in the stock–flow architecture. Taken together, these sectors form an integrated system in which water collection, treatment, desalination, salinity dynamics, allocation to the hydrogen hub and electrolysis-driven hydrogen output evolve endogenously through interconnected feedbacks and delays. By decomposing the model into modular components, the formulation phase provides a clear visual and mathematical foundation for the subsequent validation procedures, where the structural assumptions, parameter choices and behavioural properties of the model are examined in detail. This completes the

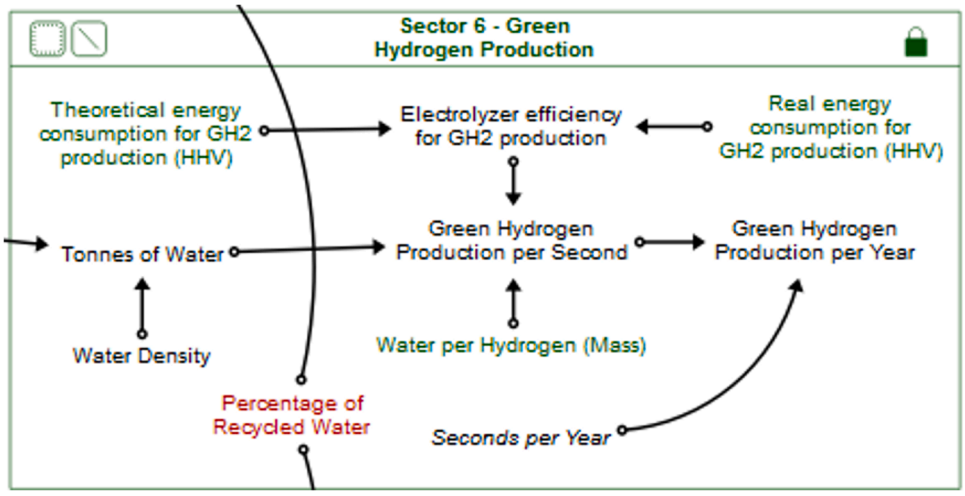

Fig. 8. Green hydrogen production.

construction of the stock–flow representation that underpins all simulations reported in the following sections.

3.4. Validation phase

This section encompasses the collection of tests used to validate the proposed model. The conducted tests were dimensional consistency test, structure confirmation test, parameter confirmation test, and sensitivity test.

3.4.1. Dimensional consistency test

A dimensional consistency check is performed in Stella Architect using the automated unit-verification tool. All stocks, flows, auxiliaries, and parameters in the model were assigned explicit units, allowing the software to evaluate the dimensional coherence of every equation. The model returned no unit warnings, indicating that all mathematical expressions comply with the required dimensional relationships between mass, volume, time, energy, and concentration variables. This outcome confirms that the internal structure of the model is dimensionally consistent [77].

3.4.2. Structure confirmation test

Following Barlas[77] and Forrester and Senge[78], a structure confirmation test was conducted to assess whether the model's causal structure, route distinctions and decision rules are consistent with empirical evidence. Insights were obtained from interviews. The profile of each interviewee was already presented on Table 4, section 3.1 Problem Articulation Phase.

Most of interviewees consistently emphasise that Ceará's water challenge stems from the management of highly variable flows rather than absolute scarcity. Interviewee E2 explains that "for eight months of the year, river flows fall to zero… the only way to have water in the dry season is by building reservoirs," adding that "no country faces water-management challenges like the northeastern semi-arid in Brazil" because supply fluctuates sharply while demand remains relatively steady. Interviewee E6 argues that diversification of water sources is essential to avoid dependence on any single route.

Even under ambitious hydrogen development projects, interviewee E1 notes that 8 GW of electrolysers would require "<1 m^3 s-1″ of demineralised water and he stated that the initial capacity of treated effluent, already available on the region, is sufficient to start the green hydrogen production process. Interviewee E4 reinforces this point by emphasising that the infrastructure required to transport recycled water to the Pecém Green Hydrogen Hub currently exists, with the capacity to transport up to 4.5 m^3/s of water. However, interviewee E11 notes that project developers often underestimate total water requirements by considering only the stoichiometric 9 Liters of water for each Kilogram of green hydrogen ratio rather than the full cooling demand: "what you spend to produce hydrogen, you spend almost four times to cool the hub," implying that four large projects with pre-contract signed to produce green hydrogen at Pecém could reach >3 m^3/s. Interviewee E11 adds that just one major construction licence authorises up to 1.6 m^3/s of seawater desalination plant.

Across interviews, raw surface water and reservoirs are described as unsuitable structural route for green hydrogen. Interviewee E2 states that "it is unlikely that reservoirs will be the water source for green hydrogen" because they are "already heavily committed to human supply, irrigation and industrial uses," and because high hydrological uncertainty makes them unreliable for long-term planning. Most of the time, the hydrological balance in the State of Ceará is negative. Annually, precipitation in Ceará is around 800 mm and evapotranspiration is around 2,000 mm [13].

Interviewee E3 argues that recycled water for green hydrogen production should be treated as a dedicated route to preserve higher-quality raw water for households, while Interviewee E4 remarks that raw water can be considered only as a contingency supply to cover short interruptions in the recycled water pipeline. Interviewee E5 adds that a study conducted in the State of Ceará concluded that raw water "cannot reliably supply the Industrial and Port Complex of Pecém during droughts season." Interviewee E8 is categorical in stating that " using raw water to produce green hydrogen makes no sense… there is nothing to discuss" given competing human and agricultural uses. These convergent assessments justify the model's exclusion of a long-term raw-water-to-hydrogen pathway.

Most of interviewees also converge that recycling urban effluent is the preferred route but is volumetrically and logistically bounded. Interviewee E2 reports that Fortaleza's water supply averages "10 m^3/s" and that approximately "3 m^3/s" of the urban effluent is treated before being discharged into water bodies; diverting this flow to the industrial zone would recover a resource currently "wasted," reducing pressure on the hydrology matrix. Interviewee E3 underscores that urban effluent is "99.9 % water," and its treatment has negligible losses, however, he states that the average losses during the distribution phase in Brazil is 50 %.

Interviewees E4 and E5 describes that the recycled water project consisting of lifting aggregated secondary effluent to a treatment facility and conveying it via the Axes 5 to a recycled-water plant. At the first-stage, the initial treatment effluent capacity is up to 1 m^3/s and at the second-stage, this capacity can be expanded up to 3 m^3/s. Interviewee E11 details that the effluents from eleven lagoon-based plants in Fortaleza, Caucaia and Maracanaú will be centralised for biological, physical and tertiary treatment and subsequently polished at the industrial site. Interviewee E6 stresses that aggregation from multiple wastewater treatment plant is essential for hydrogen-scale volumes, and interviewee E9 illustrates the systemic importance of aggregation by citing Barueri plant, in São Paulo, which treats "16 m^3/s" that could be kept on the system instead of being discharged into the Tietê river.

Interviewees also confirm the causal drivers of infrastructure expansion. Interviewee E1 stresses that investment depends on "firm demand and firm commitment." Interviewee E4 describes a mutually dependent dynamic in which both the recycled water company and hydrogen developers wait for long-term off-take contracts, asking "why would the recycled water company invest if no one will buy the water?" Interviewee E3 adds that relying exclusively on recycled water would require expansion of the effluent collection capacity because "our effluent network is very limited… much of it is open drains."

Interviewees further confirm that final water quality for electrolysis is a plant-level responsibility and does not differentiate bulk routes. Interviewee E4 states that recycled water, and reservoir water arrive at similar bulk quality and that users will perform the necessary polishing, noting that "recycled water may even be better in terms of quality than raw water." Interviewee E6 emphasises that purity levels are technologically achievable for recycled water and seawater desalination. These elements support the model's representation of hydrogen water demand as a near-linear function of output, with route differences arising from feed salinity, energy use and residue generation.

Interviewee E5 recalls that the major recycled water initiative started to be designed during the last long drought season, during from 2012 to 2020, as stated by E2. Interviewee E9 highlights that long-term anchor contracts with fixed flows and prices underpin project finance, closing the financial loop. These institutional and operational characteristics align with the model's treatment of recycled capacity as a concession-based subsystem whose growth and decline follow the time-dependent dynamics of infrastructure delivery and asset ageing. These statements align with the model's representation of recycled water as constrained by effluent collection volumes, aggregation requirements and the hydraulic capacity of regional conveyance infrastructure.

Interviewee E6 points out that aggregating flows from multiple wastewater treatment plants implies "ten pipelines crossing several areas," creating significant logistical complexity. Interviewee E11 emphasises that tariff levels, contractual duration and ramp-up paths (e.g. 0.1 to 0.5 m^3/s over years) are central to viability, adding that

regulatory obligations may be required because "voluntary uptake will remain low" unless industries are compelled by law to replace part of their raw-water consumption with recycled water. She adds that much of Fortaleza's secondary effluent is discharged into rivers under standards that do not require nutrient removal, contributing to eutrophication and health risks. These observations support the model's decision rules in which commissioning flows respond to industrial demand and institutional arrangements, while adjustments occur only after delays.

In the model, recycled water capacity and infrastructure of effluent collection capacity are represented as stocks whose expansion occurs through commissioning flows subject to planning–construction delays, and whose decline follows lifetime-based decommissioning through an ageing chain. Interviewee E3 and E11 describe recycled water provision as a specialised industrial subsystem that reflects these dynamics.

Regarding to seawater desalination, interviewees describe that this source as a higher-OPEX route, yet one that offers greater autonomy to hydrogen producers because its deployment depends almost exclusively on private decision-making. Interviewee E3 notes that recycled water can be "much more attractive than desalination" from a technical and economic standpoint, since effluent contains far fewer salts, a point reinforced by interviewee E6. Interviewee E7 estimates costs of roughly USD 2/m^3 for recycled water and USD 5–6/m^3 for seawater, while interviewee E9 contrasts reverse osmosis pressures of "about 8 bar" for recycled water with "30 bar" for seawater.

Despite this higher-operating costs, interviewee E7 notes that companies will avoid recycled water due to "legal uncertainty," "contractual risk," and exposure to the "Brazil cost," since participating in public infrastructure or Public and Private Partnerships may entail long-term liabilities. By contrast, desalination units can be developed autonomously—"each hydrogen plant would have its own desalination unit," as highlighted by interviewee E6—allowing firms to expand water supply whenever they decide to scale hydrogen output, without depending on effluent collection expansion, effluent aggregation, inter-agency agreements or municipal infrastructure. Interviewee E8 adds that, although desalination requires hydrodynamic studies and careful intake design due to underwater sandbanks, these engineering tasks lie entirely within the developer's scope, unlike the multi-actor coordination required for recycled water. As a result, desalination capacity tends to follow firm-driven investment cycles: when electrolysers need to expand, companies can directly reinvest in additional desalination modules, accelerating capacity growth relative to routes constrained by public infrastructure. This dynamic supports modelling desalination capacity as a stock governed by commissioning delays and an ageing-chain retirement structure, where reinvestment is autonomous, incremental and aligned with private expansion decisions rather than dependent on multi-agency coordination.

These accounts show that, although desalination is more expensive, its institutional simplicity and private-sector autonomy allow capacity to expand based on firm-level decisions rather than inter-agency negotiation. This justifies representing desalination capacity in the model as a stock governed by commissioning delays and lifetime-based ageing-chain decommissioning: expansion occurs when firms individually decide to invest, but capacity still becomes available only after multi-year permitting and construction, making supply constraints emerge through delayed expansion rather than instantaneous adjustment.

Interviewees also corroborate the model's environmental feedbacks associated with residual streams and near-field salinity. Interviewee E2 describes desalination as "not without controversy solution," citing uncertainty about brine impacts. Interviewee E5 recalls that the Fortaleza seawater desalination project required extensive marine studies and one-year monitoring of marine ecosystem. Interviewee E6 stresses that both recycled and desalination generate residuals that can only be concentrated, not eliminated, and that seawater brine must be released through engineered diffusers. Interviewee E8 provides ecological mechanisms by which dense saline plumes can settle over benthic habitats, potentially altering community composition even when far-field salinity later recovers.

Broader long-term dynamics described by interviewees are consistent with the model's feedback structure. Interviewee E9 expects green hydrogen to expand similarly to wind and solar, arguing that viable recycled water projects depend on sanitation universalisation and long-term anchor contracts. Interviewee E11 sees hydrogen as the "main utility" for recycled water but notes that industries have not yet committed substantial volumes due to cost, risk perception and the lack of regulatory obligations. She also emphasises that Ceará is structurally advantaged because the Axes 5 directly links sewage-generating regions to the industrial zone, a configuration that "does not exist elsewhere." In the model, recycled water capacity therefore evolves through commissioning delays and lifetime-based decommissioning, reflecting realistic infrastructure turnover.

In sum, the interviews collectively confirm that hydrogen's water demand can be constrained by infrastructure, governance and business models; that reservoirs are unsuitable as a long-term structural route; that recycle water is bounded by effluent availability, aggregation requirements and conveyance capacity; that seawater desalination is easier for companies; and that infrastructure expansion depends on firm demand, long-term contracts and coordination among agencies. Interviewees also validate the model's structural choices thereby satisfying the criteria for a structure confirmation test in the sense of Barlas [77] and Forrester and Senge [78].

3.4.3. *Parameter confirmation test*

Following Barlas [77] and Forrester and Senge [78], a parameter confirmation test was used as a direct structure test to assess whether constant parameters and initial values are conceptually meaningful and numerically plausible. For this model, all parameters were systematically checked against the sources cited on the supplementary material A, and their values were fixed accordingly. The complete list of equations, parameters, and documentation is available on the supplementary material A.

Regarding to the sector 1, the initial installed recycled-water capacity is contained in the stock Recycled Water Installed Capacity(t). The baseline capacities were derived from the EIA for the Pecém Green Hydrogen Hub [71], which estimates an annual demand of 6.5 million m^3 of seawater and 650,000 m^3 of recycled water, with reuse representing up to 10 % of total water use. These values were converted to flow units, yielding initial capacities of 0.206 $m^3\ s^{-1}$ for seawater desalination and 0.026 $m^3\ s^{-1}$ for recycled water.

The construction and commissioning delay for recycled water capacity, Time to Increase Recycled Water Installed Capacity, is fixed at 4 years. This is based on Apex Water[79], Brown & Caldwell and Carollo [80], and Lakeside Equipment Corporation[81], who describes planning and construction of permanent land-based recycled water plants within 1.5–8 years. The electricity consumption on this sector, Recycled Water Energy per Water Cubic Meters, is set to 0.000594 MWh per m^3, the value reported Kehrein et al. [82]., and based on interview E6, which stresses that the much lower salinity of wastewater relative to seawater translates into lower pressure and energy requirements. The recovery parameter Recycled Water Recovery Rate is fixed at 0.99 (dimensionless). This choice is backed by Khangaonkar et al. [73]., Sperling[83], Yang et al. [84]., and interviewer E3, all of which state that domestic wastewater typically contains about 98–99.9 % water by weight, with only 0.1–2 % solids; adopting 0.99 is therefore consistent with the order of magnitude indicated for municipal effluent.

Losses in the water distribution system between Infrastructure of Effluent Collection Capacity(t) and the Recycled Water Installed Capacity(t) are represented by Water Losses During Distribution in Northeast Brazil and set to 0.463. The is based on the annual report from the Brazilian National System of Information about Basic Sanitation [85], which affirms that 46.3 % of water is wasted during the distribution phase in the North-East of Brazil, region where the State of Ceará is located. The national values often around 40 % and sometimes above 60

%. The losses are confirmed also by interview E3, which also emphasised that the losses in wastewater treatment are negligible compared to those in drinking-water networks.

Membrane replacement in the recycled-water RO (reverse osmosis) units is governed by Years for Reverse Osmosis Recycled Water Decommissioning, fixed at 3 years. The documentation combines two sources. Yokogawa[86] reports a typical RO membrane life expectancy of roughly three years and Muñoz et al. [87]. report annual replacement rates up to 33 % in tertiary wastewater treatment. Setting a decommissioning time of three years is therefore consistent the reported for RO membranes in tertiary wastewater applications.

The parameter fraction of treated water available for recycled water plant is set to 0.085, corresponding to the midpoint of the 5–12 % reuse range reported for Greece, Italy and Spain [88]. This anchors the model in current European practice, while remaining well below the higher reuse levels observed in Cyprus (above 90 %) and Malta (around 60 %) [88].

Regarding to sector 2, Green Hydrogen Hub - Water Supply, to define a single parameter representing how total water availability is divided between hydrogen production and the cooling system, we drew on the estimates developed by Arup [24] for large-scale green hydrogen deployment in dry regions of Australia, as these conditions closely resemble those of Ceará, Brazil, as confirmed in interview E2. Arup [24] provides detailed values for both process water and total water requirements with evaporative cooling under dry-zone conditions for PEM electrolysers at the beginning and end of life, and for both recycled water and seawater feedstocks. For each dry-zone scenario, we calculated the ratio between process water and total water demand. These ratios ranged across the different combinations of asset condition (beginning/end of life) and asset performance (high/low end).

To obtain a single, representative value suitable for model implementation, we computed the arithmetic mean of all ratios for dry-zone scenarios using recycled water and seawater, resulting in an average fraction of 0.26, meaning that roughly 26 % of total water use is associated with hydrogen production and 74 % with the evaporative cooling system. This value are even more optimistic than the values assumed by Fortescue[11]. In the EIA, the company states that 9216 tonnes of water per day will being use for green hydrogen production and 41,624 tonnes of water per day for cooling system, being 0.18 the ratio between water for green hydrogen and water for cooling.

The sector 3, which encompasses variables related to green hydrogen production, assume the values of electrolyser energy performance are represented by Theoretical energy consumption for GH2 production (HHV) and Real energy consumption for GH2 production (HHV). The theoretical parameter is set to 39.4 kWh kg^{-1} H_2, following Jang et al. [89]. The real parameter is fixed at 50 kWh kg^{-1} H_2, based on Samsatli et al. [90]. The documentation explicitly interprets this as representative of current PEM technology under practical conditions, and the 39.4/50 ratio is consistent with efficiency gaps highlighted in the electrolysis literature. The water requirement per unit of hydrogen is represented by Water per Hydrogen (Mass), set to 10 tonnes of water per tonne of hydrogen. We use the value assumed by Simões et al. [21]. and Fortescue[11], who report that electrolysers require 10 litres of water per kilogram of hydrogen.

On Sector 4, the stock Seawater Desalination Installed Capacity(t) shares the same documentation as the recycled-water capacity stock. As noted above, the initial capacity of 0.206 m^3 s^{-1} is drawn directly from the annual seawater consumption of 6.5 million m^3 reported by the Complexo do Pecém[71]. Membrane lifetime in seawater RO units is represented by Years for Reverse Osmosis Seawater Decommissioning, set to 3 years. The documentation combines Yokogawa[86], Somrani et al. [91]. and Muñoz et al. [87]., which together indicate membrane lifetimes in the range of 3–5 years and annual replacement rates of 10–33 % depending on feedwater and application. Adopting a three-year decommissioning time is therefore consistent with both the average lifespan and higher replacement rates reported for seawater applications.

The construction and commissioning delay for desalination capacity, Time to implant seawater desalination, is fixed at 3 years. The documentation references Voutchkov et al. [92]., who describe planning and construction of permanent land-based desalination plants within 2–3 years, as well as Piedra et al. [93]. and Acciona[94], which report engineering, procurement and construction periods on the order of two years for large SWRO expansions. Taken together, these sources justify modelling a three-year implementation time as a central estimate for large coastal RO plants.

Regarding to specific electricity consumption of seawater desalination, Seawater Desalination Energy per Water Cubic Meters, to 0.004 MWh per m^3 (4 kWh m^{-3}). This values are based on Xevgenos et al. [95], which report a typical range of 2–5 kWh m^{-3} for reverse-osmosis desalination depending on feed-water salinity, while Silva et al. [96]. find a consumption of approximately 4 kWh m^{-3} for Brazilian RO seawater desalination plants. Interview E6 further confirms that high salinity drives high osmotic pressure and energy demand. The chosen value of 4 kWh m^{-3} thus lies squarely within empirically observed ranges for modern SWRO plants.

The initial recovery ratio of seawater RO, Seawater Initial Recovery Rate, is set to 0.45. Panagopoulos et al. [42]. describe recovery as the ratio between freshwater produced and total feedwater, and Kim and Hong[97] report that real SWRO facilities typically operate between 40 % and 50 % recovery. We therefore adopt 45 % as a representative upper-middle value in this empirical range. This value is consistent with Fortescue[11], which states that the daily estimated flow of tonnes of water for green hydrogen production is 9216 and for cooling the system is 41,624, while 55,318 is brine water, representing 52 % of the water daily captured.

The effective recovery used in the model, Seawater Recovery Rate, is computed as Expected decreasement in Recovery Rate efficiency and Seawater Initial Recovery Rate. Missimer and Maliva[15] show that increases in local seawater salinity reduce plant recovery and raise production costs. In the model, this relationship is implemented through the graphical function Expected Decreasement In Recovery Rate Efficiency, which monotonically decreases recovery as near-field salinity rises, while keeping recovery within the physically plausible band implied by the 40–50 % range.

On Sector 5, Salinity near-field parameters, the Near Field Dilution, defined as the dilution of brine immediately after discharge for Fortaleza, is set to 31.8 (dimensionless). According to the documentation, this value is taken from hydrodynamic simulations by Pereira et al. [76]., who model diffuser performance for the seawater desalination plant of Fortaleza, aimed to supply the south region of the capital with potable water. Fortaleza is the capital of Ceará and is located next to the cities where the green hydrogen hub will be installed, São Gonçalo do Amarante and Caucaia. The model therefore adopts this value as the volumetric dilution in the first tens of metres downstream of the outfall. The salinity of the brine stream, Salinity of Brine Water, is fixed at 67.33 kg m^{-3}, and the background salinity stock, Salinity Near Field(t), is initialised at 36.03 kg m^{-3}, again based on Pereira et al. [76]..

Longer-term dispersion of salt away from the near field is captured by the parameter Salt Spreading, set to 0.94 kg m^{-3} $year^{-1}$. The documentation notes that basin-scale salinity effects of desalination are small: Paparella et al. [74]. estimate changes below 0.5–1.0 psu, and Ibrahim et al. [75]. find that current brine discharge does not destabilise regional salinity equilibria. Interview E8 further indicates that strong coastal currents in Ceará promote rapid dispersion, although local ecological impacts may still occur. Given this evidence and the simplified purpose of the model, the chosen coefficient is framed as a conservative annualised leakage term which, when combined with the near-field dilution, reproduces salinity ranges consistent with Pereira et al. [76]..

On sector 6, Effluent-collection infrastructure, for the effluent network, the structural lifetime parameter Life span of Effluent

Collection Infrastructure is set to 62.5 years. We draw on Younis and Knight[98], who show that many Canadian buried water and wastewater pipes have design lives between 50 and 75 years. The adopted value is simply the mid-point of this range and reflects the long-lived nature of buried sewer infrastructure.

The implementation delay for new collection infrastructure, Time to implant effluent collection, is fixed at 4 years. The documentation assembles several sources: the Apex Water[79] design report for the Delmore Wastewater Treatment Plant, which estimates around 18 months for design and construction phases; Brown and Caldwell & Carollo[80], who show that complex wastewater projects requiring detailed environmental review can take "almost four years"; and guidance from Lakeside Equipment[81], which note that pre-construction stages can take up to three years and that total construction durations can extend to five years for large plants. Placing the model parameter at four years therefore lies within the reported 2–5-year window and is particularly consistent with the upper bound identified for complex projects. The Table 5 shown the list of parameters and initial values from the Stock and Flow Diagram.

Taken together, the sources reviewed above establish that all constant parameters and initial conditions used in the model fall within empirically documented or technically justified ranges. Table 5 consolidates these values and their respective units, providing a transparent reference for all variables used in the stock–flow formulation. With the parameters validated, the next step is to examine the robustness of model behaviour through a structured sensitivity analysis.

3.4.4. Sensitivity test

A behaviour sensitivity test was conducted to assess the robustness of the model under uncertainty in the most influential parameters. Following Barlas[77], the objective was to evaluate whether the qualitative behaviour of the system remains stable when key parameters are varied within wide, yet still conceptually defensible, ranges. Seven parameters were selected based on their structural role in the model: the fraction of treated water available for recycled water plant (FT), water losses along the distribution system (WL), the implementation delay for recycled-water capacity (TR), the fraction of total water demand allocated to cooling (FC), the implementation delay for effluent-collection infrastructure (TI), the recovery rate of seawater reverse osmosis (SI), the implementation delay for seawater desalination capacity (TS), and the Percentage of recycled water into the system (P). These parameters influence the main stocks and feedback loops associated with water supply, infrastructure expansion and hydrogen production, and are therefore suitable candidates for behavioural sensitivity testing. To account for uncertainty and operational variability, each parameter was varied within a broad but technically coherent interval. Table 6 shows the parameters and sensitivity ranges.

A Sobol low-discrepancy sequence was used to generate one hundred simulations across the multidimensional parameter space as indicated in Borges et al. [99].. The outputs were examined to determine the extent

Table 5
Parameter and initial values of the stock and flow diagram.

Parameter name (full)	Abbreviation	Unit	Value	Short reference
Initial Recycled Water Installed Capacity	CR_0	m^3/s	0; 0.0206; 0.206 (scenario-dependent)	Complexo do Pecém 2023
Initial Seawater Desalination Installed Capacity	CS_0	m^3/s	0; 0.206 (scenario-dependent)	Complexo do Pecém 2023
Initial Infrastructure of Effluent Collection Capacity	EC_0	m^3/s	1	Interviews E1, E2, E5, and Secretaria dos Recursos Hídricos (2018)
Time to Increase Recycled Water Installed Capacity	TR	years	4	Apex Water 2025; Brown & Caldwell 2011
Time to Implement Effluent Collection	TI	years	4	Apex Water 2025; Brown & Caldwell 2011
Time to Implement Seawater Desalination	TS	years	3	Voutchkov et al. 2017
Years for Reverse Osmosis Recycled Water Decommissioning	YD	years	3	Yokogawa 2015; Muñoz et al. 2014
Years for Reverse Osmosis Seawater Decommissioning	YS	years	3	Yokogawa 2015; Somrani et al. 2025
Recycled Water Energy per Water Cubic Metre	EW	MWh/m^3	0.000594	Kehrein et al. 2021
Water Losses During Distribution in Northeast Brazil	WL	dimensionless	0.463	SNIS 2024
Recycled Water Recovery Rate	RR	dimensionless	0.99	EPA 2004; Yang et al. 2020
Solid Effluent in Water	SE	Effluent Cubic Meter/Water Cubic Meters	1	Standard assumption for unit conversion
Fraction of Treated Water Available for Recycled Water Plant	FT	dimensionless	0.085	Malinauskaite et al. 2024
Fix Year Unit	FY	1/year	1	Model definition
Life Span of Effluent Collection Infrastructure	LS	years	62.5	Younis & Knight 2010
Near-Field Dilution	ND	dimensionless	31.8	Pereira et al. 2024
Brine Salinity	SB	kg/m^3	67.33	Pereira et al. 2024
Initial Near-Field Salinity	SN_0	kg/m^3	36.03	Pereira et al. 2024
Salt Spreading	SS	kg/m^3/year	0.94	Assumption based on Paparella (2022) and Ibrahim (2020)
Seawater Desalination Energy per Water Cubic Metre	SD	MWh/m^3	0.004	Xevgenos et al. 2014; Silva et al. 2018
Seawater Initial Recovery Rate	SI	dimensionless	0.45	Panagopoulos et al. 2019
Seconds per Year	SY	Seconds/Year	31,536,000	Constant
Fraction of Water for Cooling	FC	dimensionless	0.74	Arup 2022
Fraction of Water for GH_2 Production	FP	dimensionless	0.26	Arup 2022
Theoretical Energy Consumption for GH_2 (HHV)	TE	kWh/kg H_2	39.4	Jang et al. 2022
Real Energy Consumption for GH_2 (HHV)	RE	kWh/kg H_2	50	Samsatli et al. 2016
Water per Hydrogen	WM	tonnes water / tonne H_2	10	Simões et al. 2021; Fortescue 2023
Water Density	ρ^W	$tonnes/m^3$	0.998	Physical constant
Percentage of Recycled Water	P	dimensionless	Scenario variable	Scenario design

Table 6
Parameters included in the sensitivity analysis and tested ranges.

Parameter name	Abbreviation	Baseline value	Sensitivity range	Justification
Fraction of Treated Water Available for Recycled Water Plant	FT	0.085	0 – 1	Represents operational uncertainty in the proportion of secondary effluent that can be routed to tertiary treatment.
Water losses during distribution	WL	0.463	0 – 1	Captures the entire possible spectrum from no losses to full loss.
Time to expand recycled-water capacity (years)	TR	4	2 – 8	Reflects feasible variation in project delivery times for recycled-water infrastructure.
Fraction of total water allocated to cooling	FC	0.74	0.3 – 0.8	Encompasses differences in cooling-system configurations in hydrogen projects.
Time to expand effluent-collection infrastructure (years)	TI	4	2 – 8	Represents variability observed in sanitation-network expansion timelines.
Seawater recovery rate	SI	0.45	0.40 – 0.60	Reflects the documented operational range of seawater RO systems.
Time to expand seawater desalination capacity (years)	TS	3	2 – 4	Reflects feasible variation in project delivery times for private initiative.
Percentage of Recycled Water	P	0.1	0.0 – 1.0	Reflects different compositions of Recycled Water into the system.

to which parameter uncertainty affects long-term trajectories of hydrogen production, water supply composition and infrastructure expansion. The results, presented in Section 4.1, demonstrate that although variations in these parameters affect the magnitude of outcomes, the qualitative behaviour of the model remains stable across all runs.

3.5. Scenarios development phase

Four scenarios were proposed based on the percentage participation of recycled water in the system, represented by the variable P. The first scenario (S1) took into consideration the EIA of the green hydrogen hub at Industrial and Port Complex of Pecém [71], which proposes that the P participation on green hydrogen production will be 10 %. In this scenario, the CS_0 starts at 0.206 m^3 per second, and the CR_0 starts at 0.0206 m^3 per second. The second scenario (S2) considered that the P variable will be of 0 %, meaning that only seawater desalination will be utilised. This scenario is based on the EIA for the green hydrogen plant of Fortescue Future Industries [11] and interviews E5, E7, E8, E9, and E11. In this scenario, the CS_0 starts at 0.206 m^3 per second, and the CR_0 is 0 m^3 per second.

The third scenario (S3) proposed that variable P would start at 10 %, the same baseline value adopted in scenario S1, and gradually increase until it reached 50 % of the water in the system by the end of the simulation, in the year 2050. This scenario is based on the Strategic Action Plan for Water Resources of Ceará [14], CAGECE's strategic management and business plan (2023–2027) [69], and interviews E1, E3, E4, E7, E9, and E11. In this scenario, the CS_0 starts at 0.206 m^3 per second, and the CR_0 starts at 0.0206 m^3 per second. This scenario is marked by the competition between linear economy and circular economy approaches. In addition, the variable Fraction of Treated Water Available for Recycled Water Plants assumed to increase from 0.085 in 2026 to 0.58 by 2050. This projection is inspired by the case of Kuwait, where 58 % of the effluent becomes available for reuse [100].

Although the Metropolitan Region of Fortaleza has a different climate from Kuwait, the broader state of Ceará shares important similarities: around 90 % of its territory lies within Brazil's semi-arid region, and, according to interviewee E2, most of the water consumed in the Metropolitan Region of Fortaleza is sourced from these semi-arid zones. Furthermore, the population of Metropolitan Region of Fortaleza —3903,946 in 2022 [101] — is comparable to Kuwait's population of 4973,861 in 2024 [102], reinforcing the demographic relevance of this international reference. Taken together, these climatic and demographic parallels support the technical plausibility of reaching a reuse fraction of 0.58 by 2050 in the context of Ceará.

The fourth and final scenario (S4) assumes that 100 % of the water used in the green hydrogen hub will come from recycled sources, i.e., $P = 1.0$. In this case, the water supply will rely entirely on treated wastewater, with CR_0 starting at 0.206 m^3/s and no contribution from seawater desalination. This scenario is grounded in recommendations from interviewees E1, E3, E4, E7, and E11.

Also, this scenario assumes that all the sewage collected will be treated and made available to the recycled water company. This assumption is grounded in the case of Orange County, a region in California (USA), where the Water and Sanitation Districts have successfully implemented an advanced water reuse program. Since 2023, they have been able to purify and recycle 100 % of the reclaimable wastewater [103]. This example was chosen not only because Orange County had a population similar to that of the Metropolitan Region of Fortaleza in 2022—3,151,184 and 3,903,946 inhabitants, respectively [101,104] —but also because California shares important environmental similarities with Brazil's semi-arid Northeast, such as water scarcity, seasonal droughts, and high evapotranspiration rates [13]. These commonalities strengthen the relevance and applicability of this precedent to the scenario being proposed.

This scenario also accounts for a slightly better water distribution system. We assume that the losses in Northeast Brazil will be 34.1 %, the same level of losses in the Centre-West region of Brazil, and the lowest level among all the Brazilian regions [85]. Thus, the parameter Water losses during distribution in Northeast Brazil for this scenario will be 34.1 %. Besides, based on the available literature and insights from interviews E3, E5, E6, E9, and E11, we assume that the technological processes for wastewater treatment and recycled water production will efficiently remove pollutants and ensure high water quality [105,106].

4. Results

This section presents the outcomes of the modelling process in three parts. Subsection 4.1 reports the validation results, summarising the tests that confirm the model's dimensional coherence, structural soundness, parameter plausibility and behavioural robustness. Subsection 4.2 then examines the simulated behaviour of the system under the four water-supply scenarios, describing how hydrogen output, water flows, energy use and waste generation evolve over time. Subsection 4.3 provides an integrated comparison of these scenarios, highlighting their broader technological, environmental and infrastructural implications within linear and circular water-use frameworks.

4.1. Validation results

The validation phase combined structural and behavioural tests to examine whether the model is internally coherent, empirically grounded and robust to uncertainty in key parameters. The set of tests performed follows the standard procedure proposed by Barlas [77] and Forrester and Senge [78], covering dimensional consistency, structure confirmation, parameter confirmation and behaviour sensitivity. The dimensional consistency test confirmed the correctness of all unit assignments. Stella Architect's automated unit-checking returned no warnings,

indicating that all equations respect dimensional balance across stocks, flows, auxiliary variables and parameters.

The structure confirmation test compared the model's causal routes and decision rules with the evidence obtained from the interviews. This qualitative validation examined whether the direction and logic of the model's feedback loops match the operational realities described by practitioners. Statements from interviewees consistently highlighted (i) the bounded nature of recycled water supply due to effluent availability and aggregation constraints, (ii) the autonomy and modularity of seawater desalination as a private investment route, (iii) the long construction delays of wastewater infrastructure, and (iv) the predominance of cooling demand relative to electrolytic water use. These observations directly correspond to the model's structural decisions, such as the use of commissioning delays in all infrastructure stocks, the ageing-chain structure for decommissioning, the functional link between effluent collection and recycled water capacity, and the representation of desalination as firm-driven.

The parameter confirmation test examined whether all numerical values assigned to constant parameters and initial conditions were supported by literature and interview-based evidence. Each parameter was cross-checked against empirical estimates, engineering reports or hydrological studies. Overall, all parameter values fall within empirically observed ranges, satisfying the conditions for parameter confirmation.

Across all variables included in the sensitivity experiment, the ensemble of one hundred Sobol-generated simulations displays behaviour that is qualitatively robust and consistent with the reference run. The 50 %, 75 %, 95 % and 100 % envelopes expand gradually from 2026 onwards, with the most substantial dispersion occurring during the build-out phase between 2030 and 2045. This pattern is expected for infrastructure-dependent systems, in which implementation delays and recovery efficiencies determine the pace at which water supply expands to support hydrogen production. By 2050, the mean trajectories for all variables remain in the 50 % probability band, indicating that the model behaves smoothly across the tested parameter space and does not exhibit structural instabilities.

Green hydrogen production shows a widening of uncertainty during the expansion period, consistent with the sensitivity ranges applied to parameters that directly affect water availability and the timing of capacity additions. All simulations follow the same qualitative pattern: production rises rapidly between 2026 and the mid-2030s and then moves into a gentler stabilisation phase. In 2050, the 100 % envelope spans 1.11 thousand to 2.14 million tonnes per year, and the central trajectories remain close to the mean of approximately 599 thousand tonnes. The shape of the upper envelopes resembles the curves of recycled-water supply because, in the simulations where production reaches higher levels, the recycled-water route scales more rapidly, supplying a larger share of total water.

The effluent-collection capacity exhibits a smooth and monotonic increase across all sensitivity ranges. Because this stock is influenced only by the parameters FT, WL and TI, and not by multiplicative dependencies, its envelopes are relatively narrow and maintain similar shapes across percentiles. All trajectories converge gradually toward 3 m^3/s, with 2050 values ranging from 2.27 to 3.0 m^3/s. The curves show early divergence followed by steady convergence as the expansion delay becomes less influential over time.

Recycled-water installed capacity shows wider dispersion and a characteristic convex shape in the outer envelopes. This arises because

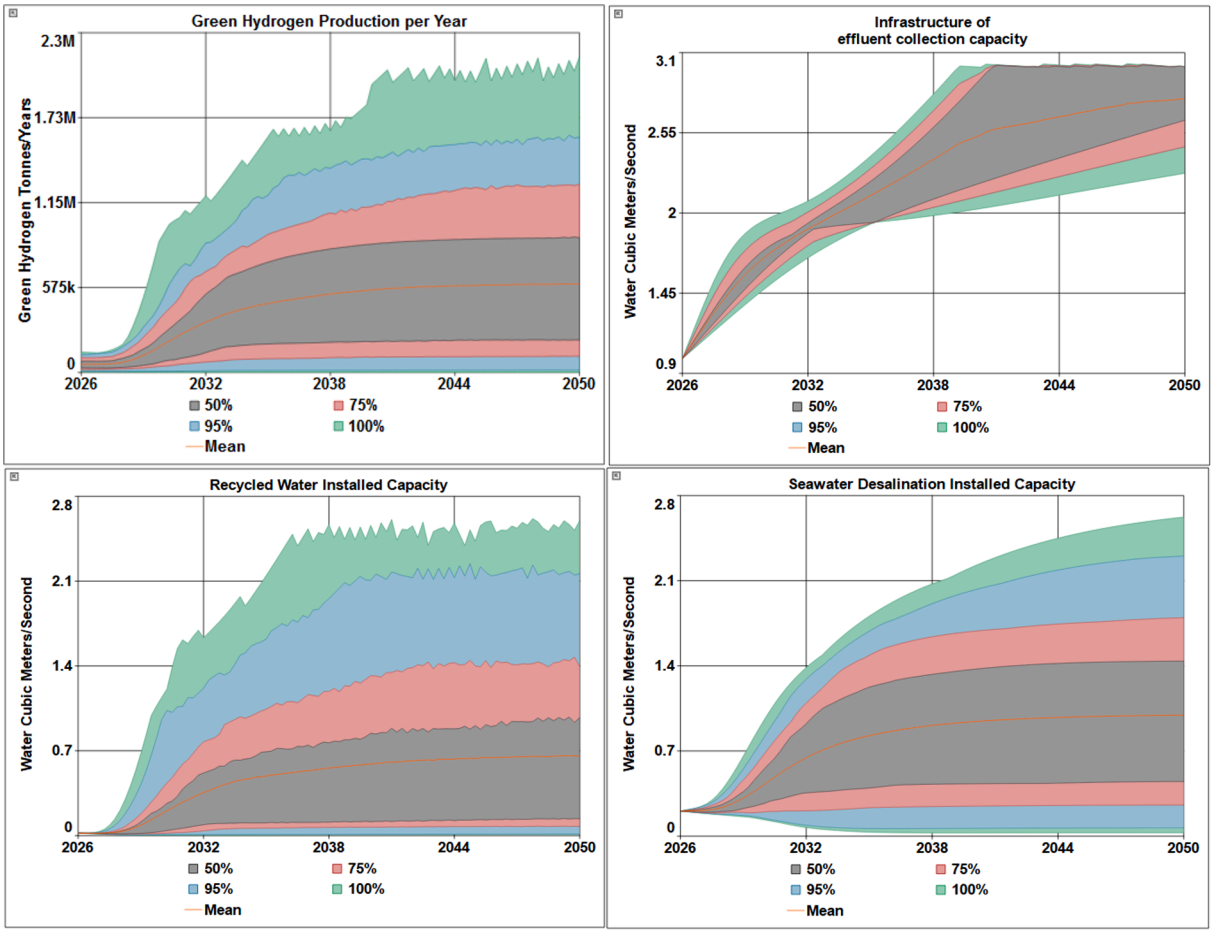

Fig. 10. Green hydrogen and installed capacities sensitivity test results.

the stock depends simultaneously on effluent availability (FT, WL), its own implementation delay (TR), and upstream collection capacity. Variations in these parameters alter the timing at which recycled-water expansion becomes active. As a result, the upper percentiles increase more quickly and exhibit a temporary "hump" before levelling off. By 2050, the 50 % band lies between 0.139 and 0.975 m^3/s, and the 100 % envelope ranges from 0.0087 to 2.6 m^3/s. The similarity between the upper recycled-water curves and the upper hydrogen-production curves reflects the direct dependence of hydrogen production on available water.

The seawater-desalination installed capacity displays a smoother, more symmetric profile across all sensitivity bands. Because this stock depends on a single delay parameter (TS) and is not constrained by upstream availability, the envelopes rise steadily and stabilise without the convexity seen in the recycled-water case. In 2050, desalination capacity ranges from 0.0274 to 2.62 m^3/s in the 100 % envelope, with the 50 % band spanning 0.449 to 1.44 m^3/s. The consistent S-shaped form across percentiles reflects the model structure, where desalination responds directly to hydrogen-production requirements and changes only in pace, not in sequence, under parameter variation. Fig. 10 shown the results from the variables depicted above.

The supply-side variables, total water for the hydrogen hub, recycled water, seawater supply and brine discharge, exhibit distinct behavioural patterns that arise from the structure of the model's capacity-expansion mechanisms. In all cases, the envelopes widen sharply during the early expansion period, when infrastructure constraints and parameter uncertainty interact most strongly, and then gradually narrow or stabilise as the system approaches its long-term operating regime.

Total water demand grows rapidly in the first decade, producing a steep and smooth rise across all percentile envelopes. This shape reflects the fact that demand scales directly with hydrogen production, a driver largely unaffected by upstream uncertainties. As desalination and recycled-water capacities approach their effective operating levels, the envelopes flatten and stabilise. By 2050, the 50 % interval spans 6.59 to 19.4 million m^3/year, while the 100 % band extends from 636 thousand to 22.5 million m^3/year, but the important feature is the convergence in curvature: the system transitions from a regime dominated by infrastructure build-out to one governed by steady-state delivery rates.

Recycled-water trajectories show a markedly different shape: all envelopes exhibit an early convex "hump" as the simultaneous expansion of effluent-collection and tertiary-treatment capacity introduces compounding delays. During this period, the sensitivity ranges widen abruptly because small changes in parameter values, particularly FT, WL, TR and TI, alter how quickly upstream constraints relax. The irregularity and amplitude of the envelopes between roughly 2032 and 2042 arise from this multi-layer dependency: the recycled-water route is only fully operational once two separate capacity stocks and a high-loss conveyance pathway have aligned. As a result, the outer envelopes tend to diverge before gradually reconverging once installation and retirement cycles dominate the dynamics. In 2050, recycled-water supply ranges from 292 thousand to 9.38 million m^3/year in the 50 % band and 234 thousand to 15.3 million m^3/year in the 100 % band, but the defining feature remains the nonlinear rise-and-flatten behaviour driven by sequential bottlenecks.

Seawater supply exhibits a far smoother and more monotonic pattern. Because desalination depends on a single dominant capacity stock, and because seawater availability is effectively unconstrained, the trajectories form clean S-shaped curves, with early acceleration followed

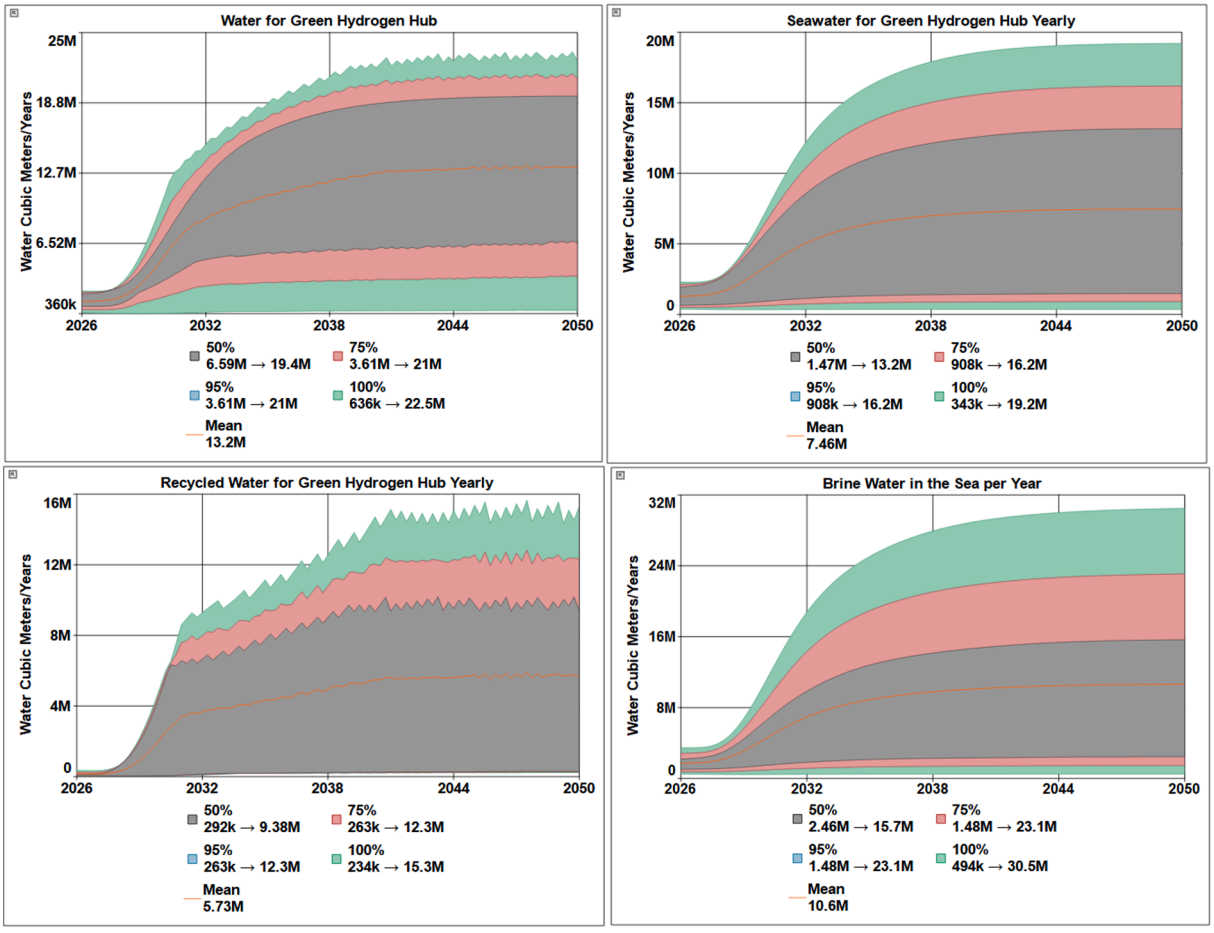

Fig. 11. Supply-side variables sensitivity test results.

by gradual stabilisation. Parameter uncertainty generates variation in slope rather than in curvature: envelopes shift upward or downward but maintain similar shapes. By 2050, seawater supply falls within 1.47 to 13.2 million m^3/year in the 50 % interval and 343 thousand to 19.2 million m^3/year in the 100 % interval. The behavioural signature here is the symmetry and stability of the bands relative to the recycled-water case.

Brine discharge inherits the shape of the seawater trajectory almost exactly, producing broad but smooth envelopes that expand as desalination capacity grows and stabilise once the system reaches its long-term throughput. In 2050, brine flows fall within 2.46 to 15.7 million m^3/year in the 50 % band and from 494 thousand to 30.5 million m^3/year in the 100 % band. The defining characteristic of these curves is the proportionality between freshwater output and concentrate generation, which preserves the stability and symmetry seen in the seawater trajectories. Fig. 11 exhibit the supply-side variables resulting from the sensitivity test.

Taken together, these results reveal a structural asymmetry: the recycled-water route produces wider, more irregular envelopes because it is contingent on the joint evolution of multiple upstream capacities and conveyance losses, whereas the seawater route generates smoother and more predictable behaviour because its performance depends primarily on a single capacity stock. This asymmetry explains the contrast between the hump-shaped recycled-water envelopes and the S-shaped seawater envelopes, and why the latter stabilise earlier and with less dispersion.

4.2. Results from scenarios simulations

This section compares the variables behaviour in four different scenarios over 2026 to 2050 comparing the utilisation of water sources under circular and linear economy frameworks, represented by the recycled water and seawater desalination, respectively. The yearly green hydrogen production differs markedly across the four scenarios, while the trajectories reflect the way each water-supply configuration constrains or enables the hub. In Scenario S1 ($P = 10$ %), green hydrogen production increases from 52.5 thousand tonnes in 2026 to approximately 397 thousand tonnes in 2050. The curve exhibits a rapid rise during the first decade followed by a long stabilisation phase, with production remaining close to a plateau after the mid-2030s. This pattern reflects the modelled interaction between the fixed recycled-water share and the evolution of desalination capacity, which together determine the water availability feeding hydrogen production in this scenario.

Scenario S2 ($P = 0$ %) shows a smooth, monotonic trajectory, rising from 57.5 thousand tonnes to approximately 509 thousand tonnes by 2050. Because this scenario relies exclusively on seawater desalination, its curve maintains a consistent S-shaped form, with early acceleration and gradual convergence toward a stable level. The absence of oscillations in this case reflects the steady nature of the desalination-capacity pathway as represented in the model.

Scenario S3, in which the recycled-water share increases over the simulation horizon, grows from 52.5 thousand tonnes to approximately 252 thousand tonnes in 2050. Its curve rises rapidly in the early years and then becomes flatter, with mild oscillations around the mid- and late-period values. These features correspond to the timing effects

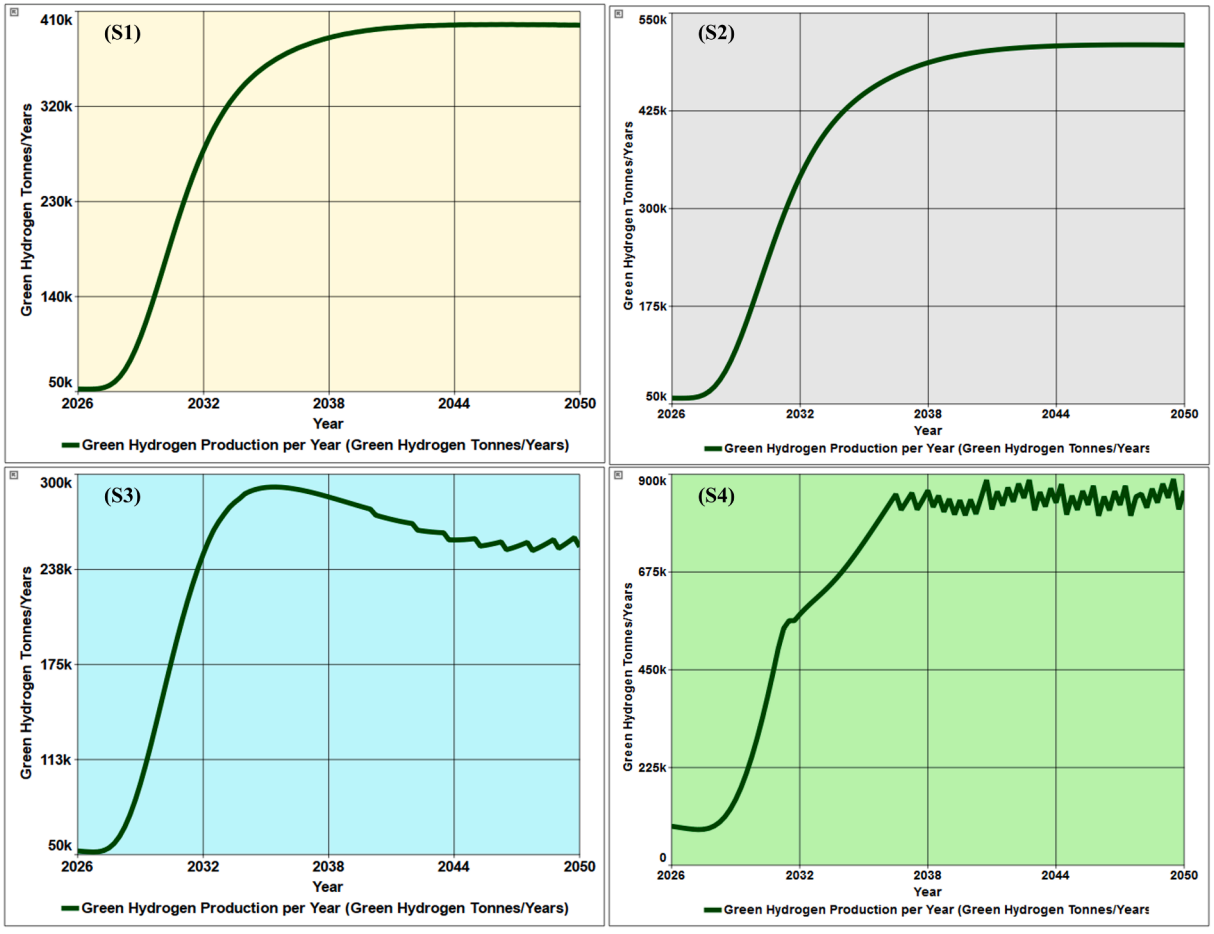

Fig. 12. Green hydrogen production yearly of the four scenarios.

generated by the water-supply components in this scenario, where both desalination and recycled-water supply contribute to hydrogen production with different temporal profiles. The resulting trajectory shows a slower approach to its long-run level compared with S1 and S2.

Scenario S4 ($P = 100$ %) presents the most distinct shape among the four trajectories. Production rises from 89.7 thousand tonnes in 2026 to approximately 862 thousand tonnes in 2050, and the curve displays two visible growth phases: a first acceleration around 2030 and a second, more pronounced increase from roughly 2032 to 2036. After these two periods of expansion, production fluctuates slightly around a high plateau. Because this scenario relies fully on recycled water, the trajectory reflects the timing and interaction of the variables governing water availability in the model, producing the multi-phase growth pattern seen in the simulation results. Fig. 12 shows how the green hydrogen production varies across the scenarios.

The evolution of installed capacities for effluent collection, seawater desalination and recycled water reflects how each scenario structures the water-supply backbone of the hub. In Scenario S1, the infrastructure of effluent collection capacity increases from 1.00 to 1.98 m^3/s, displaying a steep rise during the early 2030s and stabilising close to its upper bound thereafter. Seawater desalination installed capacity grows from 0.206 to 1.61 m^3/s, following a smooth S-shaped trajectory with rapid early expansion and slower gains toward the end of the period. Recycled water installed capacity remains small, increasing only from 0.0206 to 0.0837 m^3/s, and its curve stays nearly flat after the mid-2030s. The resulting configuration shows a system in which desalination becomes progressively more dominant, while recycled water remains a marginal supply route. The effluent-collection network grows substantially despite the low reliance on recycled water, suggesting that, in this scenario, its evolution is driven by the model's structural dynamics rather than by recycled-water uptake.

Scenario S2 relies entirely on seawater desalination, and this is clearly reflected in the behaviour of the installed capacities. Seawater desalination capacity increases from 0.206 to 1.88 m^3/s, exhibiting a smooth and continuous rise similar to S1 but reaching higher long-run values. Recycled water installed capacity remains at zero throughout the simulation. In contrast, effluent-collection capacity declines from 1.00 to 0.62 m^3/s, following a gently downward trajectory. The divergence between the two capacities, growth in desalination and contraction in effluent collection, illustrates the structural shift that occurs when recycled water is excluded from the supply portfolio: all expansion concentrates in desalination, while the collection network is gradually phased down.

Scenario S3 produces a more balanced configuration between the two water routes. Effluent-collection capacity increases from 1.00 to 2.50 m^3/s, rising quickly in the early years and then continuing on a slower upward trend until the end of the horizon. Recycled water installed capacity grows substantially, from 0.0206 to 0.698 m^3/s, with its steepest rise around the early 2030s. Seawater desalination installed capacity increases from 0.206 to 0.978 m^3/s, but its curve begins to level off earlier than in S1 and S2. By 2050, the recycled-water capacity approaches, but does not surpass, the desalination capacity, and both remain well below the effluent-collection capacity. The simultaneous presence of both expanding sources characterises S3 as a transitional configuration between linear and circular supply structures.

In Scenario S4, the system evolves toward full dependence on recycled water. Effluent-collection capacity increases sharply from 1.00 to 3.00 m^3/s, with most of the growth occurring before the mid-2030s,

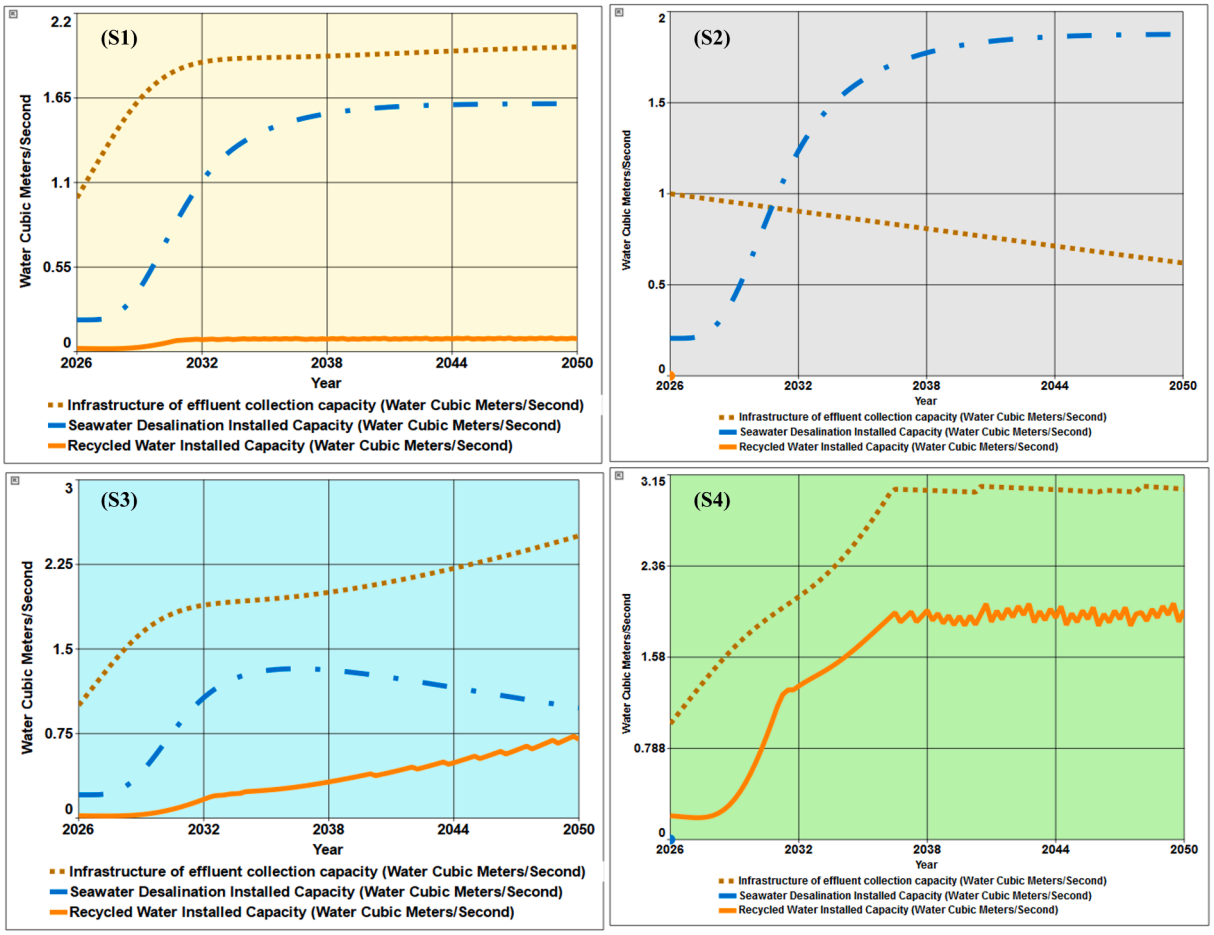

Fig. 13. Installed capacities of the four scenarios.

after which the curve stabilises close to its maximum level. Recycled water installed capacity rises from 0.206 to 1.98 m^3/s, showing two clearly identifiable growth phases: an initial acceleration around 2030, followed by a second, more pronounced expansion between approximately 2032 and 2036. After this dual expansion, recycled-water capacity fluctuates slightly around a high plateau. Seawater desalination remains at zero throughout the period. The combination of a high and stable collection capacity with a rapidly expanding recycled-water plant produces the most circular water-supply configuration among the four scenarios. Fig. 13 shows the pattern behaviour of the four scenarios for these variables.

The yearly water supplied to the hub from recycled water and seawater desalination displays distinct and highly dynamic trajectories across the four scenarios, reflecting how each water system responds to changes in installed capacity, effluent availability and the percentage of recycled water in the mix. In Scenario S1, seawater remains the dominant source of supply. Seawater deliveries rise from 2.53 million m^3/year to 19.3 million m^3/year, following a smooth upward trajectory that stabilises after the mid-2030s. Recycled water contributes only marginally, increasing from 34.6 thousand m^3/year to 140 thousand m^3/year, and its curve remains almost flat throughout the horizon. The visual separation between the two curves reflects the modest role that recycled water plays under a fixed 10 % share, combined with the rapid scaling of desalination capacity observed in this scenario. The overall pattern is one in which seawater progressively takes on the full burden of meeting the hub's rising water demand.

In Scenario S2, the recycled-water pathway is entirely absent, and seawater accounts for all supply. Deliveries grow from 2.81 million m^3/year to 24.9 million m^3/year, forming a monotonic curve that rises sharply in the early years and then converges smoothly toward an upper plateau. The absence of the recycled-water curve (flat at zero) highlights the exclusive reliance on desalination, and the shape of the seawater trajectory reflects the steady expansion of desalination capacity seen in the installed-capacity results. The pattern resembles S1 but with higher long-run values, consistent with the complete allocation of water-infrastructure expansion to desalination.

Scenario S3 exhibits the most balanced pattern between the two water sources. Seawater supply increases initially from 2.53 million m^3/year to a peak of approximately 13–14 million m^3/year, after which the curve declines and settles around 6.49 million m^3/year by 2050. Recycled-water supply shows the opposite profile: it starts at 34.6 thousand m^3/year, grows steadily across the horizon, and reaches 5.85 million m^3/year by 2050. The crossing of the two curves around the mid-2030s indicates the point at which recycled water becomes the main contributor. The combined pattern reflects the gradual transition from a desalination-dominated configuration to one in which recycled water supplies an increasingly larger share of the hub's needs.

Scenario S4 displays the most distinct behaviour, with water supplied exclusively from the recycled-water route. Deliveries rise from 4.39 million m^3/year to 42.2 million m^3/year, and the curve shows two clearly identifiable growth phases: an initial acceleration around 2030, and a second, more pronounced increase from approximately 2032 to 2036. After these phases, the trajectory stabilises at a high level but exhibits small oscillations consistent with the fluctuations seen in recycled-water capacity in this scenario. Because the model applies a 31.8 % distribution loss, the effective water delivered to the hub corresponds to the post-loss volume, meaning that the supply reaching the electrolyser is substantially lower than the total treated and collected

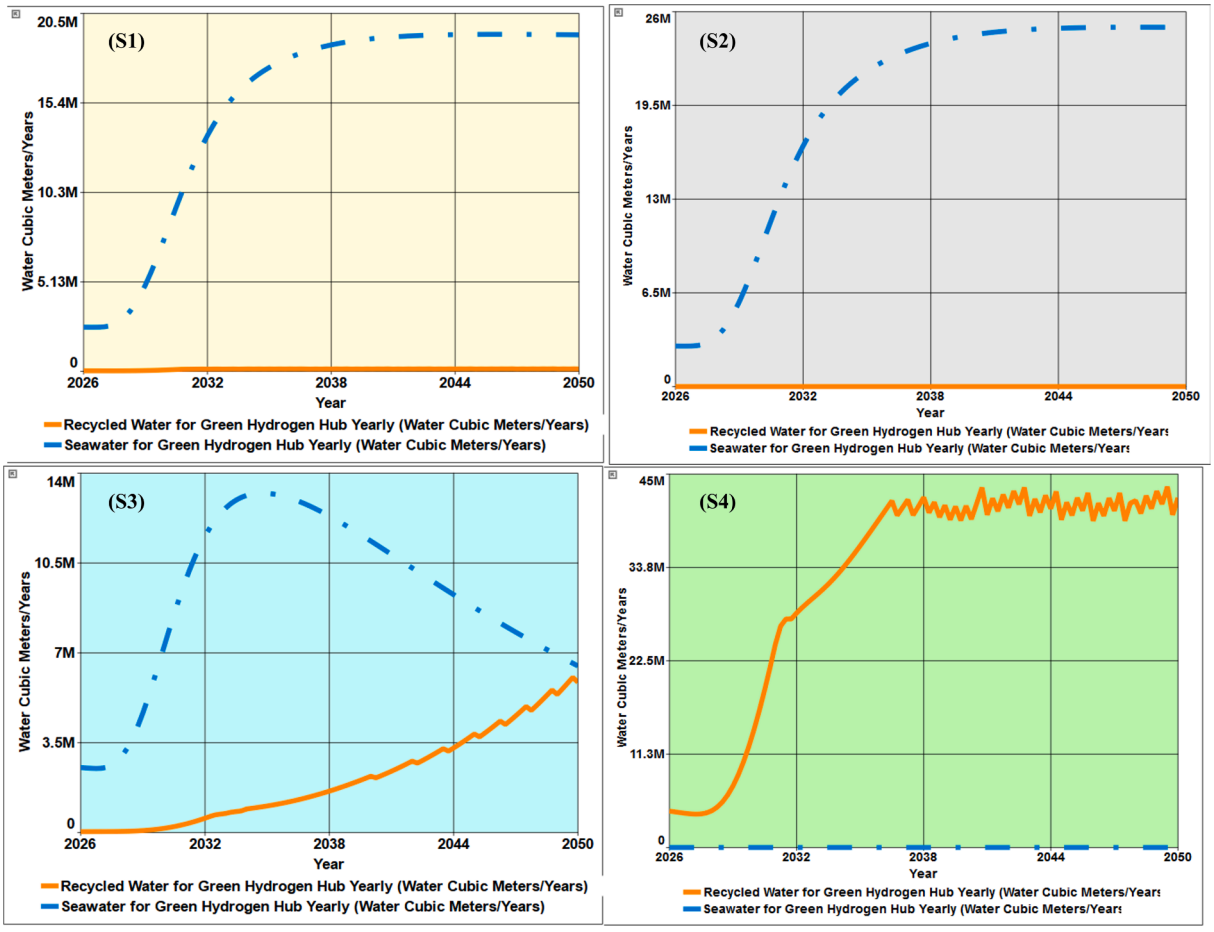

Fig. 14. Annual water supply per source in the four scenarios.

wastewater. Even under this loss rate, S4 achieves the highest long-run flows due to the rapid expansion of both effluent-collection and recycled-water capacities. Fig. 14 shows how the yearly water supplied to the hub from seawater and recycled water evolves under each scenario.

The yearly water required for green hydrogen production and cooling exhibits distinct growth patterns across the scenarios, shaped by differences in water availability, installed capacity expansion and the scale of hydrogen generation. In Scenario S1, both cooling water and electrolysis water follow smooth, monotonic trajectories that stabilise early. Cooling demand rises from 1.9 million m^3/year to around 14.4 million m^3/year, while water for electrolysis increases from 667 thousand m^3/year to 5.05 million m^3/year. The shape of both curves reflects the gradual approach to a stable operating regime: after an initial phase of rapid growth, the increments become progressively smaller, resulting in long, flat plateaus. This is consistent with the broader behaviour of S1, where total water supply expands relatively quickly but does not change substantially after the mid-2030s.

Scenario S2, which relies exclusively on desalination, exhibits the highest long-run cooling demand among the desalination-based configurations. Cooling water increases from 2.08 million m^3/year to 18.4 million m^3/year, maintaining a smooth rise similar to S1 but reaching higher values. Water for electrolysis grows from 731 thousand m^3/year to 6.48 million m^3/year, closely tracking the shape of hydrogen production in this scenario. The absence of recycled water leads to a monotonic and uninterrupted expansion pathway, reflected in the consistent curvature of both cooling and electrolysis trajectories.

Scenario S3 shows a distinct turning-point pattern in both uses. Cooling water increases from 1.9 million m^3/year to a peak of about 11–12 million m^3/year around 2034 and then gradually declines, stabilising near 9.13 million m^3/year by 2050. Water for electrolysis follows the same temporal structure: it rises from 667 thousand m^3/year to just over 3.4 million m^3/year before decreasing slightly to 3.21 million m^3/year at the end of the horizon. These inflection points mirror the evolution of total water supply in S3, where seawater availability begins to decline while recycled-water supply continues to grow, yielding a combined profile with early expansion followed by mild contraction. The resulting curves highlight the transitional nature of this scenario.

Scenario S4 shows the highest water use for both cooling and electrolysis, with trajectories marked by the two-phase growth pattern also observed in other S4 variables. Cooling water increases from 3.25 million m^3/year to 31.2 million m^3/year, and water for electrolysis rises from 1.14 million m^3/year to 11 million m^3/year. Both curves display two accelerations: an initial rise in the early 2030s, followed by a second expansion between roughly 2032 and 2036, after which the curves stabilise with small fluctuations. These oscillations reflect the dynamic adjustment of water supply within the model once recycled water becomes the sole source available to the hub. The sustained high levels at the end of the horizon highlight the markedly different long-run behaviour of S4 relative to the mixed and desalination-only scenarios. Fig. 15 shows how the yearly water required for green hydrogen production and cooling evolves across the four scenarios.

The near-field salinity exhibits only minimal variation across the scenarios, remaining within a narrow range because the dilution capacity of the receiving marine environment is large relative to brine volume. In Scenarios S1, S2 and S3, salinity starts at approximately 36 kg/m^3 in 2026 and rises slightly to about 36.8 kg/m^3 by 2050. This behaviour results from the limited magnitude of brine discharge relative

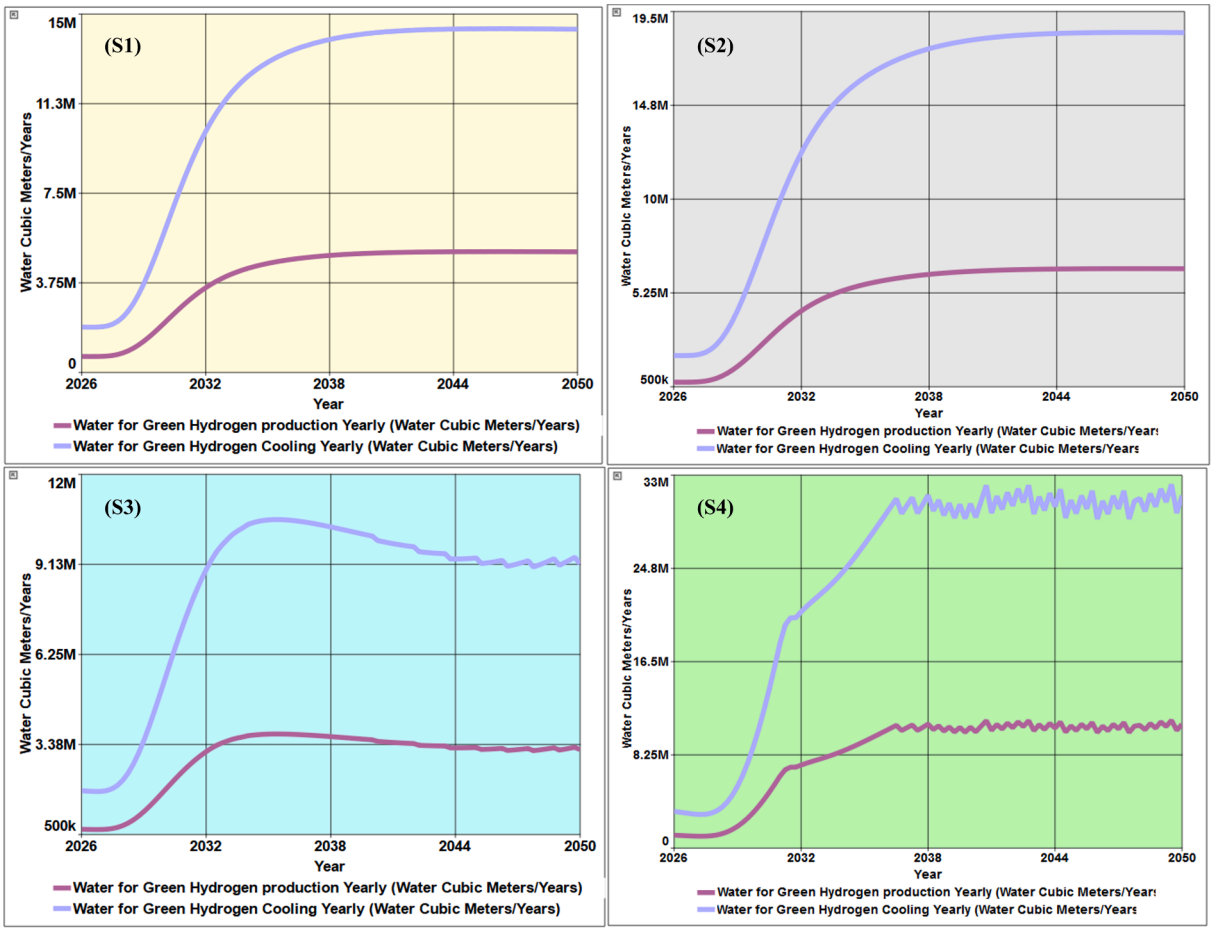

Fig. 15. Water required for the cooling system and for green hydrogen production in all scenarios.

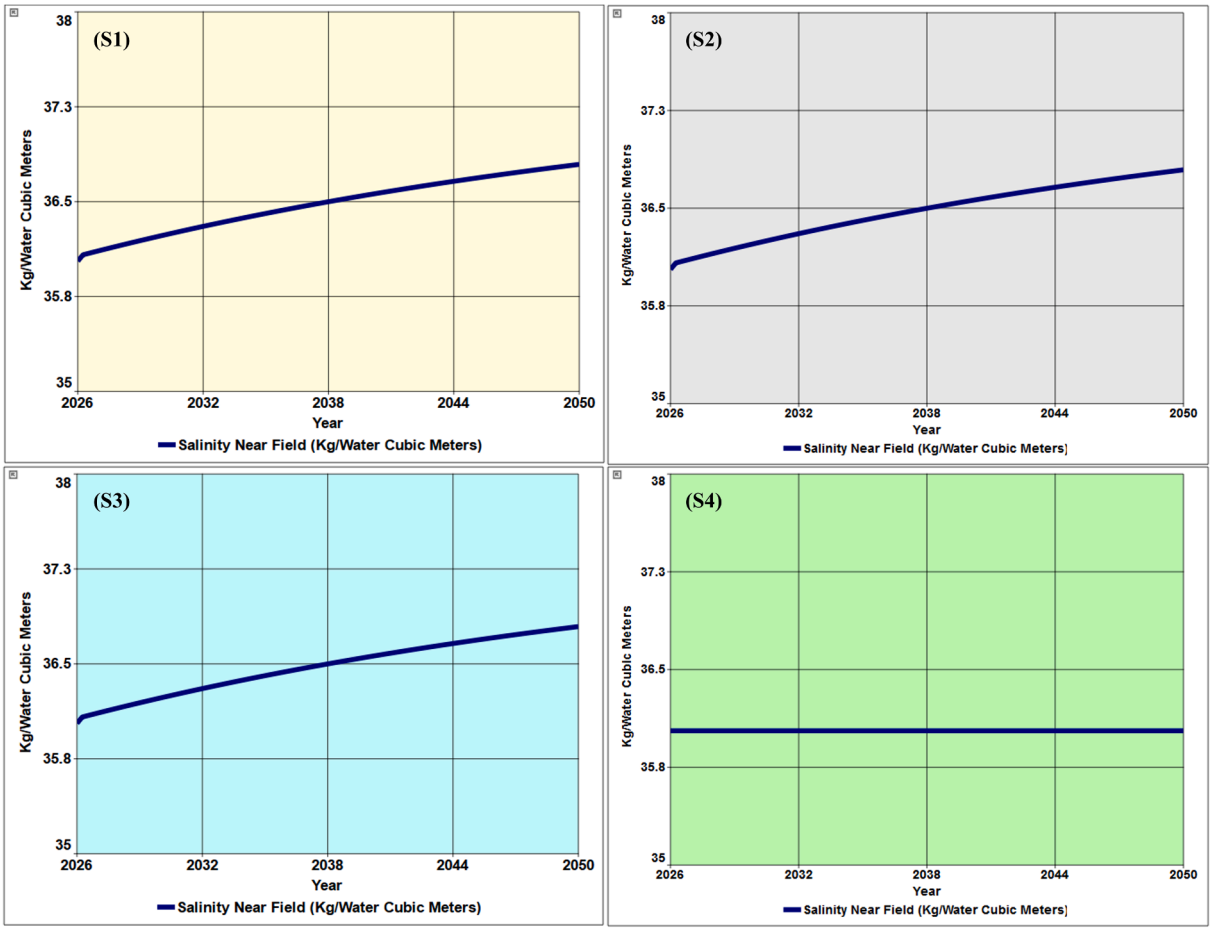

Fig. 16. Near-field salinity results for each scenario.

to the large receiving marine volume and from the strong mixing and dispersion, which constrains salinity increases even when desalination output grows. In Scenario S4, salinity remains constant at 36 kg/m^3 over the entire simulation horizon because no brine is discharged into the sea. Fig. 16 shows this behaviour across the four scenarios. The curves remain nearly flat, reflecting the strong dilution and dispersion processes in the receiving environment, which yield small changes in salinity over time. While desalination does increase brine discharge in scenarios S1–S3, the resulting changes remain well below 1 kg/m^3, and therefore the trajectories display very little dynamical structure.

The yearly energy consumption associated with seawater desalination and recycled-water treatment follows distinct trajectories across the four scenarios, reflecting differences in water-supply configurations and in the scale of hydrogen production. In Scenario S1, seawater desalination is the dominant contributor to energy use, with consumption rising from 23.4 thousand MWh/year to 183 thousand MWh/year. The curve shows a steep early increase followed by a gradual flattening, closely matching the S-shaped expansion pattern of desalination supply observed earlier. Recycled-water energy consumption remains minimal, increasing from 20.5 to 83.4 MWh/year, and is almost invisible in the Fig. 17 due to its scale. An important feature of S1 is the stability of the desalination curve after the mid-2030s, indicating that once desalination capacity reaches its long-run level, yearly energy consumption becomes nearly constant.

Scenario S2 shows the highest desalination energy use among all configurations. Seawater desalination energy consumption increases from 26 thousand MWh/year to 237 thousand MWh/year, and the curve maintains a smooth upward trajectory throughout the horizon. A distinctive aspect of S2 is the wider vertical separation between the early-phase and late-phase values compared with S1, reflecting the higher water throughput in this configuration. As recycled water is absent, recycled-water energy consumption stays at zero, and the resulting energy profile is the most desalination-intensive of the four scenarios. The curve also exhibits a clear stabilisation trend after the mid-2030s, although at a higher level than in S1.

Scenario S3 presents a transitional energy pattern that is visible directly in the shape of the curves. Seawater desalination energy consumption rises early in the simulation, reaching approximately 125 thousand MWh/year around 2033, and then declines to 61.7 thousand MWh/year by 2050. This decline mirrors the decreasing seawater supply observed for this scenario. Recycled-water energy consumption, by contrast, grows from 20.5 MWh/year to 3.48 thousand MWh/year, reflecting the rise in recycled-water supply over time. The key visual feature of S3 is the pivot between the two routes: desalination energy declines while recycled-water energy increases, producing the only scenario in which the two curves move in opposite directions.

Scenario S4 relies exclusively on recycled water, and its energy profile is therefore fully determined by advanced wastewater treatment. Recycled-water energy consumption increases from 2.61 thousand MWh/year to 25 thousand MWh/year, with mild oscillations after the mid-2030s. Compared with the desalination scenarios, the scale of energy use is considerably lower, even though S4 processes the largest volumes of water. This contrast reflects the underlying parameterisation of the model, in which recycled-water treatment has much lower specific energy consumption than seawater desalination. Seawater desalination energy remains at zero for the entire horizon. The Fig. 17 shows the results for energy consumption in each scenarios.

In Scenario S1, sludge generation reflects the modest but steady use

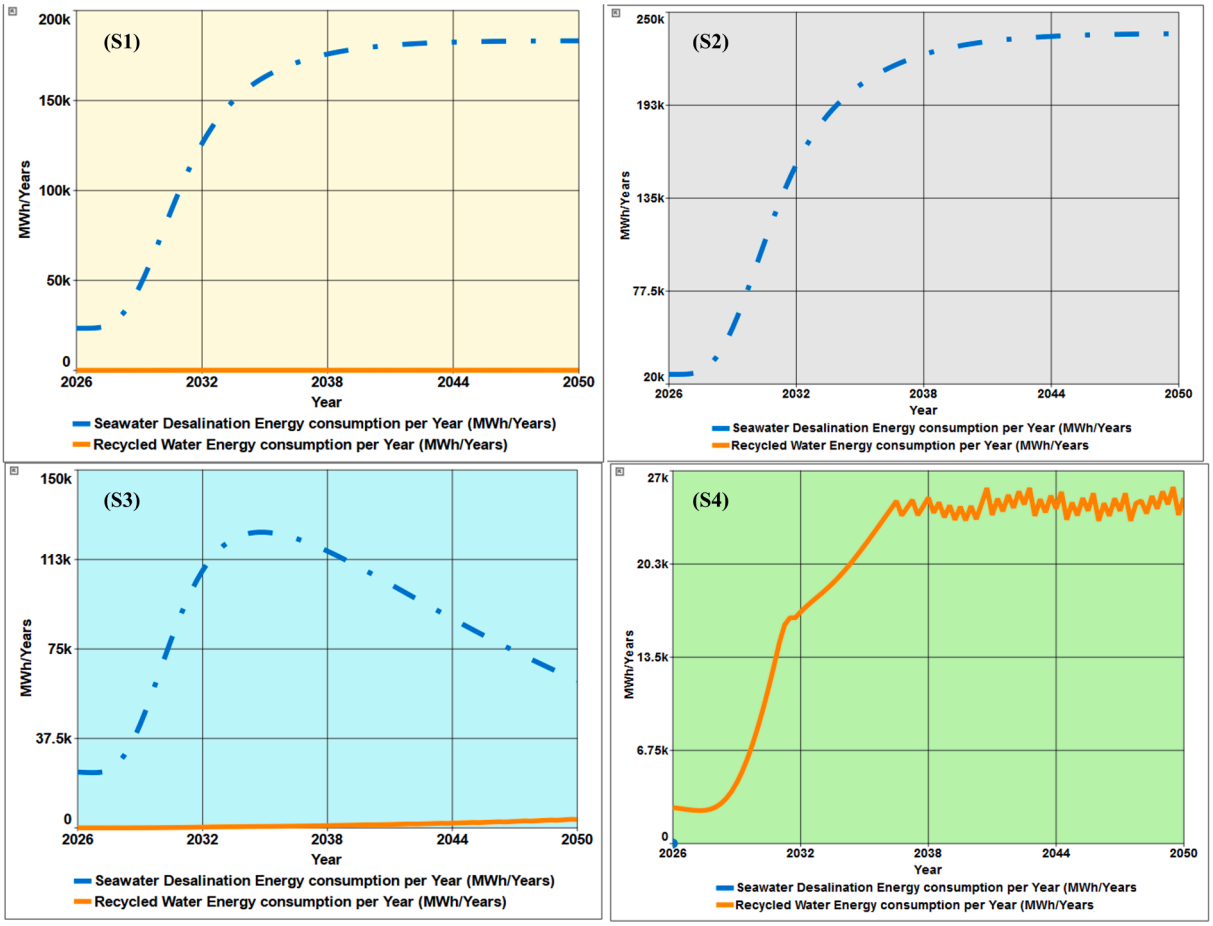

Fig. 17. Energy consumption across the four scenarios.

of recycled water permitted under the 10 % cap. Sludge to landfill begins at 349 m^3/year in 2026 and follows a brief initial dip, after which the curve rises sharply during the early 2030s as the recycled-water pathway reaches its stable operating scale. Once this adjustment phase concludes, the trajectory settles into a narrow band between 1.3 and 1.4 thousand m^3/year, showing only small oscillations. The long period of near-constancy indicates that, after the early expansion of recycled-water use, no further increases in recycled-water throughput occur, and the associated waste stream stabilises accordingly. This generates a behaviour profile in which sludge production is present but remains structurally limited. Scenario S2 produces no sludge at any point in the simulation, since recycled water is not used and the wastewater-treatment route is never activated.

Scenario S3 presents a markedly different pattern, with sludge increasing continuously throughout the horizon. Sludge to landfill starts at around 650 m^3/year, rises steadily through the 2030s, and reaches 110 thousand m^3/year by 2050. The curve shows a smooth upward trend punctuated by mild oscillations, signalling sustained growth rather than early stabilisation. This behaviour reflects the sustained increase in recycled-water use in S3, in which recycled-water availability expands year after year rather than levelling off early. As a result, sludge grows in parallel with the increasing contribution of recycled water to the hub's supply. Among the mixed scenarios, S3 is the one in which sludge continues to intensify through the entire period, without a mid-term plateau.

Scenario S4 generates the highest sludge levels across all configurations. Sludge production begins at 65 thousand m^3/year in 2026 and increases rapidly during the early 2030s as recycled-water supply expands. By the mid-2030s, yearly sludge reaches values between 550 and 600 thousand m^3, after which the trajectory stabilises at a high plateau with characteristic short-term fluctuations. Unlike S3, S4 shows a clear transition: an initial acceleration phase followed by sustained operation at large volumes. Because this scenario relies entirely on recycled water, sludge becomes a structural feature of the system, matching the magnitude of water flows processed for reuse. Fig. 18 shows how yearly sludge to landfill evolves across the four scenarios.

The yearly volume of brine discharged into the sea presents distinct structural behaviours across the scenarios, directly reflecting how much seawater desalination each configuration relies upon. In Scenario S1, brine discharge increases from 3.32 million m^3/year in 2026 to 26.5 million m^3/year in 2050. The curve rises steeply during the early expansion of desalination capacity and then transitions into a long, smooth upward path that gradually flattens as desalination approaches its operating ceiling. Because recycled water remains limited throughout the horizon, desalination continues to scale with hydrogen production, generating a persistently increasing brine load that dominates S1's waste-stream profile.

Scenario S2 shows the highest brine volumes among the scenarios that rely on desalination. Brine discharge grows from 3.69 million m^3/year to 34.3 million m^3/year, following a smooth and strongly monotonic curve. With no recycled water in operation, all additional water required by the hub is supplied through desalination, and the brine trajectory follows the same acceleration–stabilisation pattern seen in the installed-capacity curve. The absence of any secondary supply route results in a cleaner curve: the rise is continuous, and no mid-horizon dampening occurs, making S2 the scenario in which marine brine loading intensifies most sharply.

Scenario S3 displays a markedly different behaviour, characterised

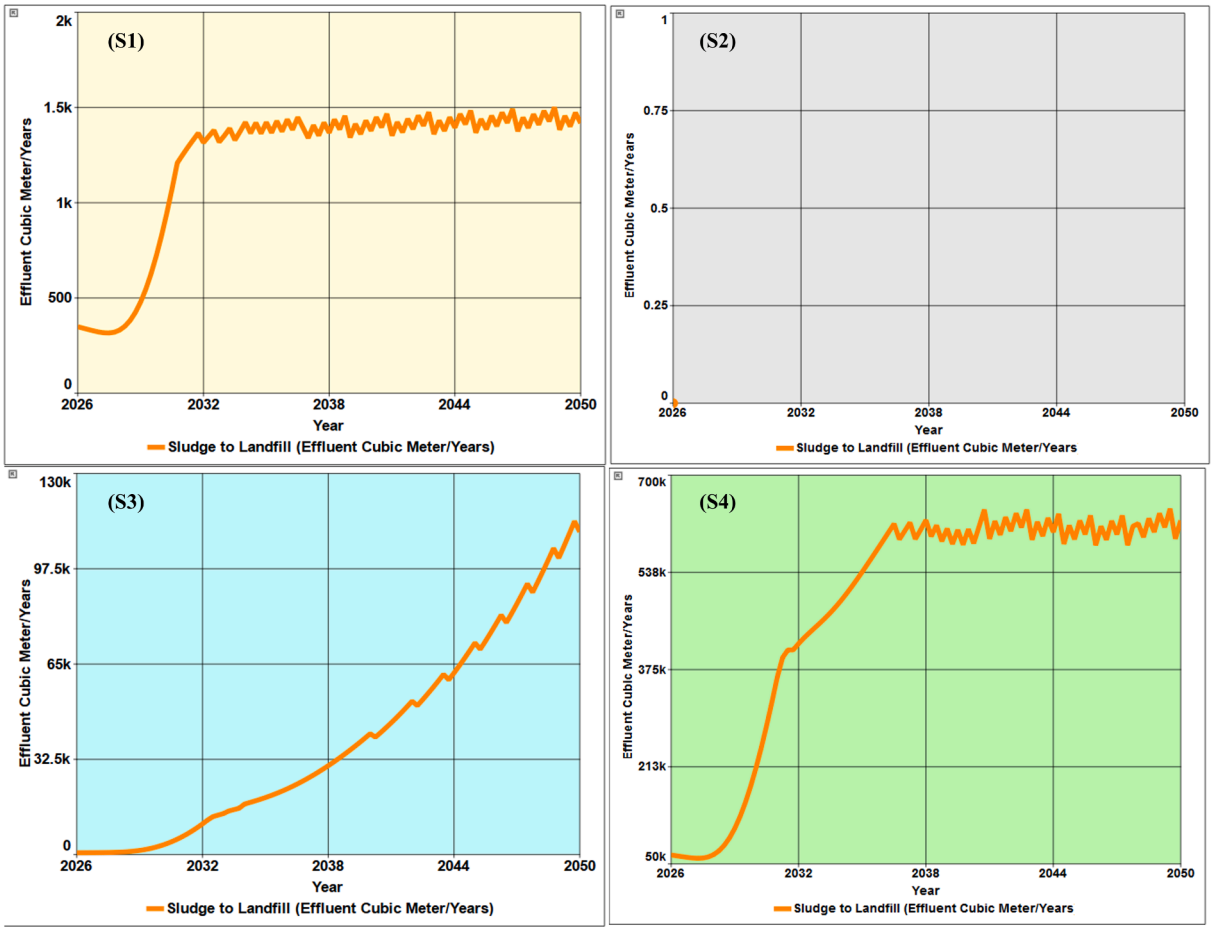

Fig. 18. Sludge production yearly across the four scenarios.

by an inverted-U trajectory. Brine discharge begins at 3.32 million m^3/year, climbs rapidly to a peak of 17.8 million m^3/year in the early 2030s, and then declines steadily to 8.93 million m^3/year by 2050. This turning point corresponds to the moment when recycled water becomes increasingly important in the supply mix. As recycled-water availability expands, desalination no longer scales in parallel with hydrogen production, and brine generation gradually decreases. Among all scenarios, S3 is the only one in which brine first accelerates and later recedes, producing a distinctive rise-and-fall pattern. Scenario S4 yields zero brine discharge over the entire simulation period. This produces a flat line at zero, sharply contrasting with the brine-intensive trajectories observed in S1–S3 and highlighting how the shift to a fully circular water-supply configuration eliminates this waste stream entirely. Fig. 19 shows how yearly brine discharge to the sea evolves across the four scenarios.

The integrated analysis of the simulated variables shows that each water supply configuration reorganises water, energy and waste flows differently over time, producing specific operating regimes for the hydrogen hub. Scenarios based on desalination concentrate pressures on energy consumption and brine discharge, while those that increase recycled water increase sludge production and reduce dependence on the sea as a source and destination. The comparison shows that the structural choices made in the system design, especially the participation of recycled water, shape not only water availability but also the potential environmental and social impacts associated with the hub's operation.

4.3. *Overall results of the four scenarios*

The comparative assessment of the four scenarios shows how different water-supply architectures shape hydrogen output, resource allocation, environmental pressures and the co-benefits associated with strengthening sanitation systems. Each scenario represents a distinct configuration of linear and circular water use, and the results demonstrate how these choices reverberate across technological, environmental and social dimensions. Table 7 summarises these outcomes qualitatively.

Scenarios S1 and S2 illustrate the implications of desalination-centred strategies. In S1, the persistent 10 % ceiling on recycled water keeps circularity marginal, and desalination becomes progressively dominant as demand rises. This produces medium–high hydrogen output, but at the cost of a continuously increasing brine load and a sustained rise in energy use. Effluent-collection expansion is moderate, and although some co-benefits emerge from improvements in collection infrastructure, these remain limited and do not significantly reconfigure the supply system. Overall, S1 reliably delivers hydrogen but accumulates marine pressures over time, generating only moderate improvements in sanitation.

Scenario S2 amplifies these characteristics. With recycled water fully excluded, desalination becomes the sole operational pillar of the hub, delivering high hydrogen production among the linear scenarios but also the highest energy intensity and the largest brine discharge. Effluent-collection capacity declines steadily, offering no sanitation co-benefits, and the scenario aligns exclusively with a linear water-use model. Its overall sustainability performance remains low because environmental pressures concentrate in one dimension while no

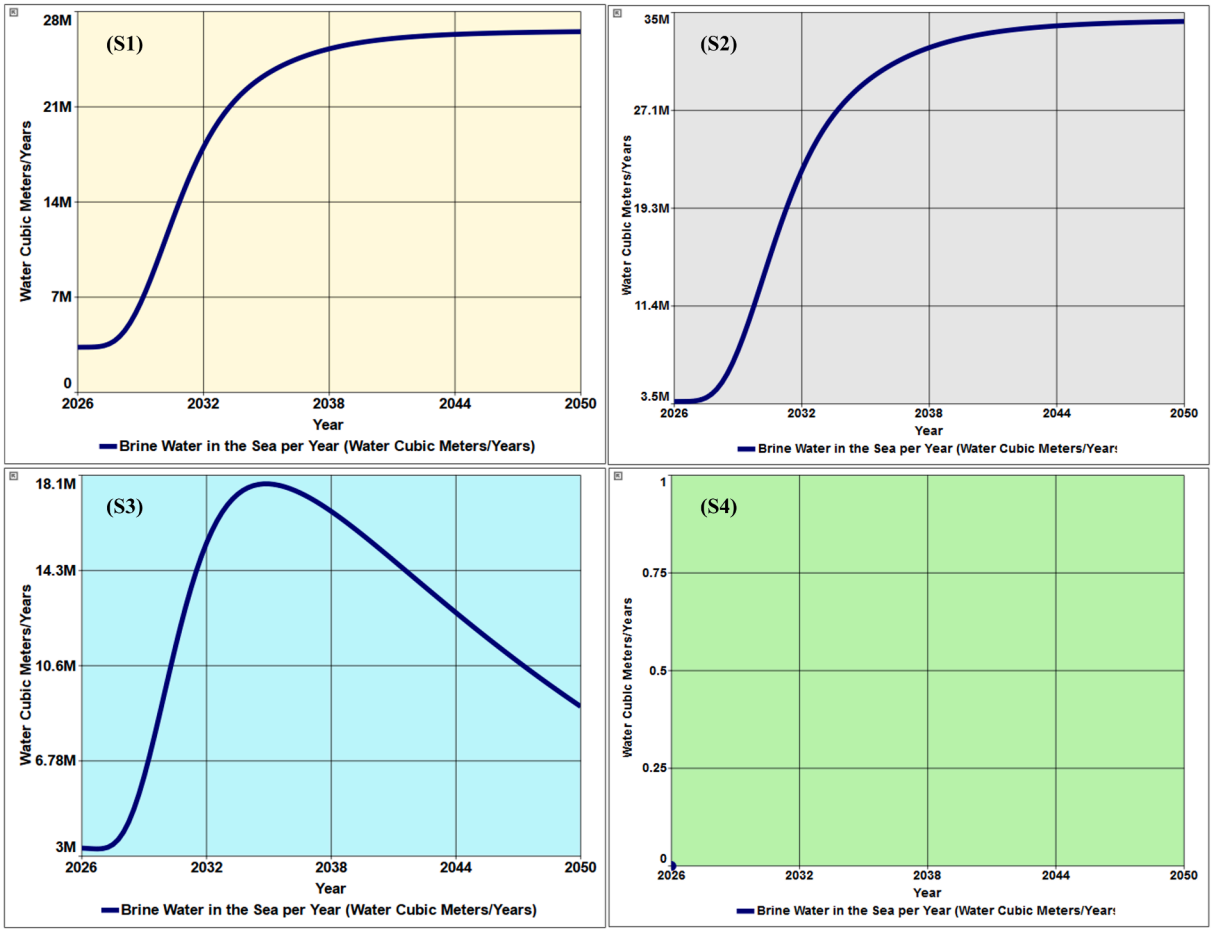

Fig. 19. Brine water production yearly across the four scenarios.

compensatory benefits arise elsewhere.

Scenario S3 stands apart not because it maximises or minimises any single outcome, but because it represents a genuine transition between two competing architectures. Hydrogen production is the lowest among the scenarios, yet the trajectory that produces this result is structurally meaningful. Desalination dependence declines over time, reducing brine discharge after an initial inverted-U peak. Meanwhile, the recycled-water chain expands: effluent collection increases, treatment capacity grows, and sludge volumes become high and rising as more wastewater is processed. Total water availability becomes increasing and balanced, and moderate co-benefits for sanitation and public health accumulate as circular infrastructure strengthens. S3 exemplifies a transitional regime in which sustainability indicators improve, but technological output remains constrained because the circular pathway matures slowly within the time frame considered. Its overall sustainability performance is medium.

Scenario S4 demonstrates the systemic implications of a fully circular configuration. By relying exclusively on recycled water, the hub reorients all expansion dynamics toward the terrestrial domain. Effluent collection undergoes strong expansion and saturates early, recycled-water capacity grows in two clear stages, and no brine is discharged at any point. Hydrogen production becomes very high, and the system achieves the lowest energy intensity per unit of water because it operates without desalination. Sludge volumes are very high, reflecting the large quantities of wastewater treated in this scenario, an impact concentrated on land rather than offshore and consistent with a model that internalises and manages its own outputs. S4 therefore presents the strongest alignment with circular-economy principles and reaches a mature circular state within the simulated period, in which resource availability, infrastructure performance and environmental outcomes reinforce each other. Its overall sustainability performance is very high.

Although near-field salinity remains almost constant across the scenarios, this indicator does not fully capture the environmental relevance of brine discharge. In desalination systems, the magnitude of impacts is influenced not only by changes in salinity concentration, but also by the large volumes of effluent released, the formation of dense bottom-hugging plumes, thermal contrasts with receiving waters and the presence of pre-treatment chemicals. These processes may generate pressures on the marine environment even when salinity values in the water column appear stable. As a result, scenarios with higher desalination use (S1 and especially S2) still impose greater marine loading through brine disposal, whereas S3 reduces this pressure as desalination becomes progressively marginal, and S4 removes it entirely by relying exclusively on recycled water.

Across the four scenarios, three insights become clear. First, higher circularity consistently shifts environmental pressures from the marine environment to the terrestrial wastewater system, while also reducing energy intensity. Second, transition pathways such as S3 tend to produce mixed outcomes when the maturity of competing supply chains diverges over time. Third, fully circular architectures such as S4 offer the most balanced configuration, achieving high hydrogen output while reinforcing sanitation infrastructure and avoiding marine degradation. In semiarid regions, where water scarcity and environmental sensitivity converge, the structural advantages of circular water systems become particularly pronounced.

Table 7
Qualitative comparison of the four scenarios.

Dimension	S1 (10 % recycled)	S2 (0 % recycled)	S3 (10 %–50 % recycled)	S4 (100 % recycled)
Green hydrogen production	Medium–high	High	Low (lowest among scenarios)	Very high
Water availability for the hub	Moderate	High (but linear)	Increasing and balanced	Very high (fully circular)
Energy intensity of the system	Medium–high	Highest	Low–medium	Lowest per unit of water
Dependence on desalination	High	Total	Declining	None
Brine discharge (marine impact)	Medium and rising	Highest	Declining (inverted-U)	None
Sludge generation (urban impact)	Very low	None	High and rising	Very high
Effluent collection expansion	Moderate expansion	Declining	Increasing	Strong expansion
Co-benefits for sanitation and public health	Moderate	None	Medium	Very High
Alignment with circular-economy principles	Low	None	Medium	High
Overall sustainability performance	Moderate–low	Low	Medium	Very high

5. Discussion

The simulation results demonstrate that water-supply choices shape not only the technological feasibility of green hydrogen production in semi-arid regions but also its long-term environmental and socio-economic consequences [107]. Across all scenarios, the share of recycled water restructures the energy footprint, waste profile and spatial distribution of impacts. The findings support existing literature that emphasises the need to frame hydrogen development not as a purely technical optimisation problem, but as a socio-environmental decision embedded in local resource constraints, institutional arrangements and procedural justice [26,28,108,109].

Across the four scenarios, the dynamics of hydrogen production follow the structure of the underlying water system. When desalination dominates (Scenarios S1 and S2), hydrogen output grows steadily because investments concentrate on a single technology that expands predictably with installed capacity. These patterns align with broader evidence showing that reverse osmosis systems exhibit stable recovery rates around 40–45 % and scale linearly with capacity additions [41,42]. The updated simulations reinforce this behaviour: S1 and S2 both show continuous increases in hydrogen production, but S2, relying exclusively on seawater, achieves substantially higher output and considerably larger environmental burdens than S1.

However, the transitional architecture of Scenario S3 reveals a dynamic rarely discussed in the hydrogen literature: a transition penalty. As the share of recycled water increases, the expansion of desalination slows; yet the recycled-water pathway, dependent on sequential improvements in effluent collection, treatment capacity and the availability of treated wastewater, matures only later in the horizon. During this prolonged period of infrastructural asymmetry, total water availability remains structurally constrained, resulting in the lowest hydrogen output among all scenarios. The updated results strengthen this interpretation: brine discharge follows an inverted-U trajectory, peaking near 17.8 million m^3/year before falling to 8.93 million m^3/year, while hydrogen output stabilises at relatively low levels without a late-period acceleration. This behaviour mirrors transition dynamics observed in other socio-technical systems, where hybrid regimes often underperform until new infrastructures become fully consolidated.

In contrast, Scenario S4 demonstrates that a fully circular configuration provides not only environmental benefits but also the highest hydrogen production. This outcome is consistent with studies identifying recycled water as a more advantageous feedstock than seawater, both technologically and economically [22]. The 99 % recovery rate assumed for recycled-water treatment systems [83,84,110] enables a substantially larger effective water supply when wastewater volumes are high. In the updated model, S4 exhibits two distinct expansion phases, associated first with early improvements in effluent collection and later with the consolidation of treatment capacity, before stabilising at a high production plateau. Although sludge generation becomes substantial (exceeding 624 thousand m^3/year), this output aligns with terrestrial circular-economy opportunities such as thermal valorisation in cement kilns [111] and nutrient recovery [112,113], provided that regulatory frameworks address contaminants including heavy metals and emerging pollutants like microplastics [105,106].

Near-field salinity dynamics further illuminate differences between linear and circular water architectures. Although modelled salinity increments remain small (<1 kg/m^3), desalination-based scenarios generate very large brine volumes, reaching 26.5 million m^3/year in S1 and 34.3 million m^3/year in S2 by 2050. Literature shows that ecological impacts often depend more on effluent volume, density-driven plume behaviour and chemical additives than on changes in average salinity [15,16,45]. These mechanisms can affect benthic communities, macroalgae and sensitive habitats such as *Posidonia oceanica*, even when salinity changes appear minimal. Similar impacts have been documented in the Red Sea and Cyprus, regions with climatic parallels to Ceará [13,95,114]. The model therefore highlights that near-field salinity is an insufficient proxy for environmental harm: desalination-based scenarios externalise ecological pressures onto coastal ecosystems and marine-dependent livelihoods, particularly artisanal fishing communities [115,116].

Energy dynamics also diverge sharply. Desalination-based scenarios maintain the highest energy burdens, consistent with the intensity of reverse-osmosis systems [41]. Scenarios S1 and S2 show sustained rises in desalination energy use over time, while S3 transitions toward greater reliance on recycled water and stabilises at intermediate levels. Despite processing the largest volumes of water, S4 exhibits the lowest energy intensity per cubic metre due to the comparatively lower requirements of recycled-water treatment [56], demonstrating that circularity can simultaneously deliver high productivity and reduced energy impacts.

The feasibility of large-scale recycled-water supply remains conditional on wastewater availability, which in Ceará is shaped by structural advantages: (1) the sewage pipeline interconnecting Fortaleza and CIPP; (2) mandatory sanitation expansion under Federal Law 14,026/2020; and (3) projections in the State Strategic Water Plan indicating potential effluent availability near 2.5 m^3/s [14]. These conditions enhance the plausibility of S4's circular configuration. Nonetheless, interviewees highlighted operational and institutional barriers, including slow public investment, outdated regulatory frameworks and tariff structures that disadvantage recycled water, as establish in Decision No 01/2022 [117]. These challenges echo those documented in São Paulo [118], such as limited sludge valorisation, insufficient biogas volumes and spatial mismatch between treatment facilities and industrial demand. Without policy alignment and sustained investment, the benefits suggested by S4 remain constrained by institutional inertia.

The socio-environmental implications of these water-supply choices are particularly significant. Previous large-scale infrastructure projects in Ceará, including wind farms and the original construction of CIPP, have generated land conflicts, displacement and heightened social vulnerability [119–121]. Fishing communities near CIPP have faced violence, land speculation and rising living costs as industrial expansion

reshaped the territory [122,123]. Without deliberate governance strategies, hydrogen development risks reproducing these patterns, prioritising corporate interests over local communities [120,124]. These dynamics resemble what Abreu & Andrade [125] describe as "wicked industrial disasters," where institutional weaknesses and environmental degradation interact to magnify harm.

Water supply decisions are therefore not neutral. A linear water system centred on desalination externalises ecological burdens onto coastal communities, whereas a circular system rooted in sewage valorisation distributes benefits more widely and reduces exposure to environmental risks. The absence of the National Water and Sanitation Agency (ANA) and IBAMA from Brazil's Legal Framework for Low-Carbon Hydrogen underscores a regulatory gap in national planning, one that mirrors broader tendencies toward licensing flexibilisation in Brazil [126]. In Ceará, the misalignment is particularly stark: while the state's Strategic Water Plan recommends recycled water for CIPP, Environmental Impact Assessments produced for hydrogen projects have prioritised desalination [11,71].

This institutional asymmetry increases the risk of path dependency on linear infrastructures, with long-term ecological and social consequences. Incorporating circular-economy principles into hydrogen governance, consistent with insights from Sauvé et al. [17]. and Müller & Pampus [23,66], would anchor hydrogen development within a regenerative rather than extractive resource regime.

Our findings advance the literature in at least three ways. First, they show that circular water systems can outperform linear systems not only environmentally but technologically, challenging persistent assumptions about desalination as the only scalable option in semiarid regions. Secondly, they reveal a novel dynamic, the transition penalty, demonstrating how hybrid configurations can underperform for extended periods due to asynchronous infrastructure evolution. Thirdly, they integrate environmental, technological and socio-political dimensions within a long-term feedback model, addressing gaps identified by Santana et al. [23]. and others regarding cumulative impacts, territorial inequalities and cross-sector feedbacks.

Finally, literature on energy justice warns that low-carbon infrastructures can reproduce historical inequalities when distributive, procedural and recognition dimensions are ignored [2,108,109,127–129]. Our results show that the choice of water system determines where impacts fall: desalination shifts burdens to coastal ecosystems and marine-dependent communities, while recycled water integrates benefits into sanitation systems, industry and territorial health. This aligns with analyses of past wind-energy conflicts in Ceará [119], where inadequate participatory governance generated community resistance and social fragmentation. If hydrogen development continues along a linear pathway, Ceará risks entering a new cycle of resource extraction, land pressure and community dispossession, contradicting the principles of a just transition.

6. Conclusion and policy implications

This study examined how alternative water-supply strategies—recycled water and seawater desalination—reshape the technological, environmental, and social outcomes of green hydrogen production in a semi-arid region. The system dynamics simulations show that fully circular configurations centred on recycled water offer the most advantageous combination of high hydrogen output, low environmental burdens, and indirect societal co-benefits. Because recycled water has a higher recovery rate than seawater desalination and can expand in tandem with sanitation infrastructure, it supports substantially larger production volumes while eliminating brine discharge and reducing energy intensity. These findings reinforce the relevance of integrating circular economy principles into the hydrogen economy of Ceará.

The results also echo longstanding governance patterns in the Industrial and Port Complex of Pecém, where previous infrastructure expansions often advanced economic interests while overlooking ecological impacts and local communities [120,122]. Similar dynamics appear in ongoing hydrogen planning, where desalination has been prioritised despite its energy intensity and marine pressures. This tendency occurs amid regulatory gaps, including the absence of water and environmental agencies in the Brazilian Legal Framework for Low-Carbon Hydrogen and licensing processes that traditionally emphasise economic feasibility over cumulative impacts [126,130].

The environmental concerns raised by desalination-based scenarios are consistent with studies documenting biodiversity loss in regions exposed to sustained brine discharge, such as the Egyptian Red Sea and Cyprus [95,114]. Such pressures have direct implications for coastal livelihoods in Ceará, where artisanal fishing remains economically and culturally significant [115]. While the model does not simulate ecological change, the brine volumes emerging from desalination-dominated scenarios highlight the scale of potential pressures on marine ecosystems and reinforce the need for precautionary governance.

Conversely, scenarios prioritising recycled water generate broader territorial co-benefits. Expanded wastewater collection reduces untreated discharges and supports the recovery of energy and nutrients from sludge [111,112]. These pathways align with Ceará's industrial structure, where cement plants and agricultural sectors could absorb processed sludge, provided that regulatory frameworks address contaminants such as heavy metals and emerging pollutants [64,105]. The potential availability of treated effluent—reinforced by Brazil's sanitation expansion commitments under Law 14.026/2020—adds to the feasibility of circular strategies for hydrogen production.

However, realising these benefits depends on institutional coordination. Interviews indicated that companies often favour desalination due to perceived inertia in public investment in recycled water infrastructure. Environmental Impact Assessments for hydrogen projects have reinforced this bias by presenting desalination as the most feasible supply option [11,71], despite the state's Strategic Water Plan recommending recycled water [14]. These asymmetries risk perpetuating social injustices observed in previous energy transitions in Ceará, including land conflicts associated with wind power deployment [119].

To guide a just and sustainable hydrogen transition, policy measures should integrate hydrogen planning with sanitation expansion, strengthen participatory governance with local communities, modernise sludge-valorisation regulation, account for cumulative marine impacts, and diversify hydrogen production pathways. Crucially, the abundance of solar and wind energy and the existing industrial infrastructure at Pecém cannot be treated as decisive arguments for hydrogen deployment in Ceará. Long-term feedback loops in ecological and socio-economic systems must be incorporated into decision-making if the hydrogen economy is to avoid reproducing historical inequalities and instead contribute to a genuinely just energy transition.

Ultimately, the model shows that water choices determine whether Ceará's hydrogen economy will reinforce extractive patterns or enable a regenerative development pathway. Desalination-centred strategies externalise impacts to coastal ecosystems and vulnerable fishing communities, while circular configurations internalise flows, strengthen sanitation, and expand productive capacity. As governments and investors rush to scale green hydrogen in semi-arid regions worldwide, the Ceará case demonstrates that infrastructure lock-ins created in the first decade will define environmental burdens and social outcomes for generations. Ensuring that hydrogen development is aligned with circular water governance is therefore not an environmental add-on but a structural condition for a just, resilient, and territorially grounded energy transition.

6.1. Study limitations and future research

Although this study provides new insights into how linear and circular water strategies shape the sustainability of hydrogen production in

semi-arid regions, several limitations should be acknowledged. First, because the green hydrogen hub at the Industrial and Port Complex of Pecém is not yet operational, all simulations are based on projected rather than observed conditions. The model draws on policy documents, interviews and existing literature to estimate water availability, infrastructure behaviour and technological performance. While system dynamics is well suited for exploring uncertainty in emerging sectors, the absence of empirical operational data limits calibration and may affect the precision of long-term trajectories.

Second, the model concentrates on the physical flows most relevant to water–hydrogen interactions: water supply, energy use and waste generation. It does not simulate ecological or socio-economic dynamics such as marine biodiversity responses, fisheries productivity, groundwater interactions, land-use change or labour-market transitions. Discussions of potential social and ecological consequences—such as risks to coastal livelihoods or opportunities arising from sludge reuse—therefore rely on external literature rather than on endogenous model behaviour. Future work could embed these processes into coupled ecological or socio-economic submodels to capture cumulative effects.

Third, infrastructure performance and wastewater availability were represented using aggregated stocks and flows. In practice, processes such as infiltration, stormwater dilution, illegal connections, seasonal variability and operational failures can influence the volume of sewage reaching treatment plants and the efficiency of collection networks. While some of these processes are indirectly reflected in variables such as distribution losses or recovery-rate functions, they are not explicitly modelled. Enhanced spatial resolution or the integration of hydrological subcomponents could help refine these dynamics.

Fourth, financial and institutional dimensions, such as capital costs, tariff structures, financing constraints and investment sequencing, were not included in the model. Because economic decisions strongly influence technology adoption and water-source selection, integrating capital-allocation dynamics could improve understanding of how financial feasibility interacts with circularity and long-term infrastructure trajectories. Similarly, regulatory factors were included qualitatively but not formally modelled; future versions could incorporate policy levers, institutional inertia or incentive structures more explicitly.

Finally, although the model includes feedback loops between water availability, installed capacities and hydrogen production, it does not yet incorporate multi-criteria decision-support approaches capable of evaluating trade-offs among environmental, social, economic and operational criteria. Combining system dynamics with methods such as AHP, ELECTRE, TOPSIS or robust decision-making could support participatory planning and allow stakeholders to explore alternative governance pathways under uncertainty.

Despite these limitations, the modelling framework provides a foundation for integrated water–hydrogen planning in semi-arid contexts. As empirical data become available from real-world hydrogen projects, the model can be calibrated, extended and coupled with ecological, economic and governance modules. This evolution will strengthen its contribution to strategic decision-making and to the design of equitable and sustainable hydrogen transitions.

Funding sources

This work was supported by the National Council for Scientific and Technological Development (grant number 409549/2022-3).

CRediT authorship contribution statement

Luís Matheus Tavares Silva: Writing – review & editing, Writing – original draft, Methodology, Investigation, Formal analysis, Data curation, Conceptualization. **Cosme Polese Borges:** Writing – review & editing, Writing – original draft, Visualization, Validation, Methodology, Formal analysis. **Mônica Cavalcanti Sá De Abreu:** Writing – review & editing, Writing – original draft, Supervision, Project administration, Investigation, Funding acquisition, Conceptualization. **Mauricio Uriona Maldonado:** Writing – review & editing, Software, Methodology, Formal analysis. **Flávia Mendes De Almeida Collaço:** Writing – review & editing, Visualization, Conceptualization.

Declaration of competing interest

The authors declare that they have no known competing financial interests or personal relationships that could have appeared to influence the work reported in this paper.

Supplementary materials

Supplementary material associated with this article can be found, in the online version, at doi:10.1016/j.sftr.2026.101721.

Data availability

Data will be made available on request.

References

[1] A. Islam, T. Islam, H. Mahmud, O. Raihan, M.S. Islam, H.M. Marwani, et al., Accelerating the green hydrogen revolution: a comprehensive analysis of technological advancements and policy interventions, Int. J. Hydrog. Energy 67 (2024) 458–486, https://doi.org/10.1016/j.ijhydene.2024.04.142.
[2] S. Griffiths, B.K. Sovacool, J. Kim, M. Bazilian, J.M. Uratani, Industrial decarbonization via hydrogen: a critical and systematic review of developments, socio-technical systems and policy options, Energy Res. Soc. Sci 80 (2021), https://doi.org/10.1016/j.erss.2021.102208.
[3] Deutsche Gesellschaft für Internationale Zusammenarbeit (GIZ) GmbH. Mapeamento do Setor de Hidrogênio Brasileiro Panorama Atual e Potenciais para o Hidrogênio Verde, 2021. Brasília.
[4] T. Longden, F.J. Beck, F. Jotzo, R. Andrews, M. Prasad, Clean' hydrogen? – Comparing the emissions and costs of fossil fuel versus renewable electricity based hydrogen, Appl. Energy 306 (2022), https://doi.org/10.1016/j.apenergy.2021.118145.
[5] L. Cremonese, G.K. Mbungu, R. Quitzow, The sustainability of green hydrogen: an uncertain proposition, Int. J. Hydrog. Energy 48 (2023) 19422–19436, https://doi.org/10.1016/j.ijhydene.2023.01.350.
[6] Y. Zhou, R. Li, Z. Lv, J. Liu, H. Zhou, C. Xu, Green hydrogen: a promising way to the carbon-free society, Chin. J. Chem. Eng. 43 (2022) 2–13, https://doi.org/10.1016/j.cjche.2022.02.001.
[7] M. Hermesmann, Müller TE. Green, Blue Turquoise, or Grey?, Environmentally friendly hydrogen production in transforming energy systems, Prog. Energy Combust. Sci. 90 (2022) 1–8, https://doi.org/10.1016/j.pecs.2022.100996.
[8] Hydrogen Council, McKinsey & Company. Hydrogen Insights an updated perspective on hydrogen investment, market development and momentum in China. 2021.
[9] Relatório Síntese 2025: Ano base 2024, Energy Research Company, Rio de Janeiro, 2025.
[10] Hidrogênio Sustentável: Perspectivas Para O Desenvolvimento E Potencial Para A Indústria Brasileira, National Confederation of Industry, Brasília, 2024.
[11] Estudo De Impacto Ambiental (EIA) – Planta Fortescue De Hidrogênio Verde: Caucaia e São Gonçalo Do Amarante, Fortescue Future Industries, 2023.
[12] S.M.O. Silva, F. Filho, A.S. de, D.A.C. Cid, S.H.S. de Aquino, L.C.P. Xavier, Proposal of integrated urban waters management as a strategy to promote water security: the fortaleza case, Eng. Sanit. Ambient. 24 (2019) 239–250.
[13] A. Souza Filho F de, Estudo Setorial Especial: Recursos Hídricos, Fortaleza, 2018.
[14] Plano De Ações Estratégicas De Recursos Hídricos Do Ceará, Secretaria dos Recursos Hídricos, Fortaleza, 2018.
[15] T.M. Missimer, R.G. Maliva, Environmental issues in seawater reverse osmosis desalination: intakes and outfalls, Desalination 434 (2018) 198–215, https://doi.org/10.1016/j.desal.2017.07.012.
[16] D. Xevgenos, M. Marcou, V. Louca, E. Avramidi, G. Ioannou, M. Argyrou, et al., Aspects of environmental impacts of seawater desalination: cyprus as a case study, Desalin. Water Treat 211 (2021) 15–30, https://doi.org/10.5004/dwt.2021.26916.
[17] S. Sauvé, S. Lamontagne, J. Dupras, W. Stahel, Circular economy of water: tackling quantity, quality and footprint of water, Environ. Dev. 39 (2021), https://doi.org/10.1016/j.envdev.2021.100651.
[18] A. van Zyl, J.L. Jooste, Retaining and recycling water to address water scarcity in the City of Cape Town, Dev. South. Afr. 39 (2022) 108–125, https://doi.org/10.1080/0376835X.2020.1801387.
[19] A. Vallejos-Romero, M. Cordoves-Sánchez, C. Cisternas, F. Sáez-Ardura, I. Rodríguez, A. Aledo, et al., Green Hydrogen and Social sciences: issues, problems, and future challenges, Sustainability (Switzerland) 15 (2023), https://doi.org/10.3390/su15010303.

[20] X. Shi, X. Liao, Y. Li, Quantification of fresh water consumption and scarcity footprints of hydrogen from water electrolysis: a methodology framework, Renew. Energy 154 (2020) 786–796, https://doi.org/10.1016/j.renene.2020.03.026.
[21] S.G. Simoes, J. Catarino, A. Picado, T.F. Lopes, S. di Berardino, F. Amorim, et al., Water availability and water usage solutions for electrolysis in hydrogen production, J. Clean. Prod. 315 (2021), https://doi.org/10.1016/j.jclepro.2021.128124.
[22] P. Woods, H. Bustamante, Aguey-Zinsou KF, The hydrogen economy - where is the water? Energy Nexus 7 (2022) https://doi.org/10.1016/j.nexus.2022.100123.
[23] L. Santana, Santos G dos, A. Santos, C. Marinho, A. Bispo, H. Villardi, et al., Evaluating the economic influence of water sources on green hydrogen production: a cost analysis approach, Int. J. Hydrog. Energy 89 (2024) 353–363, https://doi.org/10.1016/j.ijhydene.2024.09.274.
[24] Water For Hydrogen, Arup Australia Pty Ltd, Brisbane, 2022.
[25] D.R. MacFarlane, P.V. Cherepanov, J. Choi, B.H.R. Suryanto, R.Y. Hodgetts, J. M. Bakker, et al., A roadmap to the ammonia economy, Joule 4 (2020) 1186–1205, https://doi.org/10.1016/j.joule.2020.04.004.
[26] M. Blohm, F. Dettner, Green hydrogen production: integrating environmental and social criteria to ensure sustainability, Smart Energy 11 (2023) 1–11, https://doi.org/10.1016/j.segy.2023.100112.
[27] D. Peyerl, B. van der Zwaan, Analyzing the green hydrogen value chain against the sustainable development goals, Discov. Sustain. 5 (2024) 1–14, https://doi.org/10.1007/s43621-024-00374-4.
[28] F. Müller, J. Tunn, T. Kalt, Hydrogen justice, Environ. Res. Lett. 17 (2022) 1–7, https://doi.org/10.1088/1748-9326/ac991a.
[29] R. Roberts, A. Brent, J. Hinkley, R.Y. Cavana, Together, taking the next step: using system dynamics modelling to build community renewable energy programmes in Aotearoa New Zealand, J. R. Soc. N. Z. 55 (2025) 1167–1186, https://doi.org/10.1080/03036758.2024.2385082.
[30] S. Hafner, A. Anger-Kraavi, I. Monasterolo, A. Jones, Emergence of new economics energy transition models: a review, Ecol. Econ. 177 (2020), https://doi.org/10.1016/j.ecolecon.2020.106779.
[31] D. Meadows, Thinking in Systems: A Primer, Earthscan, London, 2009.
[32] Sterman John, Business Dynamics : Systems Thinking and Modeling for a Complex World, 1st ed., Irwin/McGraw-Hill, Boston, 2000.
[33] R. Panwar, E. Niesten, Advancing circular economy, Bus. Strategy. Env. 29 (2020) 2890–2892, https://doi.org/10.1002/bse.2602.
[34] J. Xijie, G.N. Rim, C.J. An, Some methodological issues in assessing the efforts for the circular economy by region or country, Sage Open 13 (2023), https://doi.org/10.1177/21582440231184863.
[35] M. Geissdoerfer, P. Savaget, N.M.P. Bocken, E.J. Hultink, The circular economy – a new sustainability paradigm? J. Clean. Prod. 143 (2017) 757–768, https://doi.org/10.1016/j.jclepro.2016.12.048.
[36] S. Lahane, H. Prajapati, R. Kant, Emergence of circular economy research: a systematic literature review, Manag. Environ. Qual.: Int. J. 32 (2021) 575–595, https://doi.org/10.1108/MEQ-05-2020-0087.
[37] O. Fitch-Roy, D. Benson, D. Monciardini, All around the world: assessing optimality in comparative circular economy policy packages, J. Clean. Prod. 286 (2021), https://doi.org/10.1016/j.jclepro.2020.125493.
[38] N.C. Darre, G.S. Toor, Desalination of water: a review, Curr. Pollut. Rep. 4 (2018) 104–111, https://doi.org/10.1007/s40726-018-0085-9.
[39] K. Elsaid, M. Kamil, E.T. Sayed, M.A. Abdelkareem, T. Wilberforce, A. Olabi, Environmental impact of desalination technologies: a review, Sci. Total Environ. 748 (2020), https://doi.org/10.1016/j.scitotenv.2020.141528.
[40] M.A. Abdelkareem, M. El Haj Assad, E.T. Sayed, B. Soudan, Recent progress in the use of renewable energy sources to power water desalination plants, Desalination 435 (2018) 97–113, https://doi.org/10.1016/j.desal.2017.11.018.
[41] E. Jones, M. Qadir, M.T.H. van Vliet, V. Smakhtin, Kang S mu, The state of desalination and brine production: a global outlook, Sci. Total Environ. 657 (2019) 1343–1356, https://doi.org/10.1016/j.scitotenv.2018.12.076.
[42] A. Panagopoulos, K.J. Haralambous, M. Loizidou, Desalination brine disposal methods and treatment technologies - a review, Sci. Total Environ. 693 (2019), https://doi.org/10.1016/j.scitotenv.2019.07.351.
[43] J. Moon, S. Son, J. Kim, K. Park, Critical challenges in high-salinity seawater reverse osmosis systems: technical, energy, and environmental reviews, Desalination 607 (2025), https://doi.org/10.1016/j.desal.2025.118811.
[44] R. Sirota, G. Winters, O. Levy, J. Marques, A. Paytan, J. Silverman, et al., Impacts of desalination brine discharge on benthic ecosystems, Env. Sci. Technol. 58 (2024) 5631–5645, https://doi.org/10.1021/acs.est.3c07748.
[45] M. Sharifinia, Z. Afshari Bahmanbeigloo, W.O. Smith, C.K. Yap, M. Keshavarzifard, Prevention is better than cure: persian Gulf biodiversity vulnerability to the impacts of desalination plants, Glob. Chang. Biol. 25 (2019) 4022–4033, https://doi.org/10.1111/gcb.14808.
[46] P.H. Gomes, S.P. Pereira, T.C.L. Tavares, T.M. Garcia, M.O. Soares, Impacts of desalination discharges on phytoplankton and zooplankton: perspectives on current knowledge, Sci. Total Environ. 863 (2023), https://doi.org/10.1016/j.scitotenv.2022.160671.
[47] W.J.F. Le Quesne, L. Fernand, T.S. Ali, O. Andres, M. Antonpoulou, J.A. Burt, et al., Is the development of desalination compatible with sustainable development of the Arabian Gulf? Mar. Pollut. Bull. 173 (2021) https://doi.org/10.1016/j.marpolbul.2021.112940.
[48] C.R. Anders, C.D.S. Fernandes, S. Dias N da, J.W. Gomes, S. da, S. Melo MR de, B. G.A. de Souza, et al., Environmental impacts of reject brine disposal from desalination plants, Desalin. Water Treat 181 (2020) 17–26, https://doi.org/10.5004/dwt.2020.25055.
[49] Y. Cai, J. Wu, S.Q. Shi, J. Li, K.H. Kim, Advances in desalination technology and its environmental and economic assessment, J. Clean. Prod. 397 (2023), https://doi.org/10.1016/j.jclepro.2023.136498.
[50] I.E. Nikolaou, K.P. Tsagarakis, An introduction to circular economy and sustainability: some existing lessons and future directions, Sustain. Prod. Consum. 28 (2021) 600–609, https://doi.org/10.1016/j.spc.2021.06.017.
[51] I.E. Nikolaou, N. Jones, A. Stefanakis, Circular economy and sustainability: the past, the present and the future directions, Circ. Econ. Sustain. 1 (2021) 1–20, https://doi.org/10.1007/s43615-021-00030-3.
[52] K. Winans, A. Kendall, H. Deng, The history and current applications of the circular economy concept, Renew. Sustain. Energy Rev. 68 (2017) 825–833, https://doi.org/10.1016/j.rser.2016.09.123.
[53] P. Fortes, R. Lopes, L. Dias, J. Seixas, J.P. Gouveia, S. Martinho, et al., Circular economy and climate mitigation: benefits and conflicts, in: International Conference on Energy and Environment: bringing together Engineering and Economics, 2019, pp. 1–7. Guimarães.
[54] L. Castellet-Viciano, V. Hernández-Chover, F. Hernández-Sancho, The benefits of circular economy strategies in urban water facilities, Sci. Total Environ. 844 (2022), https://doi.org/10.1016/j.scitotenv.2022.157172.
[55] M. Salgot, M. Folch, Wastewater treatment and water reuse, Curr. Opin. Env. Sci. Health 2 (2018) 64–74, https://doi.org/10.1016/j.coesh.2018.03.005.
[56] H. Becker, J. Murawski, D.V. Shinde, I.E.L. Stephens, G. Hinds, G. Smith, Impact of impurities on water electrolysis: a review, Sustain. Energy Fuels 7 (2023) 1565–1603, https://doi.org/10.1039/d2se01517j.
[57] R. Eneng, K. Lulofs, C. Asdak, Towards a water balanced utilization through circular economy, Manag. Res. Rev. 41 (2018) 572–585, https://doi.org/10.1108/MRR-02-2018-0080.
[58] L.L.S. Silva, C.G. Moreira, B.A. Curzio, F.V da Fonseca, Micropollutant removal from water by membrane and advanced oxidation processes—a review, J. Water. Resour. Prot 09 (2017) 411–431, https://doi.org/10.4236/jwarp.2017.95027.
[59] G. Crini, E. Lichtfouse, Advantages and disadvantages of techniques used for wastewater treatment, Environ. Chem. Lett. 17 (2019) 145–155, https://doi.org/10.1007/s10311-018-0785-9.
[60] S. Guerra-Rodríguez, P. Oulego, E. Rodríguez, D.N. Singh, J. Rodríguez-Chueca, Towards the implementation of circular economy in the wastewater sector: challenges and opportunities, Water (Switzerland) 12 (2020), https://doi.org/10.3390/w12051431.
[61] S. Jafarinejad, A framework for the design of the future energy-efficient, cost-effective, reliable, resilient, and sustainable full-scale wastewater treatment plants, Curr. Opin. Env. Sci. Health 13 (2020) 91–100, https://doi.org/10.1016/j.coesh.2020.01.001.
[62] X. Hao, X. Wang, R. Liu, S. Li, M.C.M. van Loosdrecht, H. Jiang, Environmental impacts of resource recovery from wastewater treatment plants, Water. Res. 160 (2019) 268–277, https://doi.org/10.1016/j.watres.2019.05.068.
[63] Z. Chen, D. Wang, G. Dao, Q. Shi, T. Yu, F. Guo, et al., Environmental impact of the effluents discharging from full-scale wastewater treatment plants evaluated by a hybrid fuzzy approach, Sci. Total Environ. 790 (2021), https://doi.org/10.1016/j.scitotenv.2021.148212.
[64] V. Hernández-Chover, Á. Bellver-Domingo, F. Hernández-Sancho, Efficiency of wastewater treatment facilities: the influence of scale economies, J. Env. Manage 228 (2018) 77–84, https://doi.org/10.1016/j.jenvman.2018.09.014.
[65] C.W. Lin, H.N. Tran, R.S. Juang, Reclamation and reuse of wastewater by membrane-based processes in a typical midstream petrochemical factory: a techno-economic analysis, Environ. Dev. Sustain. 26 (2024) 5419–5430, https://doi.org/10.1007/s10668-022-02880-9.
[66] K. Müller, M. Pampus, The solar rush: invisible land grabbing in East Germany, Int. J. Sustain. Energy 42 (2023) 1264–1277, https://doi.org/10.1080/14786451.2023.2260009.
[67] T.R. Silberg, R.B. Richardson, C.P. Borges, L.K.S. Olabisi, M.C. Lopez, M. Grisotti, et al., Technology adoption and weed emergence dynamics: social ecological modeling for maize-legume systems across Africa, Ecol. Soc. 29 (2024), https://doi.org/10.5751/ES-14667-290102.
[68] B. Cavicchi, Sustainability that backfires: the case of biogas in Emilia Romagna, Env. Innov. Soc. Transit 21 (2016) 13–27, https://doi.org/10.1016/j.eist.2016.02.001.
[69] Plano De Gestão Estratégica e De Negócio 2023 - 2027, CAGECE, Fortaleza, 2022.
[70] LEI N°16.033, 20 De Junho De 2016 Dispõe Sobre A Política De Reúso De Água Não Potável No Âmbito Do Estado Do Ceará, Ceará, Brazil, 2016.
[71] Estudo De Impacto Ambiental (EIA) e Relatório de Impacto Ambiental (RIMA) Do Hub de Hidrogênio Verde Docomplexo Do Pecém VOLUME I, Complexo do Pecém, Fortaleza, 2023.
[72] International Renewable Energy Agency. World Energy Transitions Outlook 2023: 1.5°C Pathway. Abu Dhabi: International Renewable Energy Agency IRENA; 2023.
[73] T. Khangaonkar, L. Premathilake, B. Cope, C. Knightes, A. Tseng, PLUMES2.0 – Dilution Model: Model Theory and User Manual, 2024.
[74] A. F. Paparella, D. D'Agostino, J. Burt, Long-term, basin-scale salinity impacts from desalination in the Arabian/Persian Gulf Sci. Rep. 12 (2022) https://doi.org/10.1038/s41598-022-25167-5.
[75] H.D. Ibrahim, P. Xue, E.A.B. Eltahir, Multiple salinity equilibria and resilience of Persian/Arabian Gulf Basin salinity to brine discharge, Front. Mar. Sci. 7 (2020) 1–5, https://doi.org/10.3389/fmars.2020.00573.
[76] S.P. Pereira, M.F. Rodrigues, P.C.C. Rosman, P. Rosman, T. Bleninger, I.E. Lima Neto, et al., A novel tool for modeling the near- and far-field dispersion of brine

effluent from desalination plants, Front. Mar. Sci. 11 (2024) 01–14, https://doi.org/10.3389/fmars.2024.1377252.
[77] Y. Barlas, Formal aspects of model validity and validation in system dynamics, Syst. Dyn. Rev. 12 (1996) 183–210, https://doi.org/10.1002/(sici)1099-1727(199623)12:3<183::aid-sdr103>3.0.co;2-4.
[78] J.W. Forrester, P.M. Senge, Testes for building confidence in SDM, Stud. Manag. Sci. 14 (1980) 209–228.
[79] Apex Water. Delmore Wastewater Treatment Plant Design Report - For Consenting. 2025.
[80] Brown and Caldwell, Carollo. Chapter 7 Wastewater Treatment Plant Master Plan 7-2. 2011.
[81] Wastewater Treatment Plant Construction, Lakeside Equipment Corporation, 2025. Website 2020, https://www.lakeside-equipment.com/wastewater-treatment-plant-construction/. accessed December 8.
[82] P. Kehrein, M. Jafari, M. Slagt, E. Cornelissen, P. Osseweijer, J. Posada, et al., A techno-economic analysis of membrane-based advanced treatment processes for the reuse of municipal wastewater, Water Reuse 11 (2021) 705–725, https://doi.org/10.2166/wrd.2021.016.
[83] Sperling M von, Wastewater Characteristics, Treatment and Disposal, 1st ed., IWA Publishing, London, 2007.
[84] J. Yang, M. Monnot, L. Ercolei, P. Moulin, Membrane-based processes used in municipal wastewater treatment for water reuse: state-of-the-art and performance analysis, Membranes. (Basel) 10 (2020) 1–56, https://doi.org/10.3390/membranes10060131.
[85] Brazilian National System of Information about Basic Sanitation, Relatório dos Serviços de Abastecimento de Água: SINISA 2024 ano de referência 2023, Brasília, 2024.
[86] Yokogawa. Understanding ultrapure water and the difficulties with pH measurement. 2015.
[87] Muñoz S., Rogalla F., Icaran P., Perez C., Simón F.X. LIFE+REMEMBRANE: RECUPERACIÓN DE LAS MEMBRANAS DE ÓSMOSIS INVERSA AL FINAL DE SU VIDA ÚTIL. 2014.
[88] J. Malinauskaite, B. Delpech, L. Montorsi, M. Venturelli, W. Gernjak, M. Abily, et al., Wastewater reuse in the EU and southern European countries: policies, barriers and good practices, Sustainability (Switzerland) 16 (2024), https://doi.org/10.3390/su162411277.
[89] D. Jang, J. Kim, D. Kim, W.B. Han, S. Kang, Techno-economic analysis and Monte Carlo simulation of green hydrogen production technology through various water electrolysis technologies, Energy Convers. Manage 258 (2022), https://doi.org/10.1016/j.enconman.2022.115499.
[90] S. Samsatli, I. Staffell, N.J. Samsatli, Optimal design and operation of integrated wind-hydrogen-electricity networks for decarbonising the domestic transport sector in Great Britain, Int. J. Hydrog. Energy 41 (2016) 447–475, https://doi.org/10.1016/j.ijhydene.2015.10.032.
[91] A. Somrani, Z. Mohamed, K. Abohelal, S. Larhrib, N. Ghaffour, M. Pontié, Transforming end-of-life SWRO desalination membranes into nanofiltration membranes for thtreatment of brackish water and wastewater, Sci. Rep. 15 (2025), https://doi.org/10.1038/S41598-025-88818-3.
[92] N. Voutchkov, Critical Review of the Desalination Component of the WRP, Cape Town, 2017.
[93] Piedra J., Planas M.R., Trillas F., Ricart J.E. CAP djinet seawater desalination plant (Algeria). 2019. https://doi.org/10.15581/018.ST-523-E.
[94] Acciona. Umm Al Houl SWRO n.d.:1–5. https://www.acciona.com/projects/swro-umm-al-houl (accessed December 9, 2025).
[95] D. Xevgenos, K. Moustakas, D. Malamis, M. Loizidou, An overview on desalination & sustainability: renewable energy-driven desalination and brine management, Desalin. Water Treat 57 (2016) 2304–2314, https://doi.org/10.1080/19443994.2014.984927.
[96] Silva WF da, Santos IFS dos, O. Botan MCC de, A.P. Moni Silva, R.M Barros, Reverse osmosis desalination plants in Brazil: a cost analysis using three different energy sources, Sustain. Cities. Soc. 43 (2018) 134–143, https://doi.org/10.1016/j.scs.2018.08.030.
[97] J. Kim, S. Hong, Optimizing seawater reverse osmosis with internally staged design to improve product water quality and energy efficiency, J. Memb. Sci. 568 (2018) 76–86, https://doi.org/10.1016/j.memsci.2018.09.046.
[98] R. Younis, M.A. Knight, A probability model for investigating the trend of structural deterioration of wastewater pipelines, Tunn. Undergr. Space Technol. 25 (2010) 670–680, https://doi.org/10.1016/j.tust.2010.05.007.
[99] C.P. Borges, J.C. Sobczak, T.R. Silberg, M. Uriona-Maldonado, C.R. Vaz, A systems modeling approach to estimate biogas potential from biomass sources in Brazil, Renew. Sustain. Energy Rev. 138 (2021), https://doi.org/10.1016/j.rser.2020.110518.
[100] M.A.U.R. Tariq, R. Alotaibi, K.K. Weththasinghe, Z. Rajabi, A detailed perspective of water resource management in a dry and water scarce country: the case in Kuwait, Front. Environ. Sci. 10 (2022), https://doi.org/10.3389/fenvs.2022.1073834.
[101] Statistics About Ceará 2025:1, Instituto Brasileiro de Geografia e Estatística, 2025. https://www.ibge.gov.br/cidades-e-estados/ce.html. accessed December 9.
[102] Kuwait Population 2024 2025:1–26, World Bank Group, 2025. https://data.worldbank.org/indicator/SP.POP.TOTL?locations=KW. accessed December 9.
[103] Orange County completes World's Largest Wastewater Recycling and Purification System 2023, State Water Resources Control Board, 2025. https://www.waterboards.ca.gov/press_room/press_releases/2023/pr20230414-orange-county-replenishment.html. accessed December 9.
[104] Our Changing Population: Orange County, USA Facts, California, 2025. https://usafacts.org/data/topics/people-society/population-and-demographics/our-changing-population/state/california/county/orange-county/. accessed December 9, 2025.
[105] F. Hassan, K.D. Prasetya, J.N. Hanun, H.M. Bui, S. Rajendran, N. Kataria, et al., Microplastic contamination in sewage sludge: abundance, characteristics, and impacts on the environment and human health, Environ. Technol. Innov. 31 (2023), https://doi.org/10.1016/j.eti.2023.103176.
[106] V. Hernández-Chover, L. Castellet-Viciano, R. Fuentes, F. Hernández-Sancho, Circular economy and efficiency to ensure the sustainability in the wastewater treatment plants, J. Clean. Prod. 384 (2023), https://doi.org/10.1016/j.jclepro.2022.135563.
[107] E.H. Krueger, S.M. Constantino, M.A. Centeno, T. Elmqvist, E.U. Weber, S. A. Levin, Governing sustainable transformations of urban social-ecological-technological systems, Npj Urban Sustain. 2 (2022), https://doi.org/10.1038/s42949-022-00053-1.
[108] B.K. Sovacool, M. Martiskainen, A. Hook, L. Baker, Decarbonization and its discontents: a critical energy justice perspective on four low-carbon transitions, Clim. Change 155 (2019) 581–619, https://doi.org/10.1007/s10584-019-02521-7.
[109] E.D. Mendes, R.J.S. Sampaio, F.M. Collaço, A. de, Justice or just plans? Reviewing the energy transition strategy of Brazil's Ceará state, Energy Res. Soc. Sci. 119 (2025) 103865, https://doi.org/10.1016/j.erss.2024.103865.
[110] United States Environmental Protection Agency, Primer for Municipal Wastewater Treatment Systems, Washington, 2004.
[111] A. Hurynovich, M. Kwietniewski, V. Romanovski, Evaluation of the possibility of utilization of sewage sludge from a wastewater treatment plant – case study, Desalin. Water Treat 227 (2021) 16–25, https://doi.org/10.5004/dwt.2021.27199.
[112] X. Zhang, Y. Liu, Circular economy is game-changing municipal wastewater treatment technology towards energy and carbon neutrality, Chem. Eng. J. 429 (2022), https://doi.org/10.1016/j.cej.2021.132114.
[113] M. Lima P de, T.A. Lopes, S. de, L.M. Queiroz, J.R. McConville, Resource-oriented sanitation: identifying appropriate technologies and environmental gains by coupling Santiago software and life cycle assessment in a Brazilian case study, Sci. Total Environ. 837 (2022), https://doi.org/10.1016/j.scitotenv.2022.155777.
[114] H. Nasr, M. Yousef, H. Madkour, Impacts of discharge of desalination plants on marine environment at the southern part of the Egyptian Red Sea coast (Case Study), Int. J. Ecotoxicol. Ecobiol. 4 (2019) 66, https://doi.org/10.11648/j.ijee.20190403.12.
[115] L.D.S. Queiroz, S. Rossi, A.T. Mercander, C. Serra-Pompei, D.V. Pifarré, J. C. Domínguez, et al., The social and economic framework of Artisanal fishing in The State of Ceará, Brazil, Geosaberes 11 (2020) 180, https://doi.org/10.26895/geosaberes.v11i0.871.
[116] J.M.L. Marques, R. Cruz, C.V. Feitosa, Dynamics of artisanal fisheries performed with hook-and-line gear under different management regimes in Brazil, Ocean. Coast. Manage 200 (2021), https://doi.org/10.1016/j.ocecoaman.2020.105403.
[117] Water Resources Council of the State of Ceará, Resolução Conerh No01/2022: Dispõe Sobre A Cobrança Pelo Uso Dos Recursos Hídricos Superficiais E Subterrâneos De Domínio Do Estado Do Ceará Ou Da União (2022).
[118] M.C. Chrispim, M. Scholz, M.A. Nolasco, A framework for resource recovery from wastewater treatment plants in megacities of developing countries, Env. Res 188 (2020), https://doi.org/10.1016/j.envres.2020.109745.
[119] A. Gorayeb, C. Brannstrom, A.J. de Andrade Meireles, Sousa de, J. Mendes, Wind power gone bad: critiquing wind power planning processes in northeastern Brazil, Energy Res. Soc. Sci 40 (2018) 82–88, https://doi.org/10.1016/j.erss.2017.11.027.
[120] L.N. Nóbrega, O povo indígena Anacé e o Complexo Industrial e Portuário do Pecém, no Ceará: desenvolvimento e resistências no contexto da barbárie por vir, Rev. Ciênc. Sociais-Fortaleza 51 (2020) 165–211, https://doi.org/10.36517/rcs.51.2.d05.
[121] M. Tahir, A.A. Albahouth, M. Jaboob, A.J. Osama, U. Burki, The consumption of natural resources and its effects on environmental quality: evidence from the OECD countries, Sustain. Futures 8 (2024), https://doi.org/10.1016/j.sftr.2024.100248.
[122] P.R.B. Castro, A.F. Gomes, Análise da expansão urbana na região metropolitana de Fortaleza a partir do conceito de cidade fordista: o caso do Complexo Industrial e Portuário do Pecém – CIPP, Contrib. Las Cienc. Soc. 16 (2023) 28096–28108, https://doi.org/10.55905/revconv.16n.11-201.
[123] B.H.N. Diógenes, J.A. Farias, Dinâmicas urbanas recentes no eixo oeste de expansão metropolitana de Fortaleza, Thesis 7 (2024) 193–211.
[124] A. Meireles AJ de, J.A.T. Melo, M.A. Said, Environmental injustice in northeast Brazil: the Pecém industrial and shipping complex, in: P. Cooney, W.S. Freslon (Eds.), Research in Political Economy, 1st ed., Emerald Group Publishing Ltd., 2018, pp. 171–187, https://doi.org/10.1108/S0161-723020180000033007, vol. 33.
[125] Abreu MCS de, Andrade R de JC de, Problematizing the wickedness of the Fundão dam rupture: are cross-sector partnerships enough to bring about the Doce river basin recovery process? Env. Sci. Policy 132 (2022) 35–47, https://doi.org/10.1016/j.envsci.2022.02.013.
[126] V. Moretti, N.R. Corraini, E.L. Melo, M.E.G. Scherer, J.C. Colmenero, Progress towards the Sustainable Development Goal 14 (Life below water) in the context of Brazil: a multicriteria approach, Sustain. Futures 8 (2024), https://doi.org/10.1016/j.sftr.2024.100410.
[127] E.D. Mendes, F.M. Collaço, A. de, Justiça Distributiva em Conflitos de Energia Eólica: análise de Decisões Judiciais sobre Impactos de Parques no Ceará, Direito Público 21 (2024) https://doi.org/10.11117/rdp.v21i111.7940.

[128] K. Dillman, J. Heinonen, Towards a safe hydrogen economy: an absolute climate sustainability assessment of hydrogen production, Climate 11 (2023), https://doi.org/10.3390/cli11010025.
[129] B.K. Sovacool, Who are the victims of low-carbon transitions? Towards a political ecology of climate change mitigation, Energy Res. Soc. Sci. 73 (2021), https://doi.org/10.1016/j.erss.2021.101916.
[130] C. Brannstrom, A. Gorayeb, Geographical implications of Brazil's emerging green hydrogen sector, J. Lat. Am. Geogr. 21 (2022) 185–194, https://doi.org/10.1353/lag.2022.0006.